**Università degli Studi del Piemonte Orientale**

**"Amedeo Avogadro"**

Dipartimento di Scienze e Innovazione Tecnologica


Dottorato di Ricerca in Chemistry & Biology

*curriculum*: Drug Discovery and Development

XXXII ciclo a.a. 2018-2019

SSD: CHIM/03

# Anticancer activity of multifunctional Pt(IV) prodrugs

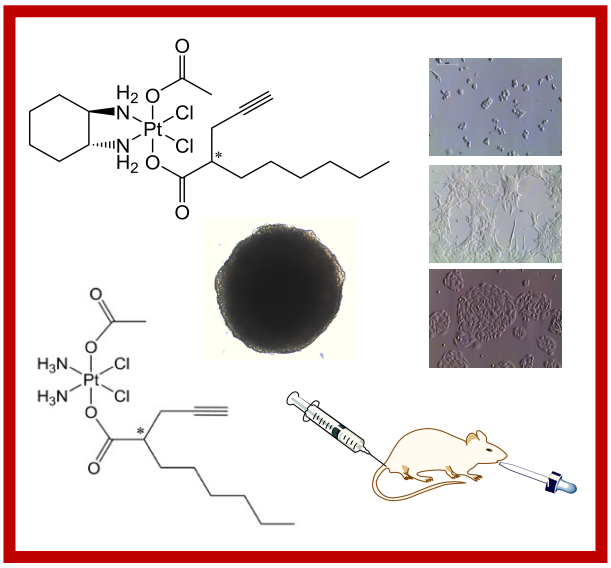



**Beatrice Rangone**

Supervised by Prof. Domenico Osella

PhD program co-ordinator Prof. Luigi Panza

**Università degli Studi del Piemonte Orientale**
**"Amedeo Avogadro"**

Dipartimento di Scienze e Innovazione Tecnologica

Dottorato di Ricerca in Chemistry & Biology

*curriculum*: Drug Discovery and Development

XXXII ciclo a.a. 2018-2019

SSD: CHIM/03

# Anticancer activity of multifunctional Pt(IV) prodrugs

**Beatrice Rangone**

Supervised by Prof. Domenico Osella

PhD program co-ordinator Prof. Luigi Panza

*Omnia venenum sunt:*
*nec sine veneno quicquam existit.*
*Dosis sola facit,*
*ut venenum non fit.*

PARACELSO

# *Contents*

## Chapter 1

***Introduction***



## Chapter 2

## Chapter 3

***Unsymmetric cisplatin-based Pt(IV) derivative containing a novel Histone DeACetylase inhibitor (HDACi): a very efficient multi-action antitumor prodrug candidate***

## Chapter 4

***Pt(IV) multifunctional 1R,2R-diamine-based Pt(IV) prodrug containing the novel HDACi, POA: induction of immunogenic cell death on colon cancer***



## Chapter 5

***Selective activity against human colon cancer cell lines of cyclohexane- 1R,2R-diamine-based Pt(IV) dicarboxylato anticancer prodrugs***

## Chapter 6

***Antiproliferative Activity of Pt(IV) Conjugates Containing the Non-Steroidal Anti-Inflammatory Drugs (NSAIDs) Ketoprofen and Naproxen***

# Chapter 1

# Introduction

## 1.1 The tumorigenesis

Most tumors do not result from a single phenomenon, hence tumorigenesis is a complex and multifactorial process characterized by the acquisition of several abnormal functionalities, needed by the cells to evolve through different premalignant steps into invasive cancers. So, they originate from normal cells that have experienced a transformation process as a result of mutations induced by errors in cell replication or by exogenous factors, as X-rays, UV light, chemicals and oncoviruses (Figure 1.1).

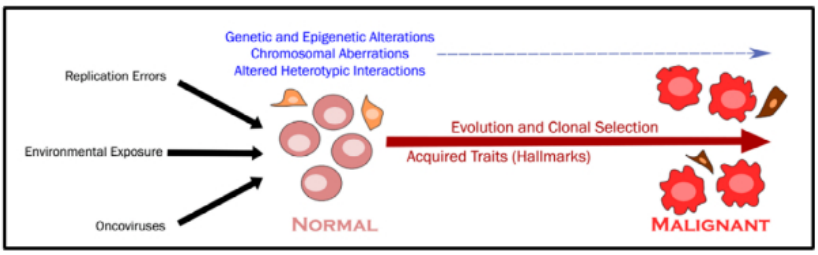


Figure 1.1: The transformation process of normal cells into malignant ones. The picture is a modification of that reported in literature [1].

These alterations confer to mutant cells a selective growth advantage, allowing them to proliferate out of control. This process, called evolutionary clonal selection, makes the cell to acquire malignant traits, which are the hallmarks of tumor [1]. The normal cell that acquire the initial cancer-promoting mutation is considered the "cell of origin". On the contrary, the subset of self-renewing cancer cells that uniquely

sustain tumor malignant growth are known as cancer stem cells (CSC). These cells have proven to be a common component in most tumors and several hypotheses have been proposed about the origin of CSC, either from stem or differentiated cells; however, until now little is known about them [2].

Tumorigenesis is the result of mutations in protein-encoding genes, which can be classified into two classes: proto-oncogenes and tumor suppressor genes. Proto-oncogenes encode for proteins which promote cell growth and proliferation, including kinases, tyrosine kinase receptors, transcription and growth factors and GTPase regulators. Their mutated form are known as oncogenes. A representative example is the RAS protein family, chronically active in 30% of cancers, due to inactivating mutations in one of its negative regulators or missense mutations in its gene. The components of downstream cascades mediating RAS functions could be mutated in similar way in different type of cancers. Thus, mutations in RAS, in its regulatory proteins and in its downstream pathways result in a panel of effects which enhance growth and proliferation [3]. On the other hand, tumor suppressor genes encode for proteins which operate in different ways in order to limit cell growth and proliferation. The most commonly mutated (in over 50% of sequenced malignancies) tumor suppressor gene encodes for P53. This protein acts as a detector of a variety of stresses, arresting further progression of cell cycle, being involved in repair mechanism, or eventually triggering apoptosis if the degree of damage is excessive [4]. Another key tumor suppressor gene encodes for retinoblastoma (RB) protein, which is commonly inactivated in a great number of cancers. It is a critical regulator of cell-cycle progression and its absence leads to persistent cell proliferation [5]. Thus, mutations, which affect both oncogenes and tumor suppressor genes, cause uncontrolled cell proliferation and, consequently, alterations in tissue homeostasis.

Despite cancer is not a single disease, but exhibit a strong heterogeneity in cellular morphology, proliferative activity, genetic lesions and response to therapy, generally malignant cells show the following features:

- selective growth and proliferative advantage, due to self-sufficiency in growth signals and insensitivity to antigrowth pathways;
- altered stress response leading to overall cell survival, for example defects in DNA repair machinery, escape of cell death (both apoptosis and autophagy) and loss of senescence ability;
- sustained angiogenesis and other modes of tumor neo-vascularization;
- acquisition of the capacity to invade surrounding tissue and to form secondary sites of growth (metastasis);
- metabolic rewiring that represents a selective advantage during initiation and progression of cancer, as the switch from aerobic to anaerobic metabolism, phenomenon known as "Warburg effect";
- creation of dynamic and rich microenvironment;
- ability to escape immune surveillance, supported by the fact that primary and acquired immunodeficiency in mice and humans are related with greater susceptibility to carcinogenesis [1].

## *1.2 Cell cycle*

Cellular replication is regulated by the cell cycle, a tightly ruled process with multifactorial and very complex control mechanisms. It is divided into several stages, each of them with very typical functional properties. Upon receiving the mitogenic stimulus the eukaryotic cell starts its cell cycle in G1 (gap 1) phase: the cell shows a rise in the expression of protein and in its metabolism, in order to set the conditions needed for the following S (synthesis) phase, which is the step involving DNA replication. This is followed by the G2 (gap 2) phase, during which the accuracy of chromosome replication is checked and further synthesis of the proteins occurs. G1, S, and G2 form the interphase. Then, the M (mitotic) phase is characterized by the separation of chromosomes in the nucleus and, finally, by the division of cytoplasm, called cytokinesis (Figure 1.2).

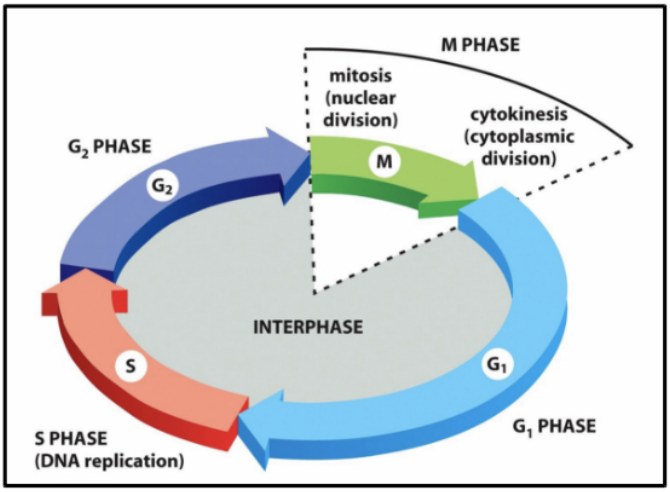


Figure 1.2: The cell cycle events. The picture is a modification of that reported in literature [6].

After M phase, cells can enter into a new G1 phase or proceed to a quiescent state, known as G0, which can persist for a long time, or even for the rest of cell life in the case of some somatic cells. The strictly correlation between a step and the correct completion of the preceding one allows the successful progression of cell cycle. The interdependency is related to surveillance mechanisms, namely checkpoints, which prevent the propagation of genetic abnormalities. If cell damage cannot be repaired, checkpoint signaling may induce apoptosis. This control system is based on two groups of proteins: the family of cyclin-dependent kinases (CdKs) and cyclins. CdKs bind cyclins and check their ability to phosphorylate appropriate targets. There are several classes of CdKs and cyclins, depending on the step of the cell cycle where they are activated (Table 1).

Loss of cell cycle regulation leads to uncontrolled cell proliferation, which is an hallmark of cancer [7].

| CYCLIN-CDK COMPLEX | VERTEBRATES | | BUDDING YEAST | |
|---|---|---|---|---|
| | CYCLIN | CDK PARTNER | CYCLIN | CDK PARTNER |
| $G_1$-Cdk | cyclin D* | Cdk4, CdK6 | Cln 3 | Cdk1** |
| $G_1$/S-Cdk | cyclin E | Cdk2 | Cln1, 2 | Cdk1 |
| S-Cdk | cyclin A | Cdk2, Cdk1** | Clb5, 6 | Cdk1 |
| M-Cdk | cyclin B | Cdk1 | Clb1, 2, 3, 4 | Cdk1 |

Table 1: The main classes of cyclins and CdKs, referred to vertebrate and budding yeast [6].

## *1.3 Cell death*

Like cell growth and proliferation, cell death plays a crucial role in tissue homeostasis. Defects in the regulation of cell death are related to a variety of human disease, including tumor. In addition, the main purpose of anticancer drugs is selectively inducing cell death in malignant cells only. Different kinds of cell death can be distinguished, according to biochemical and morphological parameters, but they are strictly interconnected and may co-exist, hence often it is difficult to discriminate them [8].

### *1.3.1 Apoptosis*

Apoptosis is a type of programmed cell death and it is a key component of cell growth control. It is fundamental for various processes involved in tissue homeostasis, as embryonic development and organogenesis. Thus, abnormal regulation of apoptosis leads to pathogenesis of several human disorders, particularly its suppression is strictly related to tumorigenesis.

This kind of cell death is characterized by a series of morphological changes, such as cell shrinkage and reduction of cell volume (pyknosis), disruption of organelles membrane, chromatin condensation, nuclear cleavage (karyorhexis) and finally cell fragmentation into apoptotic bodies, which can be engulfed by macrophages.

Apoptosis may be triggered by a plethora of signals and it is induced by two major pathways: the intrinsic and extrinsic one (Figure 1.3). Both pathways converge in the activation of a specific series of cysteine aspartyl-protease, known as caspases, which are both the initiators (like caspase 2, -8 , -9 and -10), showing autocatalytic activity, and the downstream effectors (as caspase 3, -6 and -7), activated by proteolytic cleavage by the previous ones. The effector caspases can further cleave other nuclear and cytosolic substrates, progressively activating proteolytic cascades that lead to the biochemical and morphological features of apoptosis.

The intrinsic apoptotic pathway is triggered by intracellular signals, such as DNA damage. Upon these stimuli the activation of pro-apoptotic proteins, as BAX, BAK, BAD and BID, leads to mitochondrial outer membrane permeabilization (MOMP), resulting in the release of proteins from the mitochondrial intermembrane space. Among them cytochrome c is the most important; indeed, once released in cytoplasm, it transiently binds the apoptotic protease-activating factor 1 (Apaf-1), triggering Apaf-1 oligomerization into an heptamer, which exposes the caspase activation and recruitment domain (CARD). This domain binds to pro-caspase 9, forming a multi-protein complex, namely apoptosome, in which pro-caspase 9 auto-activates and subsequently recruits the executioner caspases 3 and -7 to orchestrate apoptosis. This pathway can also be modulate by anti-apoptotic proteins (*e.g* BCL-2 and IAPs).

On the contrary, the extrinsic pathway is activated by cell transmembrane receptors in the presence of extracellular signals. These death receptors include a subset of tumor necrosis factor (TNF) superfamily, characterized by different protein motifs, called death domains (DD) and death effectors domains (DED). There are three main receptor-systems involved in this apoptotic pathway: Fas, activated by Fas ligand (Fas L); tumor necrosis factor receptor 1 (TNFR1), activated by tumor necrosis factor α (TNF-α); and death receptors 4 and 5 (DR4, DR5), activated by TNF-related apoptosis inducing ligand (TRAIL). After the activation, these receptors attract DD-containing molecules, such as Fas-associated death domain protein (FADD), thus

triggering pro-apoptotic pathways. FADD recruits other DD/DED-containing factors, including pro-caspases 8 and -10, promoting the formation of the death inducing complex (DISC) in the cytoplasm. The recruitment of these proteins in DISC favors their self-cleavage and once activated, caspases 8 and -10 directly engage the effector caspases 3, -6 and -7 to perpetrate apoptotic cell death. Alternatively, caspase 8 can activate BID, promoting the intrinsic apoptotic pathway [9] [10].

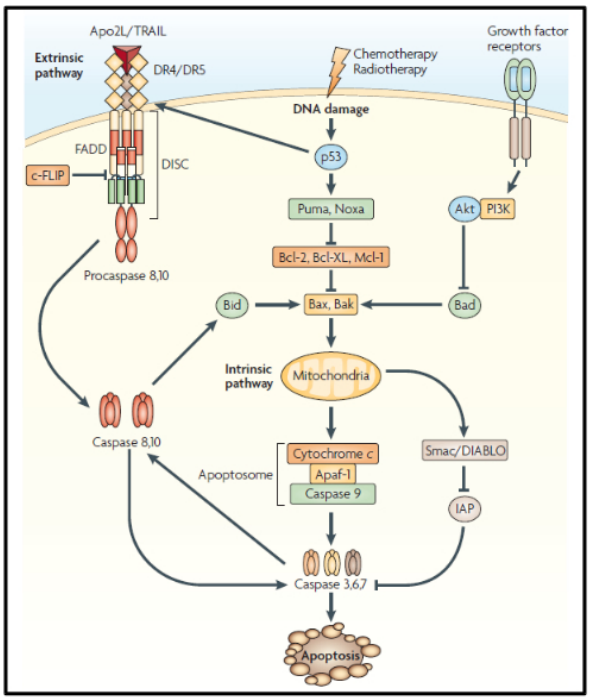


Figure 1.3: Key step in apoptotic intrinsic and extrinsic signaling pathways. The picture is a modification of that reported in literature [11].

## *1.3.2 Autophagy*

Autophagy is another type of programmed cell death. It contributes to cell homeostasis by degrading several intracellular materials, particularly dysfunctional organelles, protein aggregates, and invading pathogens. Similarly to apoptosis, aberrant autophagy seems to be linked to a wide range of human diseases, including cancer. It has been reported that autophagy plays contradictory roles in tumor initiation and progression. Hence, both stimulation and repression of autophagy should be explored as therapeutic approaches, due to the several factors that contribute to tumorigenesis.

The general term autophagy describes the process by which cytoplasmic components are delivered to lysosomes for degradation. Three main autophagy pathways have been elucidated, which may be distinguished by the delivery method of substrates: macroautophagy, microautophagy and chaperone-mediated autophagy (CMA) [12] (Figure 1.4).

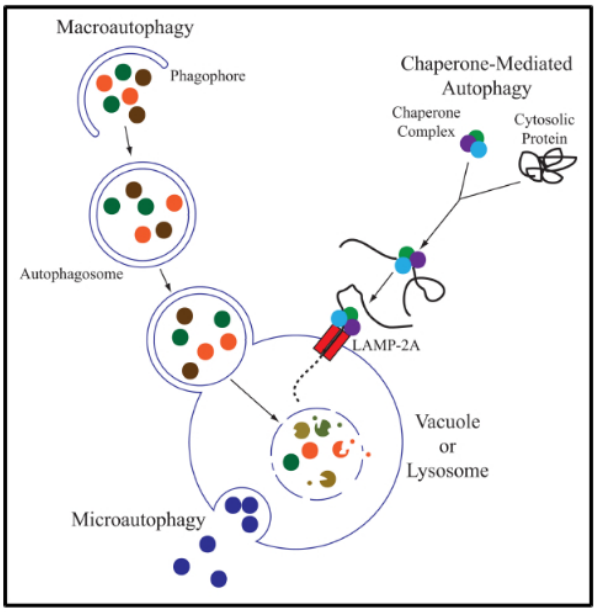


Figure 1.4: Three main autophagic pathways. The picture is a modification of that reported in literature [13].

Among the three autophagic pathways, macroautophagy represents the main and the most studied one. During this process, an isolation membrane, called phagophore, encloses a small part of unnecessary or dysfunctional cytoplasmic components, such as damaged organelles, forming a double-membraned structure, namely autophagosome. Then, its outer membrane fuses with lysosomes, to evolve into an autolysosome, in which lysosomal enzymes degrade the cytoplasmic substrates (Figure 1.4). Macroautophagy consists of different steps: initiation and nucleation, elongation, maturation, fusion and degradation (Figure 1.5). The machinery is finely regulated by a series of factors, the Atg proteins, which can assemble into many different multimolecular complexes to form autophagosome. Among them, the Unc-51 like kinase 1 (ULK1) complex plays a key role in the initiation of the process. In fact, in response to several stresses, like starvation, the serine-threonine kinase mammalian target of rapamycin (mTOR) is inhibited and dissociates from the ULK1 complex, leading to its activation and to the initiation. The activation of this complex promotes the recruitment of the class III phosphatidylinositol 3 kinase (PI3K), which is essential for the nucleation and assembly of phagophore membrane, through the phosphorylation of key factors, like activating molecule in Beclin-1-regulated protein autophagy 1 (AMBRA) and Beclin-1. The subsequent elongation process involves two conjugation reactions leading to Atg5-Atg12 and microtubule associated protein-1 light chain (LC3)-phosphatidylethanolamine (PE). The product of the second conjugation is essential for the closure of the autophagosome membrane. Finally, in the fusion stage, in which autophagosome fuses with lysosome to form an autolysosome, are involved monomeric GTPases of the Rab family. This process is followed by the lysosomal degradation of the autophagic substrate [9].

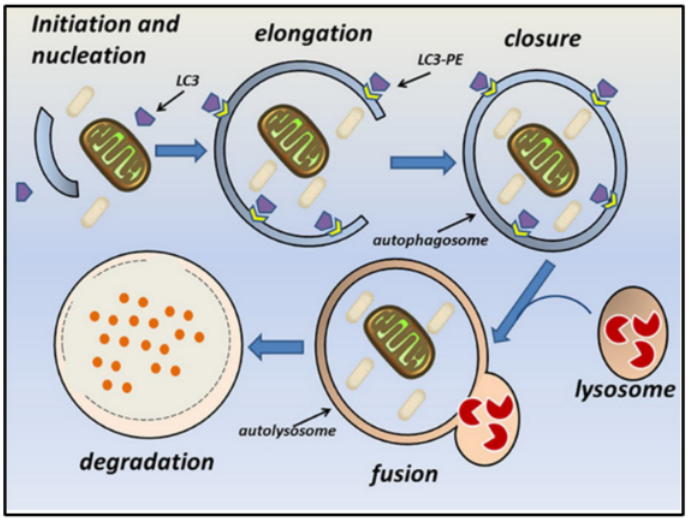


Figure 1.5: The macroautophagy steps. The picture is a modification of that reported in literature [14].

Conversely, microautophagy is the less studied. It is characterized by the direct engulfment of cytoplasmic portions by the lysosomes (Figure 1.4). Thus, the lysosomal membrane randomly undergoes invagination and differentiation into autophagic tubes, in order to enclose substrates for degradation. The main functions of microautophagy are the maintenance of membrane homeostasis, organellar sizes, and cell survival under nitrogen starvation [15].

The third type of autophagy, CMA, is a process in which the substrates are proteins containing a specific pentapeptide motif which are selectively recognized by a chaperone protein, belonging to the family of Heat Shock Proteins 70 (HSP70), the HSPA8/HSP70. The resulting chaperone-substrate complex binds the lysosomal receptor lysosomal-associated membrane protein type 2A (LAMP-2A), leading to its multimerization, with the help of the lysosomal protein HSP90. Then, the substrates are unfolded and delivered to the lysosome lumen, through the LAMP-2A-enriched translocation complex, where lysosomal proteases degrade them (Figure 1.4). Subsequently, LAMP-2A multimers undergo disassembly and degradation for the next cycle of CMA. This pathway is tightly regulated and can be activated under

protracted starvation and a variety of stresses, and it represents a quality control aimed to remove unfolded or damage proteins [16].

### *1.3.3 Necrosis*

Necrosis is another type of cell death without the typical features of apoptosis (cell shrinkage, pyknosis, karyorhexis and formation of apoptotic bodies) and without abundant autophagic vacuolization. On the contrary, the main characteristics of necrosis include an increase of cell volume (oncosis), which finally leads to a disruption of plasma membrane and to disorganized dismantling of swollen organelles. Thus, this type of cell death lacks typical biomarkers, except for the plasma membrane permeabilization. Necrosis is usually regarded as harmful, due to its association with pathological cell loss and to the capacity of necrotic cells to favor local inflammation, which can support tumor growth [17].

### *1.3.4 Non-lethal processes: cell senescence and mitotic catastrophe*

The molecular machinery involved in cell death is also related to other processes that cannot be considered as cell death *per se*, including cell senescence and mitotic catastrophe.

Cell senescence is a pathophysiological state during which the cells persistently lose their proliferative ability while remaining metabolically active and viable. Senescent cells show typical morphological features, such as intracellular vacuolization, altered chromatin structure, flattening and cellular or nuclear enlargement. The biochemical markers are: increased lysosomal galactosidase beta (GLB1) activity, inhibition of several CDKs and subsequent dephosphorylation of multiple members of the RB protein family, absence of proliferation markers, activation of the DNA damage response (DDR) machinery, and presence of senescent-associated heterochromatic

foci (SAHF). Moreover, senescent cells secrete the so-called senescent-associated secretory phenotype (SAPS), composed by mitogenic and immunomodulatory chemokines, cytokines and growth factors, which is involved in the immunological clearance of these cells, and also modulate the activity of other cells with an intact proliferative capacity. Hence, cell senescence seems to contribute to embryogenesis, as well as to several adult pathophysiological processes, such as tissue regeneration and repair, immunity and tumor suppression. Particularly, cell senescence has been reported to occur in response to potentially tumorigenic events (as tumor suppressor genes inactivation or oncogenes activation) and various sublethal cell insults (including DNA damage, telomere shortening, mitochondrial dysfunctions). However senescent cells are also implicated in the side effects of some chemotherapeutic treatments and in the recurrence of specific cancers, thus senescence plays a controversial role in cancer progression, acting both as a tumor suppressor and promoter.

Mitotic catastrophe is a regulated mechanism, hampering the proliferation and the survival of cells that cannot complete mitosis, due to extensive DNA damage, defects in the mitotic machinery and failure of cell cycle checkpoints. Mitotic defects can originate both from exogenous and endogenous sources, and the main alterations driving aberrant mitosis can derive from other cell cycle phases, especially the S phase. This process is morphologically characterized by typical nuclear alterations, as multinucleation, macro- and micronucleation, while the molecular mechanisms triggering mitotic catastrophe cascade are still unclear, but probably involve p53 in many cell types. The destiny of cells undergoing mitotic catastrophe appears to be related to the period spent under mitotic arrest, and their ability to escape from abnormal mitosis. Hence, the arrested cells may undergo cell death (most often intrinsic apoptosis) or enter cell senescence, after activating some cell cycle checkpoints. Consequently, the abrogation of mitotic catastrophe constitutes a fundamental event during tumorigenic transformation and progression [8] [17].

## *1.4 The anticancer chemotherapy*

The oldest case of cancer was described around 3000 BC in an Egyptian papyrus, in which eight cases of breast tumors were recorded along with their treatment by cauterization. Thus, surgical resections were historically the main way of cancer treatment. Later, in 1896 X-rays began to be used for recurrent breast carcinoma therapy, and since then radiotherapy and surgery represented the main treatments. Only since 1950 chemotherapy has become a valid therapeutic option, with the discovery of nitrogen mustard (now regarded as the first chemotherapeutic agent) and its application for lymphomas and solid tumors therapy. This event led to a rapid development of various chemotherapeutics. However, despite the advances in this field, nowadays cancer remains one of the major cause of death worldwide, partly due to an ageing global population [18].

The ultimate goal of conventional anticancer chemotherapeutics is to induce malignant cells to die or arrest their proliferation. Hence, they mainly modify, directly or indirectly, the cell cycle. Anticancer agents may act as cytostatic or cytotoxic drugs. Cytostatic drugs stop the cancer cells proliferation, by inhibiting signaling pathways related to processes as cancer growth, angiogenesis, invasion and metastasis. For example the current therapies include: receptor antagonists, antigrowth factors antibodies, small tyrosine kinase inhibitors and anti-receptor monoclonal antibodies [19].

Conversely, cytotoxic agents target rapidly proliferating cells, as cancer cells, leading to cell death. These represent most of anticancer drugs and, according to their main mechanism of action, they can be divided into:

- alkylating agents, which react with DNA, chemically modifying its structure;
- antimetabolites, which inhibits DNA and RNA synthesis;
- topoisomerase inhibitors, which interfere with the correct DNA unwinding during replication and transcription;

- microtubular poisons, which hamper the polymerization and depolymerization of tubulin, thus inhibiting mitosis;
- cytotoxic antibiotics, which exert anticancer effects by several mechanisms, such as DNA intercalation and over production of reactive oxygen species (ROS) [20].

Nowadays, immunostimulating- and targeted-therapies are considered among the most promising strategies to get high therapeutic antitumor effects with mild systemic toxicity. However, traditional chemotherapy is still one of the treatments of choice for several highly aggressive cancers. Most of such chemotherapeutic schedules consist of the so-called combination therapy (*i.e.* the administration of two or more additive, or better synergistic, drugs together). In order to improve patient compliance, the different drugs are usually incorporated into the same formulation. However, this is not a simple task because of pharmacokinetic differences between drugs; moreover, possible interactions between the individual components can occur. Thus, a more effective strategy to reach such a goal may involve the preparation of a single drug containing different agents, reversibly bonded, also called “combo” [21].

# *1.5 Platinum-based anticancer drugs*

## *1.5.1 History of cisplatin*

Cisplatin, *cis*-diamminedichloridoplatinum(II), is a square-planar complex of Pt(II) coordinated to two chloride ligands (leaving groups) and two ammine ligands (carrier groups). The prefix *cis* indicate the geometry of this complex, where two identical ligands are on the same side with respect to the metal, differentiating this from its *trans* isomer (Figure 1.6).

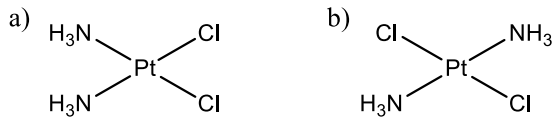


Figure 1.6: Geometric isomers of diamminedichloridoplatinum(II). a) Cisplatin and b) Transplatin.

Cisplatin was synthesized for the first time in 1845 by Michele Peyrone, and, therefore, it was known as Peyrone's chloride since the end of the nineteenth century. Then Alfred Werner elucidated its chemical structure for the first time in 1893. However, its anticancer properties were serendipitously discovered in 1965 by the physicist Barnett Rosenberg at the Michigan State University, during the investigation of the role of electric or magnetic field in *Escherichia Coli* cell division. He observed an inhibition of cell division, not due to the electric field, but to the complexes produced by the electrolysis from the platinum electrodes in contact with a growth medium containing ammonium chloride. Among the possible species, the *cis*-isomer of $[Pt^{II}Cl_2(NH_3)_2]$, *i.e* cisplatin, was identified as the major bioactive species. The results suggested that, since this molecule was able to stop bacterial cell growth, it might be active also against proliferation of cancer cells. As a result, in 1968 cisplatin showed the ability to cause a strong tumor regression when

administered intraperitoneally to mice bearing sarcoma-180 [22] [23]. After further *in vivo* tests, this compound entered clinical trials and the first patient was treated in 1971. However cisplatin was approved by the Food and Drug Administration (FDA) as anticancer agents in 1978. Since then, cisplatin was employed for the treatment of a wide range of solid tumors, including bladder, head and neck, lung, ovarian and testicular cancers (in this case cure rates have overcome 95%) [24].
The *trans* isomer is much less active than the *cis* homologue and so it is not used as an anticancer agent.

## *1.5.2 Cisplatin mechanism of action*

Cisplatin is administered to patients by intravenous infusion over a period of six to eight hours. In the bloodstream the compound does not undergo appreciable aquation reaction (hydrolysis) due to the high concentration of chloride ions (about 100 mM), although cisplatin can react with plasmatic proteins, as human serum albumin, and extracellular enzymes.
The molecular mechanism by which cisplatin enters cells is not completely clarified yet. Being a neutral molecule with moderate molecular weight, cisplatin can cross the cell membrane by passive diffusion, although active transporters, like copper transporter-1 (Ctr1), and organic cationic transporters (OCT), are also involved in cisplatin uptake [25] [26].
Once inside the cytoplasm, where the concentration of chloride ions drops to 2-10 mM, cisplatin undergoes aquation reaction with the replacement of one (monoaqua species) or two (diaqua species) chlorido groups with water molecules. The rate of the aquation of the first chloride ion at 37°C is $7 \times 10^{-3}$ $min^{-1}$ (half-life time is about 120 min) while the substitution of the second chloride ligand is two times slower [27].
Once inside the cell, cisplatin interacts with different biomolecules but its main pharmacological target is the DNA. The mono- and di-aqua species, positively

charged, represent the active forms of the complex and covalently bind to nucleophilic sites on the DNA strand. In particular platinum binds nitrogen in position 7 (N7) of the imidazole ring of the purine bases, preferentially guanine (G) and, to a lesser extent, adenine (A). Cisplatin is able to form monofunctional or bifunctional adducts. The most frequent lesions occur on the same DNA strand and are known as intrastrand adducts, involving adjacent bases as GpG 1,2 intrastrand (60-65% of DNA binding) and ApG 1,2 intrastrand (20-25%). Other binding modes, produced on the same strand, includes GpXpG 1,3 intrastrand crosslink, involving a third nucleotide X between the two platinated guanines (2%) and monofunctional adducts on guanines (2%). Finally, approximately 2% of adducts occur on opposite DNA strand (G-G "interstrand crosslinks"). These adducts cause severe distortions in the structure of the DNA, including unwinding and bending, thus preventing DNA replication and transcription [28] (Figure 1.7).

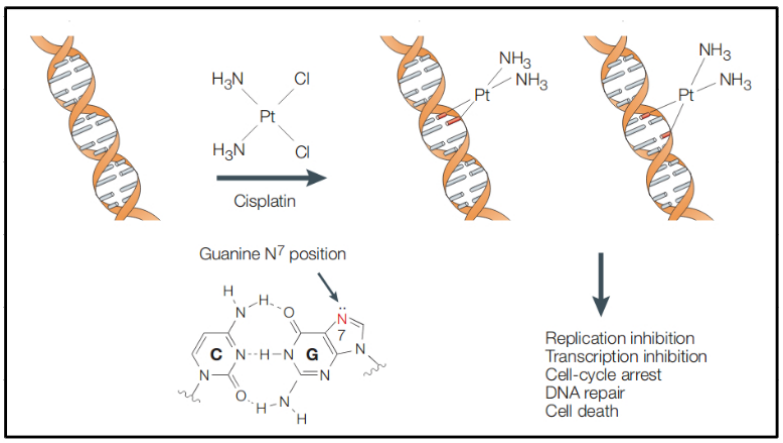


Figure 1.7: Formation and effects of cisplatin-DNA adducts. The picture is a modification of that reported in literature [29].

Cisplatin-induced DNA damage leads to cell cycle arrest in G2 phase and activation of DNA repair pathways, as nucleotide excision repair (NER), mismatch repair (MMR) and DNA-dependent protein kinase (DNA PK). Among these, NER is the main system known to remove cisplatin lesions from DNA and it is involved in repair

of intrastrand Pt-DNA crosslinks. Also the high-mobility group (HMG) proteins, a family of non-histone chromatin-associated proteins, are able to identify and bind Pt-DNA adducts, particularly 1-2 intrastrand crosslinks, but these elements have a controversial role. Indeed, on the one hand they are implicated in repair efforts, but on the other hand they may interfere with the activity of DNA repair enzyme, allowing the damage to persist.

The failure of the DNA-repair ability of the cells and the consequently persistence of DNA-adducts activate cell death pathways. Especially, cells treated with high concentrations of the drug show a necrotic-like phenotype, while an apoptotic one occurs after exposition to (and the pharmacologically optimal) lower concentrations. Cisplatin-induced DNA damage activates several proteins, including ATM and ATR sensor kinases, p21 and p53, leading to intrinsic apoptosis. Also the extrinsic apoptotic pathway may be activated [30].

Cisplatin also stresses different cellular organelles, including mitochondria, endoplasmic reticulum (ER) and lysosomes. In addition to genomic DNA, the platinum complex can bind mitochondrial DNA (mtDNA) with high efficiency, inducing characteristic mitochondrial alterations which lead to the activation of the intrinsic apoptotic pathway, due to the low efficiency of mtDNA repair. Moreover, the drug causes calcium-dependent mitochondrial swelling and depolarization, calcium release and decrease in NAD(P)H levels [31]. The mitochondrial permeabilization is also linked to ROS overproduction; at the same time cisplatin inhibits antioxidant enzymes, such as catalase, superoxide dismutase (SOD), glutathione peroxidase, glutathione S-transferase and glutathione reductase, leading to mitochondrial and cellular oxidative stress.

Furthermore, cisplatin induces the activation of ER stress pathways, due to deregulation of calcium homeostasis and accumulation of misfolded protein, which may lead to apoptosis [30]. Lysosomal alterations and injuries are also involved in cell death; cisplatin treatment results in lysosomal membrane permeabilization and

consequently release in the cytosol of proteases of the cathepsin family, which are involved in the activation of apoptotic pathways [32].

Additionally, cisplatin interacts with plasma membrane phospholipids, inducing plasmalemma destabilization and changes in fluidity, alterations in cholesterol metabolism and FAS receptor aggregation and stimulation, which activates the extrinsic pathway of apoptosis [33].

Finally, as already mentioned above, cisplatin is able to react with different peptides and polypeptides, including endogenous nucleophiles containing sulphur functionalities, such as methionine, cysteine-rich proteins as metallothioneins and reduced glutathione (GSH). However this tripeptide seems to have a controversial role toward the cytotoxicity of cisplatin. Indeed, on the one hand GSH is involved in cisplatin detoxification, but on the other hand the platinum-GSH conjugate has been shown to interfere with transcription factors, leading to the arrest of the protein synthesis. Moreover the GSH depletion alters the redox state of the cells, increasing the levels of ROS.

The formation of the Pt-DNA adducts may also interfere with the activity of DNA polymerase, preventing the DNA recognition by this enzyme. Otherwise cisplatin might directly bind the enzyme, causing its structural changes or loss of active sites [34].

## *1.5.3 Cisplatin side effects and chemoresistance*

The antitumor activity of cisplatin is associated to severe dose-limiting toxicities. Among these, nephrotoxicity represents one of the major side effects during chemotherapy. Indeed, about 20% of patients treated with high dose of cisplatin show serious renal injury and most of them experience kidney dysfunction shortly after initial administration. The pathophysiological phenomena involved in this kind of toxicity include induction of renal vasoconstriction, sequentially reduction in renal plasma flow, decrease of glomerular filtration rate and alterations of serum

creatinine, as well as of potassium and magnesium levels, which may lead to a permanent kidney dysfunction. The cisplatin-induced nephrotoxicity is mainly related to a high uptake of the platinum complex by the proximal tubular cells, due to a high renal expression of OCT2. Then, the renal injury may spread from this site to other tubular areas, such as collecting and distal tubules. However, this side effect can be largely controlled by administration of diuretics and adequate pre-hydration of the patients [35].

Also peripheral neurotoxicity is associated with cisplatin treatment. Early effects include tingling, numbness, or paresthesia and a reduction of distal vibratory sensitivity, while long term treatment may affect proprioception. The pathophysiology of this phenomenon is not completely elucidated, but it is known that the dorsal root ganglia (DRG) and peripheral neurons are the main target of the drug [36].

Another common type of cisplatin-related side effect is ototoxicity, due to injury of outer hair cells of the cochlea in the inner ear, causing functional deficits as hearing loss [37].

Moreover, hepatotoxicity, cardiotoxicity and disorders of the gastrointestinal tract (controlled by additional therapies with antiemetics) may be related to cisplatin treatment [38].

In addition to this plethora of toxicities, the clinical use of cisplatin is limited by induction of chemoresistance, which can be inherent, when the drug is inefficient from the initial treatment, or acquired, if the drug is effective at the beginning of the therapy but it loses activity over time. Resistance to cisplatin is considered a multifactorial event (Figure 1.8), which may be described as:

1) pre-target resistance: it involves processes that precede the interaction between cisplatin and its target, hampering DNA binding. This kind of chemoresistance consists of reduced influx or increased efflux or both, leading to a minor cellular accumulation of cisplatin. Thus, it includes alterations in functionality, expression level or subcellular localization of

Ctr1, which play an important role in cisplatin uptake, or of copper P-type adenosine triphosphate transporters (ATP7A and ATP7B), which significantly mediate the drug extrusion. Other plasma membrane transporters, like multidrug resistance-associated protein 2 (MRP2) and phospholipid transporting ATPase 11B (ATP11B), participate to cisplatin efflux, hence promoting this kind of chemoresistance. Moreover, pre-target resistance is ascribed to increased levels of cytoplasmic scavenger containing thiols, like GSH and metallothioneins, which contribute to drug sequestration and inactivation;

2) on-target resistance: it is directly related to cisplatin-induced molecular damage. The response of cancer cells to cisplatin is limited by the presence of an efficient DNA repair system. Thus, components of NER and MMR machinery are implicated in cisplatin resistance.
3) post-target resistance: it is ascribed to defects in the cell death signaling pathways triggered by molecular lesions caused by cisplatin. Indeed, resistance is associated with p53 mutations but also with alterations in many other pro-apoptotic factors, as mitogen-activated protein kinase 14 (MAPK14 or p38) and c-Jun N-terminal kinase 1 (JNK1), leading to a defective apoptosis. This process is also significantly affected by changes in the expression levels and functionality of BCL-2 family proteins and caspases;
4) off-target resistance: it involves the activation of compensatory survival signals, but not directly triggered by cisplatin. For example, *v-erb-b2* avian erythroblastic leukemia viral oncogene homolog 2 (ERBB2) overexpression seems to sustain cisplatin resistance in ovarian and breast carcinomas, delivering strong pro-survival signals through the *v-akt* murine thymoma viral oncogene homolog 1 (AKT1) axis, and regulating cell cycle arrest that is necessary for the repair of cisplatin-induce DNA damage. Moreover, Y-phosphorylation-regulated kinase 1B (DYRK1B) has been suggested to

promote resistance by favoring the expression of several antioxidants enzymes. Finally, various unspecific adaptive stress responses, like macroautophagy and HSPs activity, are also implicated in cisplatin resistance [39].

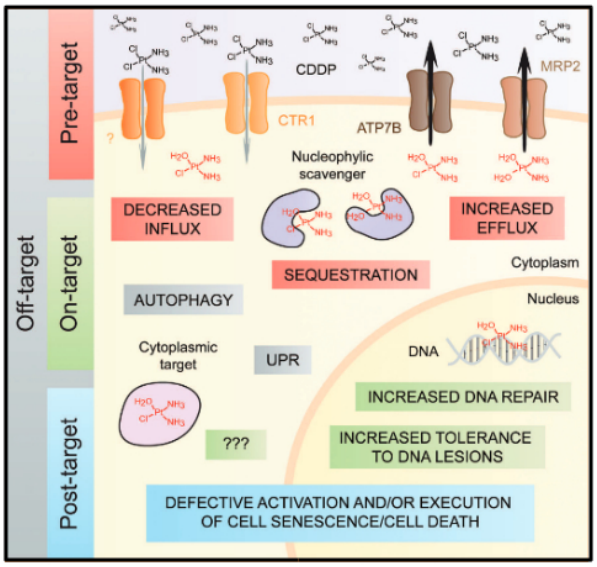


Figure 1.8: Molecular mechanisms of cisplatin chemoresistance. The picture is a modification of that reported in literature [39].

### *1.5.4 Second and third generation of platinum anticancer drugs*

Although cisplatin is a very effective anticancer drug, its benefits are limited by a panel of severe side effects and by inherent and acquired resistance. Thus, the research has moved toward the development of less toxic analogues without affecting success in cancer treatment. These efforts have led to the discovery of a second generation platinum complex, carboplatin, *cis*-diammine(1,1′-cyclobutanedicarboxylato)platinum(II), which was approved by FDA in 1989. Compared to cisplatin, this drug contains the same carrier groups, so it forms the same adducts on DNA after acquation, maintaining the same efficacy. However, the

replacement of the chloride leaving groups with a cyclobutanedicarboxylate makes carboplatin about hundred times more inert to hydrolysis reactions, allowing the compound to have a higher life time. As a consequence, the presence of a more stable ligand has contributed to reduction of nephro-, neuro- and gastrointestinal tract toxicity. By contrast, myelosuppression (especially thrombocytopenia) and anemia are dose-limiting for carboplatin [28].

Later, oxaliplatin, *cis*-(1R,2R-cyclohexanediammine)oxalatoplatinum(II), a third generation of Pt(II) compound, has proved to be effective in treatment of intrinsic platinum-resistant tumor, as colorectal cancer. The different pharmacological activity is ascribed to the modification of the carrier groups: 1R,2R-diaminocyclohexane (1R,2R-DACH) replaces the two monodentate ammine ligands of cisplatin. Moreover MMR system and HMG domain proteins recognize less efficiently oxaliplatin-induced DNA adducts. Oxaliplatin treatment is frequently associated with neutropenia, but the most common dose limiting toxicity is represented by a purely sensory peripheral neuropathy. This complex became the third platinum drug approved by FDA in 2002 [28].

Cisplatin, carboplatin and oxaliplatin are employed worldwide. On the contrary, the approval of other Pt(II)-based compounds is locally restricted: lobaplatin (1,2-di(aminomethyl)cyclobutane)lactatoplatinum(II) approved in China, nedaplatin (cis-diammineglycolatoplatinum(II)) in Japan, and heptaplatin *cis*-malonato[(4R,5R)]-4,5-bis(aminomethyl)-2-isopropyl-1,3-dioxolane] platinum(II) in Korea [40] (Figure 1.9).

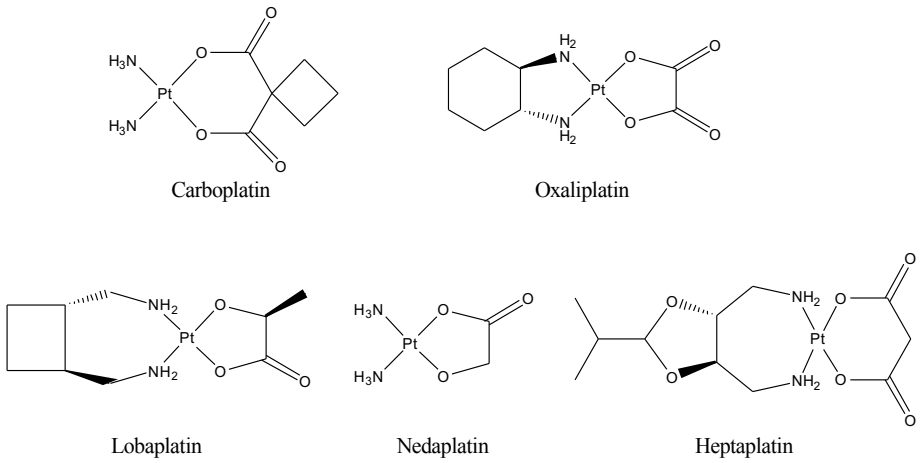


Figure 1.9: Main platinum complexes of second and third generation.

In order to overcome cisplatin inactivation by thiol containing species, like GSH and metallothioneins, a new Pt(II)-based complex providing a steric bulk around the platinum core, known as picoplatin, was designed (Figure 1.10). Its efficacy against a wide range of cisplatin- and oxaliplatin-resistant tumor has been investigated, and it has been considered a promising drug candidate for small cell lung cancer therapy. However, unfortunately, it seems not to have a considerable antitumor activity. Clinical studies with picoplatin have shown dose-limiting side effects similar to those of carboplatin, including thrombocytopenia and neutropenia, but no marked neurotoxicity and nephrotoxicity have been observed [41].

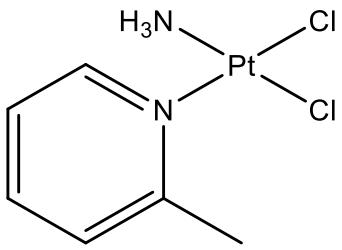

Figure 1.10: Picoplatin.

## *1.5.5 Platinum(IV) prodrugs*

Nowadays, about 50% of all chemotherapy regimens, include a platinum drug. Despite their success in cancer treatment, Pt(II)-based compounds show two main limitations: a panel of severe side effects and the induction of chemoresistance.

Moreover all platinum drugs used in clinic are intravenously administrated, via debilitating perfusion cycles, as their oral administration is hampered by acute emesis, toxicity to gastrointestinal tract and poor bioavailability. Thus, a large amount of Pt(II) complexes is lost before arriving at their final target, due to protein bindings in the bloodstream, giving rise to undesirable side reactions [42].

One strategy to overcome Pt(II) complexes limits is the use of Pt(IV) compounds. They have coordination number 6 associated to an octahedral geometry, so they are quite inert to substitution, and consequently amenable to oral administration, improving patients compliance.

Their inertness increase their lifetime in the bloodstream and so the chances of reaching the tumor target intact. Indeed, Pt(IV) agents act as prodrugs, because they are activated by reduction in hypoxic conditions, typical of cancer microenvironment, by intracellular reducing agents, such as GSH, ascorbic acid, cytochrome c and other bioreductants. Pt(IV) complexes release, upon reduction, the corresponding cytotoxic square-planar Pt(II) drug and two axial ligands, which may be identical or different [43] (Figure 1.11).

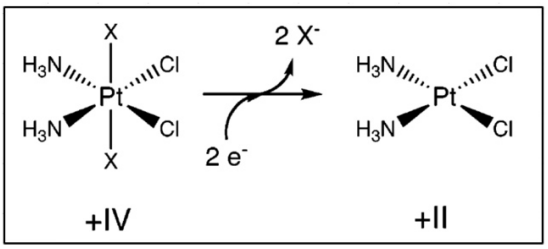


Figure 1.11: The so called "activation by reduction" of the inert octahedral Pt(IV) prodrug to square planar Pt(II) compound, with loss of the axial ligands X. The picture is a modification of that reported in literature [42].

The choice of the six ligands (axial and equatorial) around the Pt(IV) core allows to modulate the pharmacokinetic profile of these prodrugs, which is related to two critical parameters: lipophilicity and the rate of reduction. The former affects the capacity to enter cancer cells by passive diffusion and the absorption by the gastro-intestinal tract, whereas the latter refers to the kinetic of the reduction in biological conditions [44].

Up to now, some Pt(IV) compounds reached clinical trials. The most studied are tetraplatin, iproplatin and satraplatin (JM216) (Figure 1.12).

Tetraplatin (or $[PtCl_4(DACH)]$, where DACH is 1R,2R-diminocyclohexane) and iproplatin (JM9 or *cis,trans,cis*-$[PtCl_2(ipa)_2OH_2]$, where ipa is isopropylamine) were abandoned, due to a severe neurotoxicity induced by the former and the minor efficacy than cisplatin exhibited by the latter [45].

Satraplatin (JM126 or *cis,trans,cis*-$[Pt(c\text{-}C_6H_{11}NH_2)Cl_2(NH_2)(OCOCH_3)_2]$) is still undergoing clinical trials. It was evaluated in phase III in combination with prednisone for hormone refractory prostate cancer treatment. This Pt(IV) prodrug exhibits a milder toxicity and the advantage of its possible oral administration, compared to cisplatin [46].

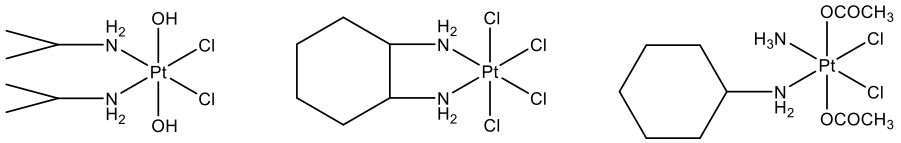


Iproplatin Tetraplatin Satraplatin

Figure 1.12: The most studied Pt(IV) compounds.

Moreover suitable axial ligands can be carefully selected to improve the pharmacological properties of the Pt(IV) complexes, as active tumor targeting agents. These ligands may selectively bind to receptors on the surface of cancer cells. However, some proteins, as essential nutrient receptors required for tumor growth,

are overexpressed in cancer cells, but are not specific for them, providing only a pseudo-active targeting. Alternatively, the targeting of other receptors, which may be unique to cancer cell, represents a very selective drug delivery method.

Furthermore Pt(IV) complexes can be bound to different macromolecules, or nanoparticles, including micelles and liposomes, polymers, carbon nanotubes and other delivery systems. Such passive drug targeting formulations exploit the enhanced permeability and retention (EPR) effect, in order to better target tumor tissue. This effect is due to the rapid growth of solid tumors, which show large fenestrations between the endothelial cells of blood vessels and an absent or inefficient lymphatic drainage. The combination of these two phenomena allows the tumor to trap and retain circulating macromolecules [47].

Finally, bioactive molecules *per se* (enzyme inhibitors, epigenetic agents or complementary anticancer drugs), can be coordinated to the Pt(IV) core, resulting in a synergistic activity with Pt(II) drug. Thus, the resulting Pt(IV) species can act on multiple targets with higher potency and fewer side effects compared to single-target drugs, being considered multi-action agents (combo) [44]. Since different mechanisms of action have been pointed out in studies about pharmacological activity, toxicity and chemoresistance of cisplatin, this drug itself may be regarded as a multi-target drug. Indeed, although genomic DNA is considered as its main cellular target, several other interactions with cisplatin are suggested by multiple disciplines, as previously described.

Moreover, Pt(IV) complexes are more or less potent oxidizing agents *per se*, which can alter the cellular redox homeostasis, increasing the ROS level and reducing the mitochondrial membrane potential. This creates a vicious cycle, inducing oxidative stress, which concurs to bringing cells to apoptosis. As previously reported, also cisplatin itself, albeit to a lesser extent, can generate ROS. This effect is especially evident for Pt(IV) compounds bearing efficient ROS-amplifying modulators. This may be a further advantage, since cancer cells are more sensitive to oxidative stress, having a higher basal level of ROS compared to their healthy counterparts [48] [49].

# *References*

[1] YA. Fouad, C. Aanei. Revisiting the hallmarks of cancer. *Am J Cancer Res* (2017) 7(5), 1016-1036.

[2] SM. Afify, M. Seno. Conversion of Stem Cells to Cancer Stem Cells: Undercurrent of Cancer Initiation. *Cancers* (2019) 11, 345.

[3] P. Csermely, T. Korcsmáros, R. Nussinov. Intracellular and intercellular signaling networks in cancer initiation, development and precision anti-cancer therapy: RAS acts as contextual signaling hub. *Semin Cell Dev Biol* (2016) 58, 55-9.

[4] G. Stracquadanio, X. Wang, MD. Wallace, AM. Grawenda, P. Zhang, J. Hewitt, J. Zeron-Medina, F. Castro-Giner, IP. Tomlinson, CR. Goding, KJ. Cygan, WG. Fairbrother, LF. Thomas, P. Saetrom, F. Gemignani, S. Landi, B. Schuster-Böckler, DA. Bell, GL. Bond. The importance of p53 pathway genetics in inherited and somatic cancer genomes. *Nat Rev Cancer* (2016) 16(4), 251-65.

[5] FA. Dick, SM. Rubin. Molecular mechanisms underlying RB protein function. *Nat Rev Mol Cell Biol* (2013) 14(5), 297-306.

[6] B. Alberts, A. Johnson, J. Lewis, et al. Molecular Biology of the Cell. 4th edition. New York: Garland Science, (2002).

[7] LH. Hartwell, TA. Weinert. Checkpoints: controls that ensure the order of cell cycle events. *Science* (1989) 246, 629 – 634.

[8] L. Galluzzi, I. Vitale, et al. Molecular mechanisms of cell death: recommendations of the Nomenclature Committee on Cell Death 2018. *Cell Death Differ* (2018) 25(3), 486–541.

[9] H. Wu, X. Che, Q. Zheng, A. Wu, K. Pan, A. Shao, Q. Wu, J. Zhang, Y. Hong. Caspases: a molecular switch node in the crosstalk between autophagy and apoptosis. *Int J Biol Sci* (2014) 10(9), 1072-83.

[10] JL. Koff, S. Ramachandiran, L. Bernal-Mizrachi. A time to kill: targeting apoptosis in cancer. *Int J Mol Sci* (2015) 16(2), 2942-55.

[11] A. Ashkenazi. Directing cancer cells to self-destruct with pro-apoptotic receptor agonists. *Nat Rev Drug Discov* (2008) 7(12), 1001-12.

[12] L. Lin, EH. Baehrecke. Autophagy, cell death, and cancer. *Mol Cell Oncol* (2015) 2(3), e985913.

[13] MA. Lynch-Da, DJ. Klionsky. The Cvt pathway as a model for selective autophagy. *FEBS Lett* (2010) 584(7), 1359-66.

[14] TT. Wu, WM. Li, YM. Yao. Interactions between Autophagy and Inhibitory Cytokines. *Int J Biol Sci* (2016) 12(7), 884-97.

[15] WW. Li, J. Li, JK. Bao. Microautophagy: lesser-known self-eating. *Cell Mol Life Sci* (2012) 69(7), 1125-36.

[16] AM. Cuervo, E. Wong. Chaperone-mediated autophagy: roles in disease and aging. *Cell Res* (2014) 24(1), 92-104.

[17] L. Galluzzi, MC. Maiuri, I. Vitale, H. Zischka, M. Castedo, L. Zitvogel, G. Kroemer. Cell death modalities: classification and pathophysiological implications. *Cell Death Differ* (2007) 14(7), 1237-43.

[18] A. Ediriwickrema, WM. Saltzman. Nanotherapy for Cancer: Targeting and Multifunctionality in the Future of Cancer Therapies. *ACS Biomater Sci Eng* (2015) 1(2), 64-78.

[19] NJ. Serkova, SG. Eckhardt. Metabolic Imaging to Assess Treatment Response to Cytotoxic and Cytostatic Agents. *Front Oncol* (2016) 6, 152.

[20] L. Galluzzi, A. Buqué, O. Kepp, L. Zitvogel, G. Kroemer. Immunological Effects of Conventional Chemotherapy and Targeted Anticancer Agents. *Cancer Cell* (2015) 28(6), 690-714.

[21] M. Ravera, E. Gabano, MJ. McGlinchey, D. Osella. A view on multi-action Pt(IV) antitumor prodrugs. *Inorg Chim Acta* (2019) 492, 32-47.

[22] B. Rosenberg, L. VanCamp, T. Krigas. Inhibition of cell division in *Escherichia coli* by electrolysis products from a platinum electrode. *Nature* (1965) 205, 698–699.

[23] B. Rosenberg, L. VanCamp, JE Trosko, VH. Mansour. Platinum compounds: a new class of potent antitumour agents. *Nature* (1969) 222, 385–386.

[24] M Galanski. Recent developments in the field of anticancer platinum complexes. *Recent Pat Anticancer Drug Discov* (2006) 1, 285–295.

[25] S. Ishida, J. Lee, D. J. Thiele, I. Herskowitz, Uptake of the anticancer drug cisplatin mediated by the copper transporter Ctr1 in yeast and mammals. *Proc Natl Acad Sci USA* (2002) 99, 14298–14302.

[26] MD. Hall, M. Okabe, DW. Shen, XJ. Liang, MM. Gottesman. The role of cellular accumulation in determining sensitivity to platinum-based chemotherapy. *Annu Rev Pharmacol Toxicol* (2008) 48, 495-535.

[27] RJ. Knox, F. Friedlos, DA. Lydall, JJ. Roberts. Mechanism of cytotoxicity of anticancer platinum drugs: evidence that cis-diamminedichloroplatinum(II) and cis-diammine-(1,1-cyclobutanedicarboxylato)platinum(II) differ only in the kinetics of their interaction with DNA. *Cancer Res* (1986) 46 (4 Pt 2), 1972-1979.

[28] L. Kelland. The resurgence of platinum-based cancer chemotherapy. *Nat Rev Cancer* (2007) 7(8), 573-584.

[29] D. Wang, SJ. Lippard. Cellular processing of platinum anticancer drugs. *Nat Rev Drug Discov* (2005) 4(4), 307-20.

[30] SM. Sancho-Martínez, L. Prieto-García, M. Prieto, JM López-Novoa, FJ. López-Hernández. Subcellular targets of cisplatin cytotoxicity: an integrated view. *Pharmacol Ther* (2012) 136(1), 35-55.

[31] Z. Yang, LM. Schumaker, MJ. Egorin, EG. Zuhowski, Z. Guo, KJ. Cullen. Cisplatin preferentially binds mitochondrial DNA and voltage-dependent anion channel protein in the mitochondrial membrane of head and neck squamous cell carcinoma: possible role in apoptosis. *Clin Cancer Res* (2006) 12(19), 5817-25.

[32] H. Appelqvist, P. Wäste, K. Kågedal, K. Öllinger. The lysosome: from waste bag to potential therapeutic target. *J Mol Cell Biol* (2013) 5(4), 214-26.

[33] S. Lacour, A. Hammann, S. Grazide, D. Lagadic-Gossmann, A. Athias, O. Sergen, G. Laurent, P. Gambert, E. Solary, MT. Dimanche-Boitrel. Cisplatin-induced CD95 redistribution into membrane lipid rafts of HT29 human colon cancer cells. *Cancer Res* (2004) 64(10), 3593-8.

[34] RN. Bose. Biomolecular targets for platinum antitumor drugs. *Mini Rev Med Chem* (2002) 2(2), 103-11.

[35] X. Yao, K. Panichpisal, N. Kurtzman, K. Nugent. Cisplatin nephrotoxicity: a review. *Am J Med Sci* (2007) 334(2), 115-24.

[36] A. Avan, TJ. Postma, C. Ceresa, A. Avan, G. Cavaletti, E. Giovannetti, GJ. Peters. Platinum-induced neurotoxicity and preventive strategies: past, present, and future, *The Oncologist* (2015) 20(4), 411-32.

[37] LP. Rybak, CA. Whitworth, D. Mukherjea, V. Ramkumar. Mechanisms of cisplatin-induced ototoxicity and prevention. *Hear Res* (2007) 226(1-2), 157-67.

[38] JT. Hartmann, HP. Lipp. Toxicity of platinum compounds. *Expert Opin Pharmacother* (2003) 4(6), 889-901.

[39] L. Galluzzi, I. Vitale, J. Michels, C. Brenner, G. Szabadkai, A. Harel-Bellan, M. Castedo, G. Kroemer. Systems biology of cisplatin resistance: past, present and future. *Cell Death Dis* (2014) 5, e1257.

[40] NJ. Wheate, S. Walker, GE. Craig, R. Oun. The status of platinum anticancer drugs in the clinic and in clinical trials. *Dalton Trans* (2010) 39(35), 8113-27.

[41] BA. Chan, JI. Coward. Chemotherapy advances in small-cell lung cancer. *J Thorac Dis* (2013) 5 Suppl 5, S565-78.

[42] MD. Hall, HR. Mellor, R. Callaghan, TW. Hambley. Basis for design and development of platinum(IV) anticancer complexes. *J Med Chem* (2007) 50(15), 3403-11.

[43] TC. Johnstone, K. Suntharalingam, SJ. Lippard. The Next Generation of Platinum Drugs: Targeted Pt(II) Agents, Nanoparticle Delivery, and Pt(IV) Prodrugs. *Chem Rev* (2016) 116(5), 3436-86.

[44] E. Gabano, M. Ravera, D. Osella. Pros and cons of bifunctional platinum(IV) antitumor prodrugs: two are (not always) better than one. *Dalton Trans* (2014) 43(26):9813-20.

[45] MR. Reithofer, AK. Bytzek, SM. Valiahdi, CR. Kowol, M. Groessl, CG. Hartinger, MA. Jakupec, M. Galanski, BK. Keppler. Tuning of lipophilicity and

cytotoxic potency by structural variation of anticancer platinum(IV) complexes. *J Inorg Biochem* (2011) 105(1), 46-51.

[46] S. Akshintala, L. Marcus, KE. Warren, RF. Murphy, TM. Sissung, A. Srivastava, WJ. Goodspeed, A. Goodwin, CC. Brewer, C. Zalewski, KA. King, A. Kim, WD. Figg, BC. Widemann. Phase 1 trial and pharmacokinetic study of the oral platinum analog satraplatin in children and young adults with refractory solid tumors including brain tumors. *Pediatr Blood Cancer* (2015) 62(4), 603-10.

[47] MG. Apps, EH. Choi, NJ. Wheate. The state-of-play and future of platinum drugs. *Endocr Relat Cancer* (2015) 22(4), R219-33.

[48] D. Tolan, V. Gandin, L. Morrison, A. El-Nahas, C. Marzano, D. Montagner, A. Erxleben. Oxidative stress induced by Pt(IV) pro-drugs based on the cisplatin scaffold and indole carboxylic acids in axial position. *Sci Rep* 6 (2016) 29367.

[49] V. Reshetnikov, A. Arkhypov, P.R. Julakanti, A. Mokhir. A cancer specific oxaliplatin-releasing Pt(IV)-prodrug. *Dalton Trans* 47 (2018) 6679–6682.

# *Chapter 2*

## *Outline of the thesis*

Nowadays cancer remains one of the major causes of death. In the field of the anticancer therapy, the FDA approved Pt(II)-based drugs, cisplatin, carboplatin and oxaliplatin, play an important role. They are DNA-damaging chemotherapeutic agents used worldwide, especially in combination therapy, being administered in 50% of chemotherapeutic regimens in the clinic. However, the antitumor activity of Pt(II) drugs is limited by severe systemic toxicity, induction of inherent or acquired chemoresistance, and poor water solubility and pharmacokinetic profile. The opportunity to overcome some of these limits is offered by octahedral Pt(IV)-based complexes. They are quite inert to substitution and reach intact cancer cells, minimizing the side effects and the off-target reactions typical of the more reactive Pt(II) counterparts. Indeed, Pt(IV) agents act as prodrugs, since they are reduced in the hypoxic cancer *milieu* to the corresponding cytotoxic Pt(II) metabolite (the so-called activation by reduction) with the simultaneous release of two ligands from the axial positions. Thus, suitable axial ligands can be carefully selected to improve the pharmacological properties of such Pt(IV) complexes. Additionally, these ligands can also be bioactive molecules *per se*, providing a synergistic or adjuvant activity with that of the Pt(II) drugs, hence the resulting Pt(IV) conjugates could be considered dual- or multi-action agents, with a great advantage in the combinatory approach.

The aim of this Ph.D. work is focused on the evaluation of the biological properties of several newly designed, synthetized and characterized bifunctional, or better multifunctional, Pt(IV) prodrug candidates.

In particular, the anticancer activity of such molecules has been investigated as reported below.

1) Cisplatin-based Pt(IV) complexes containing the histone deacetylase inhibitor 2-(2-propynyl)octanoate (POA):
   - *In vitro* studies of the antiproliferative activity, cellular accumulation, DNA platination, and epigenetic activity on human cancer cell lines with different sensitivity.
   - Evaluation of the *in vivo* activity of this multi-action prodrug in a model of solid tumor (murine Lewis lung carcinoma).
2) Pt(IV) complexes based on the oxaliplatin-analogue *cis*-dichlorido(cyclohexane-1R,2R-diamine)platinum(II) (or [$PtCl_2$(dach)]) and containing POA:
   - Evaluation of *in vitro* activity (antiproliferative activity, cellular uptake and epigenetic properties) on human and mouse colon cancer cell lines.
   - The *in vivo* activity of this compound was investigated on a pool of immunocompetent BALB/c mice bearing the highly aggressive syngeneic CT26 mouse colon carcinoma. Particularly, this part of the work is focused on the study of immunogenic cell death induction.
3) Comparisons of two series of asymmetric Pt(IV) complexes, cisplatin- or dach-based, containing the bioactive axial MCFA ligands clofibrate (2-(*p*-chlorophenoxy)-2-methyl- propionic acid, or heptanoate or octanoate:
   - Investigation of the *in vitro* biological properties of couples of complexes. In order to demonstrate the selectivity towards human colon cancer cell lines conferred by the dach carrier ligand, the antiproliferative activity, as well as the cellular uptake, of the two series of Pt(IV) complexes was evaluated.
   - Moreover, the long-term effects of the Pt(IV) treatment were studied on 3D multicellular tumor models, known as spheroids, which more accurately resemble the conditions of *in vivo* tumor tissue.

4) Cisplatin-based Pt(IV) complexes containing Non-Steroidal Anti-inflammatory Drugs (NSAIDs), ketoprofen or naproxen, acting as inhibitors of both cyclooxygenases, COX-1 and COX-2:

- Evaluation of the *in vitro* biological activity on a panel of human cancer cell lines. Particularly, antiproliferative activity, synergism between cisplatin and NSAIDs, cellular accumulation and modulation of the expression of NSAIDs target genes were studied.

# *Chapter 3*

# *Unsymmetric cisplatin-based Pt(IV) derivative containing a novel Histone DeACetylase inhibitor (HDACi): a very efficient multi-action antitumor prodrug candidate*

## *3.1 Introduction*

In order to increase antitumor efficacy of chemotherapy, usually, clinicians combine the FDA approved Pt(II) drugs with adjuvant agents. As previously mentioned (Chapter 1), the Pt(IV) derivatives are ideally suited for such a combination therapy since bioactive molecules can be coordinated as axial ligands in the octahedral assembly of the complexes, generating an ideally synergistic anticancer action when released along with the Pt(II) drug upon reduction [1].

There is growing interest in the co-administration of cisplatin with Histone DeACetylase inhibitors (HDACi) [2] [3]. They increase the acetylation level of histones (especially of their lysine residues) in chromatin, thus weakening the histone-DNA interactions and exposing nuclear DNA to the action of DNA-damaging chemotherapeutics as cisplatin. These features enhance tumor growth suppression and induce apoptosis [4] [5]. Moreover, HDACi, being epigenetic agents, alter in the meantime the expression of several genes, thus affecting the cell fate. In particular, HDACi can modulate *inter alia* the expression and functions of

DNA-repair proteins, further increasing the persistence and efficacy of the Pt-DNA adducts [6] [7].

HDACi consist of two main chemical families: hydroxamic acids (*e.g.* suberoylanilide hydroxamic acid, SAHA or Vorinostat) and medium-chain fatty acids (MCFAs) or, more precisely (at physiological pH), their corresponding anions. Unfortunately, the highly effective SAHA requires heavy chemical modifications to coordinate the metal core [8]. On the contrary, MCFAs (*e.g.* 2-propylpentanoate or valproate, VPA, clinically employed as anticonvulsant agent, and phenylbutyrate, PhB, orphan drug used to treat urea cycle disorders) [9] [10], have been easily conjugated to the metal core *via* "esterification" reaction of hydroxido Pt(IV) synthons [11] [12]. These derivatives, based on the square-plane arrangement of cisplatin or oxaliplatin and containing one or two MCFA molecules linked in axial position, have been actively studied in the context of the antitumor dual-, or better multi-action, strategy [13].

The biological properties of a new cisplatin-based Pt(IV) prodrug, containing an inert acetato and the bioactive 2-(2-propynyl)octanoato (POA) as axial ligands (**1**) are here reported. Indeed, it has been demonstrated that POA is more potent than VPA in inducing histone hyperacetylation in cerebellar granule cells, and in exhibiting antiproliferative and neurotrophic activity [14]. Since POA is a chiral molecule, the activity of the racemate (**1**), as well as that of the corresponding isomers (**1R** and **1S**), was investigated and compared to that of cisplatin and of compound **2**, a cisplatin-based Pt(IV) complex with two VPA molecules as axial ligands (Figure 3.1).

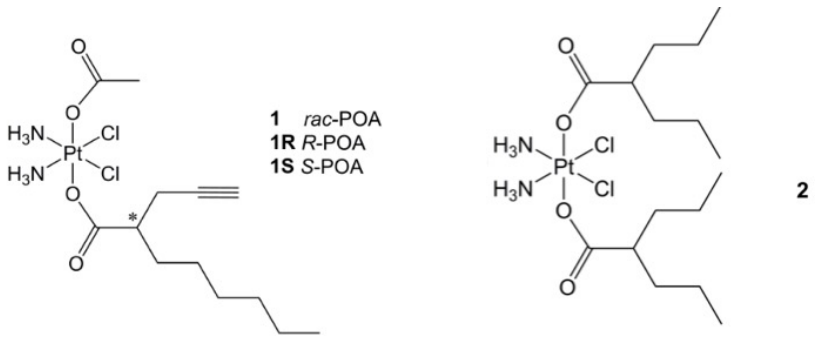


Figure 3.1: Sketch of the Pt(IV) complexes under investigation.

# *3.2 Material and methods*

## *3.2.1 Cell culture*

Human cancer cell lines were purchased from European Collection of Cell Cultures (ECACC, UK) or Interlab Cell Line Collection (ICLC, Genova, Italy): ovarian endometrioid adenocarcinoma A2780 (ICLC HTL98008), colon carcinoma HCT 116 (ECACC 91091005), breast ductal carcinoma MCF-7 (ECACC 86012803), embryonal carcinoma of the testis NTERA-2 clone D1 (also known as NT2/D1, ICLC HTL97025), and lung adenocarcinoma A549 (ICLC HTL03001). A2780 and A549 cells were grown in RPMI 1640, whereas McCoy's 5A was used for HCT 116, Dulbecco's Modified Eagle's Medium (DMEM) for NT2/D1, and Minimum Essential Medium (MEM) supplemented with non-essential amino acids for MCF-7. All media were supplemented with L-glutamine (2 mM), penicillin 100 IU $mL^{-1}$, streptomycin (100 mg $L^{-1}$) and 10% heat inactivated fetal bovine serum (FBS). Media and supplements were purchased by Sigma-Aldrich or Life Technologies.
Cell culture and treatment were carried out at 37 °C in a 5% $CO_2$ humidified chamber.

## *3.2.2 Compounds and drug candidates*

The Pt(IV) complexes under investigation were designed, synthetized and characterized in Prof. Osella's bioinorganic laboratory (University of Piemonte Orientale, Dipartimento di Scienze e Innovazione Tecnologica (DiSIT), Italy). In particular, the starting material cisplatin was oxidized with hydrogen peroxide in water or acetic acid to get di- or mono-hydroxido intermediates. These synthons reacted with the HDACi molecules through substitution of one or both their carboxylic groups [15] (Scheme 1).

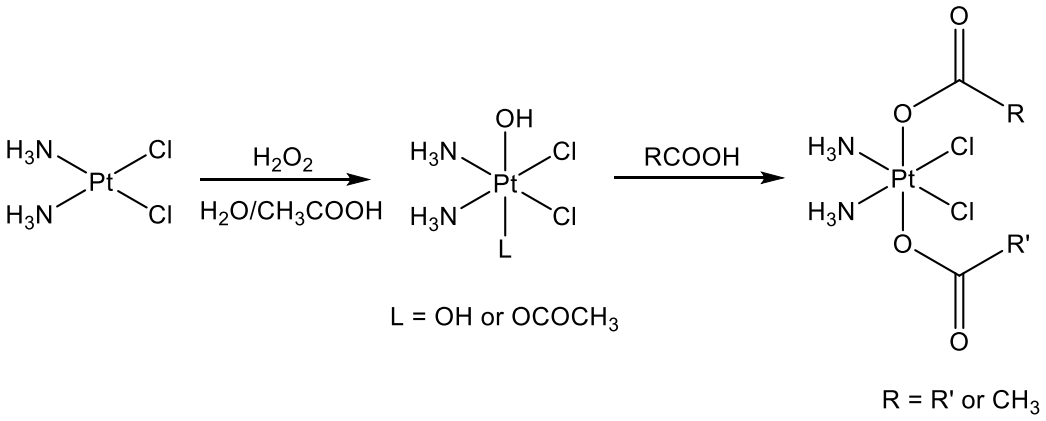


Scheme 1: Synthetic pathway for the synthesis of compounds **1** and **2**.

In order to prepare the stock solutions of the complexes under investigation for the following biological tests, cisplatin (Sigma-Aldrich) was dissolved in 0.9% w/v NaCl aqueous solution brought to pH = 3 with HCl (final stock concentration 1 mM), whereas the Pt(IV) complexes were dissolved in ethanol (final stock concentration 5 mM) and stored at -18 °C. The stock concentrations were checked by means of ICP-OES measurements. The mother solutions were diluted in complete medium to the required concentration range and, where present, the total co-solvent concentration never exceeded 0.2% (this concentration was found to be non-toxic to the cells tested). A commercial racemic mixture of POA (stock concentration 4.8 M) was

purchased by Tokyo Chemical Industry (TCI), whereas VPA (Sigma-Aldrich) was freshly dissolved in 0.9% w/v NaCl aqueous solution (final stock concentration 1 M).

## *3.2.3 Antiproliferative activity*

To assess the growth inhibition of the compounds under investigation, a cell viability test, *i.e.* the resazurin reduction assay was used [16] (Scheme 2). Briefly, $2\times10^3$/well cells were seeded in black sterile tissue-culture treated 96-well plates. At the end of the treatment, viability was assayed by 100 µg $mL^{-1}$ resazurin (Acros Chemicals, France) in fresh medium for 1 h at 37 °C, and the amount of the reduced product, resorufin, was measured by means of fluorescence, measured at excitation 535 nm and emission 595 nm with a Tecan Infinite F200Pro plate reader (Tecan Austria). In each experiment, the cells were challenged with the drug candidates at different concentrations and the final data were calculated from at least three replicates of the same experiment carried out in triplicate. The fluorescence intensities of 8 wells containing medium without cells were used as blank. Data were normalized to 100% cell viability for non-treated cells. Half inhibiting concentration ($IC_{50}$), defined as the concentration of the drug reducing cell viability by 50%, was obtained from the dose-response sigmoid using Origin Pro (version 8, Microcal Software, Inc., Northampton, MA, USA).

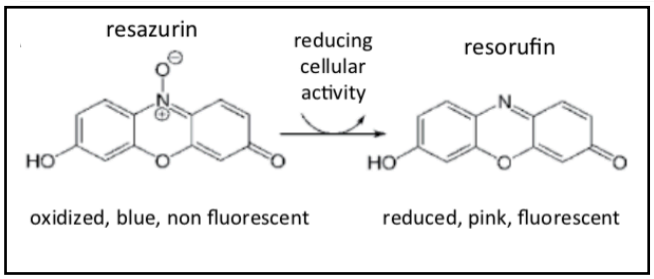


Scheme 2: Reduction of resazurin (blue, non-fluorescent) by metabolically active cells to resorufin (pink, fluorescent). The picture is a modification of that reported in literature [17].

## *3.2.4 Cellular accumulation and DNA platination*

Around $80\times10^3$ A2780 cells were seeded in 10 mm Petri dishes and treated with the complexes under investigations (1 μM for **1** and 10 μM for cisplatin) with the following schedules: 4 h CT, 24 h CT, or 4 h CT followed by 20 h R (4 h CT+20 h R), where CT is continuous treatment and R is recovery. At the end of the exposure, cells were washed three times with phosphate buffered saline (PBS), detached from the Petri dishes using 0.05% Trypsin 1X + 2% EDTA (HyClone, Thermo Fisher) and harvested in fresh complete medium. An automatic cell counting device (Countess®, Life Technologies) was used to measure the number and the mean diameter from every cell count. From the same sample, about $5\times10^6$ cells were taken out for cellular accumulation analysis, while about $20\times10^6$ cells were taken out for the DNA platination analysis. Moreover, 100 μL of medium were taken out from each sample at time zero to check the extracellular Pt concentration.

For the cellular Pt accumulation analysis, the cells were transferred into a borosilicate glass tube and centrifuged at 1100 rpm for 5 min at room temperature. The supernatant was carefully removed by aspiration, while about 200 μL of the supernatant were left in order to limit the cellular loss. Cellular pellets were stored at -80 °C until mineralization.

The measurement of the Pt content was performed by ICP-MS (Thermo Optek X Series 2). Instrumental settings were optimized in order to yield maximum sensitivity for platinum. For quantitative measurements, the most abundant isotopes of platinum and indium (used as internal standard) were measured at *m/z* 195 and 115, respectively. Mineralization was performed by addition of 70% w/w $HNO_3$ to each sample (after defrosting), followed by incubation for 1 h at 60 °C in an ultrasonic bath. Before the ICP-MS measurement, the $HNO_3$ was diluted to a final 1% concentration.

The cellular Pt accumulation was referred as ng Pt per $10^6$ cells. In order to obtain the Pt cellular concentration, the total cellular volume of each sample was obtained considering the mean cell diameter and cell number.

For the DNA platination analysis, the cells were transferred into a plastic tube and centrifuged at 1100 rpm for 5 min at room temperature. The supernatant was carefully removed by aspiration, and the cell pellets were stored at -20 °C until the total genomic DNA was extracted with a commercial kit (PerfectPure Cultured Mammalian Cells, 5Prime- Eppendorf), following the manufacturer's instructions. Briefly, during cell lysis, DNA was purified by RNAse A and proteinase K treatment, then extracted on silica-based centrifugation columns. After washing, DNA was eluted in 300 μL of elution buffer. An amount of 8 μL of sample or elution buffer (used as blank) were diluted in TE buffer (10 mM Tris-HCl, 1 mM EDTA, pH 8.0) to 80 μL, corresponding to 0.5 cm path length in UV-transparent microplates half-area wells (UV-Star®, Greiner Bio-one). Absorbance at 260 nm ($A_{260}$, relative to nucleic acids) and 280 nm ($A_{280}$, relative to proteins) were recorded from triplicate wells with a Tecan Infinite F200Pro plate reader (Tecan, Austria). For each well, $A_{260}$ and $A_{280}$ were corrected by subtraction of the background, then the purity of the samples was verified by means of the $A_{260}$ to $A_{280}$ ratio, which always resulted > 2. After the subtraction of mean $A_{260}$ of blank wells, the DNA concentration was computed from the corrected $A_{260}$ by means of a calibration curve obtained with calf thymus DNA. Under these conditions an absorbance of 1 unit at 260 nm corresponds to 100 μg of DNA per mL. The remaining amount of DNA elution buffer was transferred into a borosilicate glass tube and its precise volume measured by means of weight to compute the total amount of DNA, then stored at -20 °C until mineralization. Mineralization and Pt content determination were performed as above reported for the whole cells.

The level of Pt found in cells after drug treatment and normalized upon the cell number (cellular Pt accumulation or uptake) was expressed as ng Pt per $10^6$ cells.

This parameter considers only the intracellular concentration, without taking into account the extracellular one.

$$Cellular\ Pt\ uptake = \frac{ng\ Pt}{10^6\ cells}$$

Thus, a more correct way to indicate an effective accumulation is represented by the "accumulation ratio", AR: this value is the ratio between the intracellular Pt concentration ($[Pt]_{IC}$) and the extracellular one ($[Pt]_{EC}$) [18]. The mean cellular volume, calculated from the actual mean cell diameter measured for every sample, was used to obtain the cellular Pt concentration.

$$AR = \frac{[Pt]_{IC}}{[Pt]_{EC}}$$

Regarding DNA platination, the amount of Pt bound to DNA (experimental $P_{DNA}$) was expressed as pg of Pt per μg of DNA experimentally found [19].

## *3.2.5 HDAC assay*

A2780 cells ($50\times10^3$/well) were seeded into a transparent-bottomed, black 96-wells TC plate the day before treatment. Complexes were given at equitoxic concentrations (*i.e.* 5 mM POA and VPA; 1 μM cisplatin, **1**, **1R**, **1S**, and **2**) at that time point for 24 h. The total HDAC activity was measured by means of a commercial kit (HDAC cell-based activity assay kit, Cayman Chemical) following manufacturer's instructions. Fluorescence data were recorded at excitation λ = 360 nm, emission λ = 465 nm over a 15 min period. After blank subtraction, data were normalized on internal controls, *i.e.* the sample in the presence of trichostatin A. HDAC fold activity was rescaled on the non-treated control.

## *3.2.6 Chromatin staining*

$2\times10^5$ A2780 cells were seeded on Nunc™ Lab-Tek™ 4-chamber slides and allowed to attach for 24 h. The treatment was performed with 1 μM complex **1** or cisplatin, or 5 mM POA. After 4 h, the medium was replaced with the staining solution, consisting of 5 ng $mL^{-1}$ Hoechst 33342 in Earle's Balanced Salt solution (EBSS). Cells were incubated in the dark for 5 minutes, washed threefold with EBSS and immediately observed using a standard DAPI filter set (at 350/461 nm Exc/Em) of a fluorescence microscope (Zeiss Axiolab), equipped with a digital camera (Nikon digital Sights, DS-U3). Pictures were taken at 10× magnification.

## *3.2.7 Quantitative PCR (RT-qPCR)*

A2780 cells ($2\times10^6$) were seeded on T25 flasks and allowed to attach for 24 h. The treatment was performed in triplicate with 1 μM solutions of complex **1** or cisplatin, or a 5 mM solution of POA. After 24 h, RNA was extracted with a commercial kit (GenElute Mammalian Total RNA Miniprep Kit, Sigma-Aldrich), then it was quantified and checked for purity by means of absorbance at $\lambda$ = 260, 280, and 340 nm in UV-Star half area UV transparent plate (Brand) with the above-mentioned microplate reader. For each sample, 1 μg of RNA was retrotranscribed to cDNA with the Revertaid cDNA First strand kit (Thermo Fisher) using random hexamer primers at 42 °C, following the manufacturer's instructions. RT-qPCR was performed in triplicate on each sample to detect the expression levels of p53, p21, Cyclin D1, E, and A1, and COX-2, and the housekeeping genes RNA18S, HPRT1, GAPDH. Primer sequences were designed using the NCBI tool and checked for target specificity including splice variants. Reactions were based on the SsoFast EvaGreen Supermix (Bio-Rad) in the presence of 0.4 μM primer pairs except for RNA18S (0.2 μM), according to the manufacturer's instructions, in a reaction volume of 10 μL. In order to compute reaction efficiency, a standard curve was performed for each master

mix. RT-qPCR was performed in triplicate using and the CFX368 thermal cycler (Bio-Rad). The reaction conditions were 95 °C for 1 min, followed by 45 cycles at 98 °C for 5 s and anneal-extend step for 5 s at 60 °C, with data collection. At the end of these cycles, a melting curve (65 °C to 95 °C, with plate read every 0.5 °C) was performed in order to assess the specificity of the amplification product by single peak melting temperature verification. Results were normalized on the reference genes and on the control according to the ΔCq and ΔΔCq method, respectively [20]. All data analyses were performed with the built-in software (CFX Manager, Bio-Rad).

| Gene | Accession n. | Forward | Reverse | Product length (bp) |
|---|---|---|---|---|
| Cyclin D1 (CCND1) | NM_053056.2 | TGAGGGACGCTTTGTCTGTC | GCCTTTGGCCTCTCGATACA | 75 |
| p21 (CDKN1A) | NG_009364 | GCGACTGTGATGCGCTAATG | GAAGGTAGAGCTTGGGCAGG | 141 |
| COX-2 | M90100.1 | CCCTGAGCATCTACGGTTTG | CATCGCATACTCTGTTGTGTTC | 107 |
| Cyclin A2 (CCNA2) | NM_001237.4 | TGGTGGTCTGTGTTCTGTGA | TGCCAGTCTTACTCATAGCTGA | 136 |
| Cyclin E (CCNE) | NM_001238 | GCAGGATCCAGATGAAGAAATG | TAATCCGAGGCTTGCACGTT | 173 |
| GAPDH | NG_007073.2 | ATCCCTGAGCTGAACGGGAA | GGCAGGTTTTTCTAGACGGC | 99 |
| HPRT1 | NM_000194.2 | TTGCTTTCCTTGGTCAGGCA | ATCCAACACTTCGTGGGGTC | 85 |
| TP53 | NG_017013.2 | GCCCCTCCTCAGCATCTTATC | CTCATAGGGCACCACCACAC | 99 |
| RNA18SN1 | NR_145820.1 | CGTCTGCCCTATCAACTTTCG | TGCCTTCCTTGGATGTGGTAG | 124 |

Table 1: Analysis of relative gene expression data using RT-qPCR. The NCBI accession number is reported along with the 5'-3' sequence of the forward and reverse primer and the expected product length.

## *3.2.8 Caspase 3/7 activity*

A2780 cells ($2\times10^4$) were seeded in 96-well tissue culture (TC) plates in complete medium, the day before treatment and then challenged with Pt complexes (1 μM) and MCFAs (5 mM) concentrations. After 24 h cells were washed with PBS and then lysed with 25 μL of lysis buffer (10 mM HEPES, 2 mM EDTA, 2 mM DTT, 0.1 % CHAPS, pH 7.4). The caspase 3/7 inhibitor N-Acetyl-Asp-Glu-Val-Asp-CHO (Ac-DEVD-CHO, final concentration 0.01 g $L^{-1}$) (Sigma-Aldrich) was added to control wells. Then, 200 μL of the caspase 3/7 fluorescent substrate N-Acetyl-Asp-Glu-Val-Asp-7-amido-4-trifluoromethylcoumarin (Ac-DEVD-AFC, 0.01 g $L^{-1}$ in lysis buffer) (Sigma-Aldrich) was added to all the wells and mixed. A volume of 200 μL of each sample was transferred to a black microtiter plate and the activity was followed for 1 h by means of fluorescence at excitation $\lambda = 390$ nm, emission $\lambda = 520$ nm, normalized *vs.* the blank. Data were normalized to residual viability and final fold activity (with respect to control wells) was calculated as the mean of at least three independent replicates performed in duplicate for each condition.

## *3.2.9 Experiments with animals*

All studies involving animal testing were carried out in accordance with the ethical guidelines for animal research adopted by the University of Padua, acknowledging the Italian regulation (D.L.G.S. 116/92) and European Directive 86/609/EEC as to the animal welfare and protection and the related codes of practice. The experimental protocol was approved by the Italian Health Department according to the art. 7 of above mentioned D.L.G.S. 116/92. The mice were purchased from Charles River (Italy), housed in steel cages under controlled environmental conditions (constant temperature, humidity, and 12 h dark/light cycle), and alimented with commercial standard feed and tap water *ad libitum*.

## *3.2.10* In vivo *antitumor activity*

Lewis Lung Carcinoma (LLC) cell line was purchased from ECACC (U.K.) and maintained in DMEM (Euroclone) supplemented with 10% heat-inactivated fetal bovine serum (FBS; Euroclone), 10 mM L-glutamine, 100 U $mL^{-1}$ penicillin, and 100 μg $mL^{-1}$ streptomycin in a 5% $CO_2$ air incubator at 37 °C. The LLC was implanted intramuscularly (i.m.) as a $2\times10^6$ cell inoculum into the right hind leg of 8-week old male and female C57BL mice (24 ± 3 g body weight). After 24 h from tumor implantation, mice were randomly divided into five groups (8 animals per group, 10 controls) and treated orally with a single daily dose of Pt(IV) complexes (20 mg $kg^{-1}$ dissolved in a vehicle solution composed of Cremophor EL 20% v/v, PEG400 20% v/v, and saline solution 60% v/v) or with a daily intraperitoneal (i.p.) dose of cisplatin (1.5 mg $kg^{-1}$ in 0.9% w/v NaCl solution) from day 7 after tumor inoculation (visible tumor). At day 15, animals were sacrificed, the legs were amputated at the proximal end of the femur, and the inhibition of tumor growth was evaluated based on the difference in weight of the tumor-bearing leg and the healthy leg of the animals expressed as a percentage referred to the control animals. Body weight was measured every two days and was taken as a parameter for systemic toxicity. All the values are the means ± SD of not less than three measurements.

For Biodistribution studies, C57BL mice were inoculated i.m. into the right flank with LLC cells ($2\times10^6$). After 9 days from tumor implantation, **1** and **2** were administered orally (by gavage) at a dose of 20 mg $kg^{-1}$. After 1 and 4 h, blood samples were collected and subsequently animals were sacrificed. Tumor, lung, kidney, intestine and liver were excised. Tissues were washed in ice-cold saline and weighed after removing excess fluid. All samples were mineralized in $HNO_3$ and Pt content in each sample was measured by graphite furnace-atomic adsorption spectroscopy (GF-AAS).

### 3.2.11 Statistical analysis

Data are expressed as mean ± standard deviation of at least three experiments performed in triplicate and compared with a one-way ANOVA-Tukey test, even when not expressly indicated. The statistical significance values (p) are referred to control values (* $p<0.05$; ** $p<0.01$; *** $p<0.001$).

## 3.3 Results and discussion

### 3.3.1 Antiproliferative activity

The Pt(IV) compounds **1**, **1R**, and **1S** were tested on five human cell lines with different chemosensitivity: cisplatin highly sensitive ovarian carcinoma A2780 and testicular cancer metastatic cell tumor NT2/D1, moderately sensitive colorectal cancer HCT 116 and lung carcinoma A549, and scarcely sensitive breast adenocarcinoma MCF-7. The free ligands POA and VPA, as well as cisplatin and **2**, were tested as reference compounds. As expected, POA resulted one order of magnitude more active than VPA, albeit both showed only a very modest antiproliferative activity when employed as a single agent. Complexes **1**, **1R** and **1S** exhibited $IC_{50}$ values from the low micro- to the nano-molar range, thus, they are one-two orders of magnitude more active than cisplatin, depending on the chemo-sensitivity of the cell line (Table 2). Surprisingly, the mono-POA derivative **1** showed antiproliferative activities equal or even better than those found for the *bis*-VPA derivative **2** for all the cancer cell lines under study, except MCF-7. Generally, Pt(IV) derivatives having two hydrophobic HDACi molecules, as VPA or PhB, resulted to be more active *in vitro* than their homologues containing only one HDACi molecule [12].

| Compound | $IC_{50}$ (μM) | | | | |
|---|---|---|---|---|---|
| | **A2780** | **NT2/D1** | **A549** | **HCT 116** | **MCF-7** |
| POA | 237 ± 65 | 94 ± 18 | 520 ± 288 | 439 ± 279 | 320 ± 120 |
| VPA | 1833 ± 734 | 1180 ± 120 | 835 ± 516 | 1280 ± 184 | 4800 ± 1131 |
| cisplatin | 0.5 ± 0.1 | 0.10 ± 0.04 | 3.6 ± 0.9 | 2.3 ± 0.3 | 3.3 ± 0.2 |
| **1** | $(8 \pm 1)\times10^{-3}$ | $(4 \pm 1)\times10^{-3}$ | $(129 \pm 44)\times10^{-3}$ | $(29 \pm 12)\times10^{-3}$ | $(474 \pm 56)\times10^{-3}$ |
| **1R** | $(13 \pm 4)\times10^{-3}$ | $(5 \pm 2)\times10^{-3}$ | $(115 \pm 27)\times10^{-3}$ | $(50 \pm 24)\times10^{-3}$ | $(215 \pm 119)\times10^{-3}$ |
| **1S** | $(14 \pm 5)\times10^{-3}$ | $(4 \pm 2)\times10^{-3}$ | $(84 \pm 40)\times10^{-3}$ | $(37 \pm 2)\times10^{-3}$ | $(301 \pm 68)\times10^{-3}$ |
| **2** | $(11.1\pm0.3)\times10^{-3}$ | $(8\pm5)\times10^{-3}$ | $(158 \pm 35)\times10^{-3}$ | $(77 \pm 1)\times10^{-3}$ | $(155 \pm 49)\times10^{-3}$ |

Table 2: Antiproliferative activity ($IC_{50}$) obtained after 72 h of treatment of a panel of cancer cell lines (ovarian carcinoma A2780, testicular cancer metastatic cell tumor NT2/D1, colorectal cancer HCT 116, lung carcinoma A549, and breast adenocarcinoma MCF-7). $IC_{50}$ data are means ± standard deviation of at least three independent replicates.

This suggests the highest HDACi ability of a single molecule of POA, released by **1,** since it is able to offer a contribution to the overall antiproliferative activity similar to that produced by two molecules of VPA, released by **2**. Particularly, the POA contribution appears to be more significant for cisplatin-sensitive cancer cell lines (Figure 3.2).

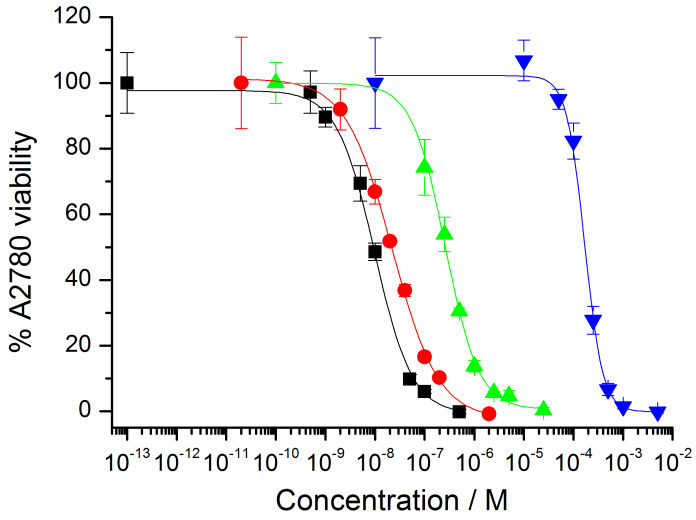


Figure 3.2: Concentration-response curve of A2780 treated for 72h with **1** (black squares and line), **2** (red circle and line), cisplatin (green upward triangles and line), POA (blue downward triangles and line).

Remarkably, the anti-proliferative activity of racemic **1** is similar to those of the enantiomers **1R** and **1S**. Chirality is intrinsically present in the DNA structure, thus, cytotoxic cisplatin analogues containing chiral diamines were reported to produce different conformations of DNA adducts, which, in turn, affect the DNA damage and hence the antitumor activity. The main example is represented by oxaliplatin: the (1*R*, 2*R*)-enantiomer resulted to be more potent and less toxic than its (1*S*, 2*S*) counterpart; indeed the former enantiomer entered the clinical use [21]. In this case, the chirality of the ligand plays a negligible role in the cytotoxicity, which, in principle, is related to the amount and kind of DNA-Pt adducts formed. Actually, the

electrophilic metabolite produced by **1** after reduction (*i.e.* cisplatin) no longer contains the chiral POA molecule.

Since most of the following experiments had to be carried out at shorter time intervals with respect to the $IC_{50}$ evaluation (72 h), an optimal concentration for the compounds under study had to be sought. Such a concentration should maintain an extensive cell viability but, in the meantime, should elicit a measurable cellular response. The concentrations chosen were 1 μM for the all Pt complexes and 5 mM for the free ligands, respectively.

## *3.3.2 Cellular uptake*

Literature data demonstrated that the trafficking of Pt(IV) complexes is unassisted by transport proteins, as Ctr1 as far as the influx is concerned. This seems to confirm the previous view that Pt(IV) complexes are internalized by cells (mainly, if not exclusively) through passive diffusion [22]. However, recent findings suggest that some, still unidentified) active transport mechanisms play a role for the high cellular uptake of selected Pt(IV) complexes having a cisplatin-like core [23]. Moreover, highly lipophilic derivatives containing fatty acids could be delivered to cells by serum albumin and/or by lipoproteins via energy-dependent endocytosis [24].

The cell uptake of **1** was compared with that of **2** and cisplatin by using the accumulation ratio, AR. The AR is the dimensionless ratio between the intra- and extra-cellular Pt concentrations allowing the comparison of the uptake even at different concentrations of drugs, as in the actual case [18].

The AR of **1** was measured after 4 h continuous treatment (CT) followed by 20 h recovery (R) in fresh, drug-free complete medium, and 24 h CT on A2780 ovarian cancer cells. The recovery experiment was planned to highlight any efflux process. The AR of **1** enormously increased from 4 h to 24 h CT and partially dropped when, after 4 h CT, the incubation was prolonged in drug-free medium for additional 20 h (4 h CT + 20 h R) (Figure 3.3 A).

Moreover, the AR values of **1** (21.8±0.6), **1R** (22.3±1.3) and **1S** (22.9±1.4), measured after 4 h CT on A2780, were almost identical within the experimental error, indicating that the two enantiomers were taken up equally by cells.

Since the Pt(IV) derivatives are believed to enter cells by passive diffusion, surprisingly, the AR values of **1** and **2** are very similar (21.8 *vs.* 18.6) [11], pointing out the lack of correlation between lipophilicity, due to the presence of MCFAs molecules as axial ligands, and cellular accumulation.

The DNA platination level (expressed as pg of Pt per μg of DNA, $P_{DNA}$) of complex **1** was also evaluated and compared with that of cisplatin: after a 4 h CT was similar to that obtained from the treatment with cisplatin at tenfold higher concentration (*i.e.* 1 *vs.* 10 μM, respectively). Although the recovery period (20 h) caused a significant ($p < 0.05$) decrease for both complexes, the $P_{DNA}$ of **1** remained higher than that of cisplatin, and the gap hugely increased after a 24 h CT (Figure 3.3 B). So, **1** produced more abundant Pt-DNA adducts than a tenfold cisplatin concentration treatment.

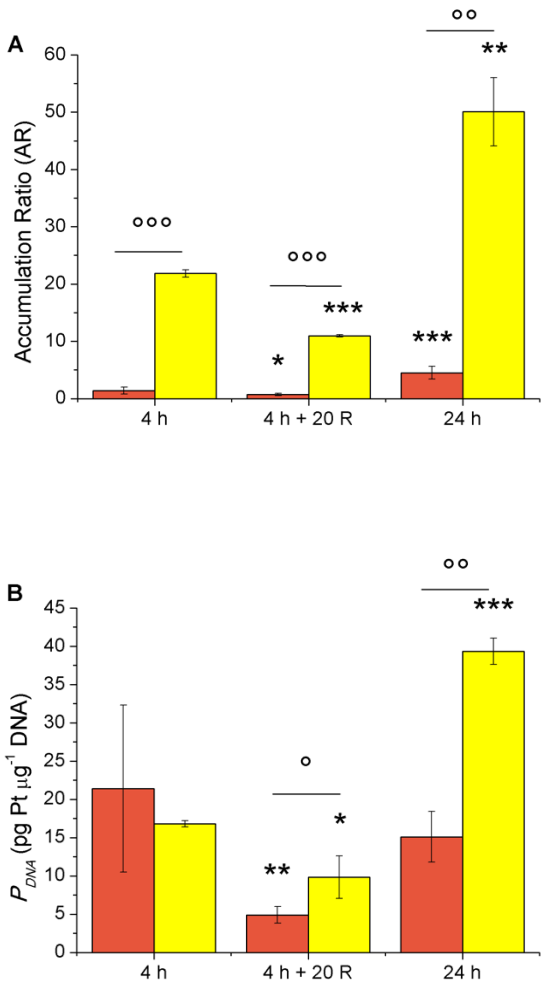


Figure 3.3: (**A**) Accumulation ratio (AR) and (**B**) DNA platination $P_{DNA}$ (pg Pt µg$^{-1}$ DNA) measured on A2780 cells after treatment with cisplatin (10 µM, red bars) and **1** (1 µM, yellow bars) for i) 4h continuous treatment (CT), ii) 4h CT followed by 20h recovery in fresh, drug-free complete medium, and iii) 24h CT. Data are means ± standard deviations of three experiments in triplicate, compared with a one-way ANOVA-Tukey test (* $p<0.05$; ** $p<0.01$; *** $p<0.001$ for the comparison with the data at 4h and 24h; ° $p<0.05$; °° $p<0.01$; °°° $p<0.001$ for the comparison between **1** and cisplatin).

## *3.3.3 Epigenetic activity*

Because of the well-known HDAC inhibition activity of free POA (it induces a strong histone H3 acetylation [14]), a HDAC activity assay on whole cells was performed after 24 h treatment with the drugs under investigation, in order to reveal the average activity of all the HDAC enzymes.

A robust inhibition (around 40%) of HDAC activity following a 24 h treatment with the free MCFAs, POA and VPA (both 5 mM) was observed, whereas the Pt(IV) complexes **1** and **2** (both 1 μM) caused a slight decrease (around 20%). Interestingly, racemic POA and enantiomeric-enriched R-POA and S-POA caused identical HDCA inhibition (within the experimental error). The same trend was found for the corresponding Pt(IV) derivatives, **1**, **1R** and **1S** (Figure 3.4).

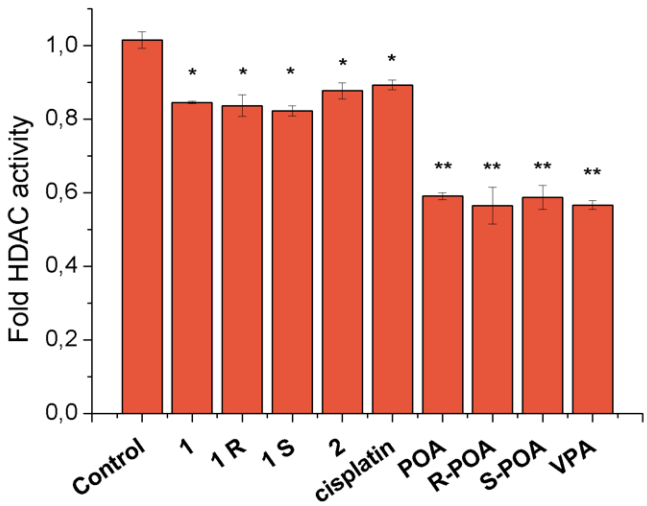


Figure 3.4: Whole cellular HDAC activity in A2780 cells after 24h of treatment with 1 μM cisplatin, **1**, **1R**, **1S**, **2** and 5 mM POA, R-POA, S-POA, VPA. Data are means ± standard deviations of three experiments in triplicate, compared with a one-way ANOVA-Tukey test (* $p<0.05$; ** $p<0.01$).

Despite the relatively modest inhibition of the overall HDAC activity, chromatin decondensation and DNA relaxation were clearly observed by fluorescence microscopy after 4h treatment of A2780 cells with **1** and POA and staining with Hoechst 33342 (Figure 3.5 c and d). On the contrary, the nuclei of cells exposed to cisplatin resulted to be more condensed (pyknotic) (Figure 3.5 b).

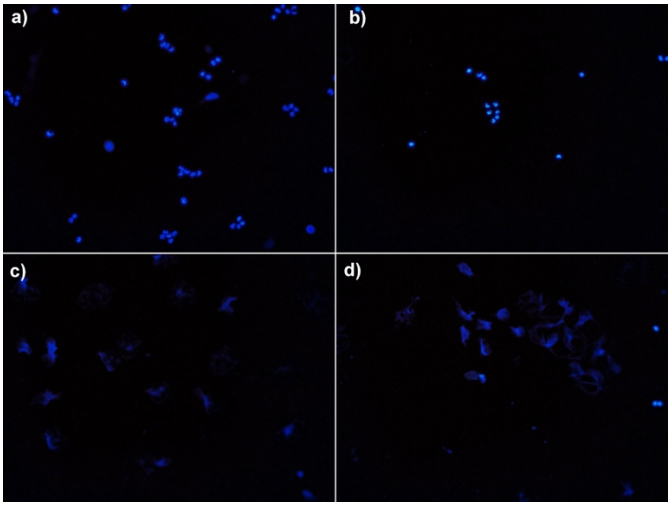


Figure 3.5: Representative pictures of Hoechst 33342 stained A2780 cells after a 4h treatment: a) control; b) cisplatin; c) **1**; d) POA.

In order to better investigate the epigenetic activity of **1**, a quantitative reverse transcription polymerase chain reaction (RT-qPCR) analysis (a powerful method to quantify gene expression) was performed [25]. The experiment was focused on the expression level of a HDACi target genes, in particular cyclooxygenase-2 (COX-2). Cyclooxygenases, COX-1 and COX-2, are the key enzymes in the formation of biological mediators of inflammation, such as prostaglandins, prostacyclin and thromboxane. COX-1 is constitutively expressed in most tissue, whereas COX-2 is induced in response to several intracellular stimuli. Thus, this enzyme plays an important role in inflammation and carcinogenesis. Moreover, it has been demonstrated that COX-2 expression is affected by treatment with HDACi [26]. As

expected, a striking increase of COX-2 was observed after treatment of A2780 with POA (5 mM) along with a significant increase caused by treatment with complex **1** (1 µM). Conversely, cisplatin showed a negligible effect *per se*.

The expression of other genes, mostly related to cisplatin activity, such as p53, p21 and some cyclins, previously mentioned in Chapter 1, were additionally analyzed. A significant gene upregulation was observed for p21 after 24 h treatment with both cisplatin (1 µM) and POA (5 mM), whereas a more pronounced induction was caused by the treatment with **1** (1 µM). This underlines the synergistic activity of **1**, because the upregulation of endogenous inhibitors of cell cycle progression, as p21, is one of the well-recognized mechanisms of HDACi lethality [27]. Interestingly enough, at the concentration (1 µM) and in the time interval (24 h) employed, the expression of p53 was not significantly affected (Figure 3.6).

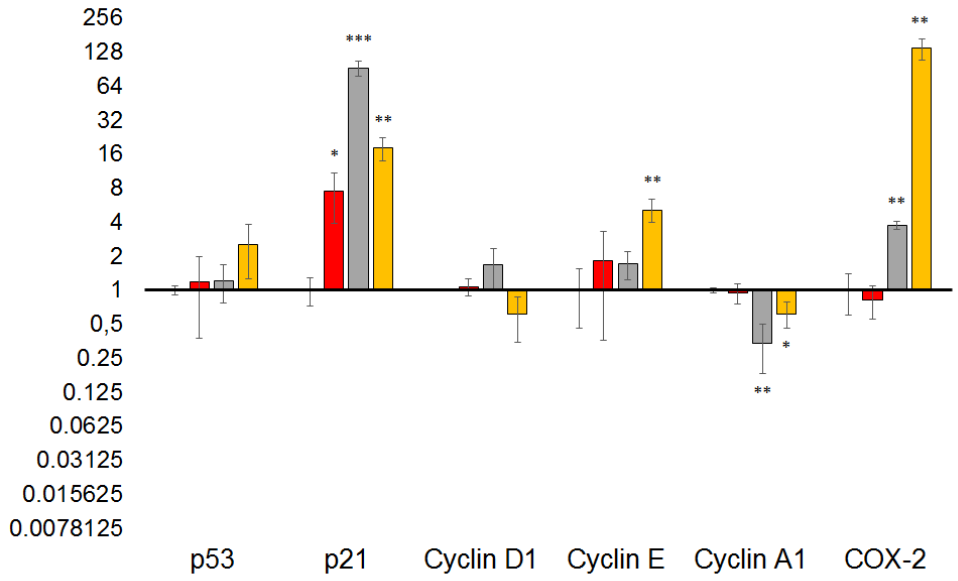


Figure 3.6: Relative expression of target genes after a 24h treatment of A2780 cells with 1 µM cisplatin (red bars), or **1** (grey bars), or 5 mM POA (yellow bars). Data are means ± standard deviations of three experiments in triplicate, compared with a one-way ANOVA-Tukey test (* $p<0.05$; ** $p<0.01$; *** $p<0.001$ with respect to not treated cells).

## *3.3.4 Cell death*

As described above (Chapter 1), the induction of apoptosis is generally related with caspases activation. Thus, the measurement of their activity is a convenient way to investigate whether the cells are undergoing apoptosis concomitant to their growing arrest. Indeed, the activity of caspase 3/7 was evaluated as an apoptosis marker in A2780 cells treated with 1 μM complex **1**, **2**, cisplatin and 5 mM POA, VPA. The ability of activation of caspase 3/7 was in the order: POA > **1** > VPA ≥ **2** ≥ cisplatin (Figure 3.7). Hence the results showed that **1** could cause apoptosis more effectively than cisplatin and **2**.

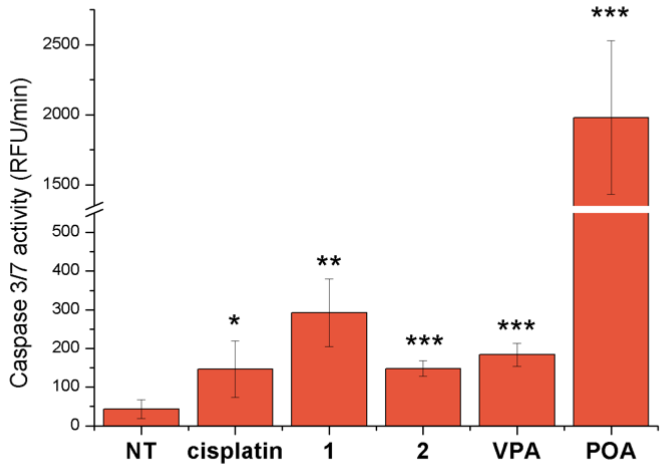


Figure 3.7: Caspase 3/7 activity assessed on A2780 cells after a 24 h treatment with 1 μM cisplatin, **1**, **2** and 5 mM VPA and POA. The activity was normalized on residual viability, and on the control. Data are means ± standard deviations of three experiments in triplicate, compared with a one-way ANOVA-Tukey test (* $p<0.05$; ** $p<0.01$; *** $p<0.001$).

## *3.3.5* In vivo *tumor growth inhibition*

The *in vivo* antitumor activity of **1** was evaluated in a model of solid tumor, the highly aggressive syngeneic murine Lewis Lung Carcinoma (LLC). Tumor growth inhibition induced by **1** was compared with that promoted by cisplatin and **2**. From day 7 after tumor inoculation, when tumors became visible, tumor-bearing mice received daily doses of **1** or **2** (both 20 mg $kg^{-1}$ by oral gavage) or cisplatin (1.5 mg $kg^{-1}$, i.p.). Cisplatin treatment schedule was selected according to standard protocols designed to optimize its efficacy and minimize the occurrence of adverse events. Tumor growth was evaluated at day 15. The results clearly show that complex **1** was able to induce an impressive reduction of the tumor mass (94%) compared to that detected in vehicle-treated animal group ($p < 0.05$), whereas chemotherapy with **2** resulted in a tumor growth inhibition lower (68%) than that promoted by **1**. Instead cisplatin induced a tumor regression of 75% (Table 3).

| **Compound** | **Daily dose [mg $kg^{-1}$]** | **Average tumor weight [g]** | **Inhibition of tumor growth [%]** |
|---|---|---|---|
| Control | 0 | 0.542±0.16 | 0 |
| cisplatin | 1.5 | 0.135±0.09 | 75 |
| **1** | 20 | 0.037±0.02 | 94 |
| **2** | 20 | 0.181±0.08 | 68 |

Table 3: The in vivo antitumor activity of **1**, **2** and cisplatin in LLC xenograft implanted intramuscularly on C57BL mice. From the day 7 to 14 the animals received daily **1** and **2** (orally) and cisplatin (intraperitoneally). At day 15 animals were sacrificed and the inhibition of tumor growth was measured. The values are means ± standard deviations of not less than three measurements.

In addition, for the assessment of the adverse side effects, changes in the body weights of tumor-bearing mice were monitored at day 1 and every two days from day 7. The time course of body weight changes attested that cisplatin induced

elevated anorexia, whereas treatment with **1** and **2** induced only a slight body weight loss (<10%) throughout the therapeutic experiment (Figure 3.8).

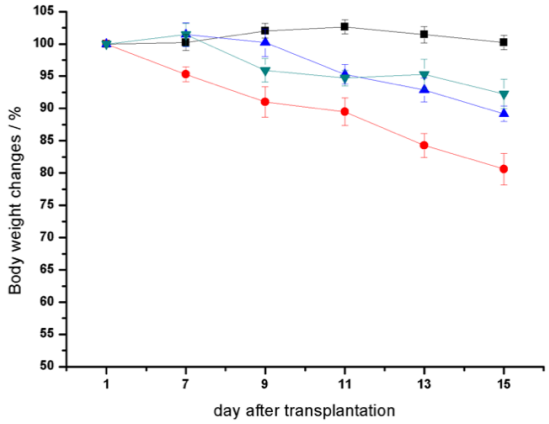


Figure 3.8: Body weight changes of LLC-bearing C57BL mice treated with vehicle (black squares), cisplatin (red circles), **1** (blue upward triangles) and **2** (green downward triangles). Body weight was measured at day 1 and every two days from day 7 and was taken as a parameter of systemic toxicity. Data are means ± standard deviations of three experiments performed in triplicate.

Moreover, blood and tissue samples were collected to estimate the biodistribution properties of **1** and **2** in LLC-bearing mice, after 1 and 4 h following administration of a single oral gavage dose, and analyzed by graphite furnace atomic absorption spectroscopy (GF-AAS).

Platinum concentrations in the whole blood of **1** and **2** treated mice were very similar, about 0.5 μg Pt $mL^{-1}$ and slightly higher in blood of mice exposed to a longer treatment (4 h) (Figure 3.9 A). Also the contents of platinum in tissues of mice treated with both **1** and **2** were similar, and the highest platinum concentrations were found in liver followed by tumor tissue and kidney. Smaller amounts of platinum were detected in intestine and lung. Noteworthy, the results showed that a significant higher platinum content was accumulated into tumor mass of **1**-treated mice with respect to that measured for **2** (Figure

3.9 B). These data show for **1** a more favorable biodistribution profile that well agrees with its superior *in vivo* antitumor efficacy.

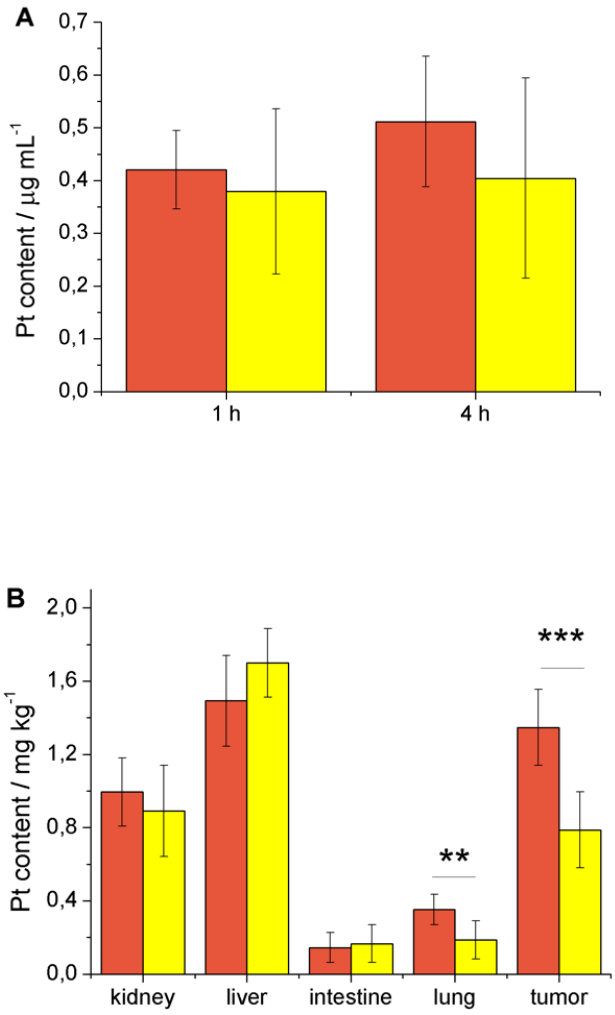


Figure 3.9: Total Pt levels in blood samples (A) or in organs (B) of mice treated with **1** (red columns) and **2** (yellow columns) after single dose oral application. Data are means ± standard deviations of three experiments in triplicate, compared with a one-way ANOVA-Tukey test (* $p<0.05$; ** $p<0.01$; *** $p<0.001$).

## *3.4 Conclusions*

The biological properties of the Pt(IV) antitumor multi-action prodrug **1**, derived from cisplatin and the potent HDACi POA, have been described. They have been compared to that of cisplatin and **2**, a cisplatin-based Pt(IV) complex with two VPA, a well-known HDACi, as axial ligands. Since POA has a chiral center, also the isomers, **1R** and **1S**, of **1** were tested. Compared to **1**, they showed almost identical *in vitro* activity.

The Pt(IV) complex **1**, albeit it contains only one molecule of the HDACi, POA, in axial position, exhibits *in vitro* performances similar or even better to those offered by the Pt(IV) compound **2**, featuring two HDACi (*i.e.* VPA) molecules. Finally, **1** shows also definitely better anticancer activity *in vivo* on LLC-bearing mice than **2** and reference cisplatin, with a more efficient biodistribution.

# *References*

[1] D. Gibson. Platinum(IV) anticancer prodrugs - hypotheses and facts. *Dalton Tran.* (2016) 45, 12983-12991.

[2] M. Bots, R. W. Johnstone. Rational combinations using HDAC inhibitors. *Clin Cancer Res* (2009) 15, 3970-3977.

[3] J. Hrebackova, J. Hrabeta, T. Eckschlager. Valproic acid in the complex therapy of malignant tumors. *Curr Drug Targets* (2010) 11, 361-379.

[4] JE. Bolden, MJ. Peart, RW. Johnstone. Anticancer activities of histone deacetylase inhibitors. *Nat Revi Drug Disc* (2006) 5, 769-784.

[5] M. Buchwald, OH. Kraemer, T. Heinzel, HDACi-targets beyond chromatin. *Cancer Lett* (2009) 280, 160-167.

[6] T. Nikolova, N. Kiweler , OH. Krämer. Interstrand Crosslink Repair as a Target for HDAC Inhibition. *Trend Pharmacol Sci* (2017) 38, 822-836.

[7] KJ. Falkenberg, RW. Johnstone. Histone deacetylases and their inhibitors in cancer, neurological diseases and immune disorders. *Nat Rev Drug Discov* (2014) 13, 673-691.

[8] D. Griffith, MP. Morgan, CJ. Marmion. A novel anti-cancer bifunctional platinum drug candidate with dual DNA binding and histone deacetylase inhibitory activity. *Chem Commun* (2009) (44), 6735-6737.

[9] S. Minucci, PG. Pelicci. Histone deacetylase inhibitors and the promise of epigenetic (and more) treatments for cancer. *Nat Rev Cancer* (2006) 6, 38-51.

[10] M. Manal, MJN. Chandrasekar, J. Gomathi Priya, MJ. Nanjan. Inhibitors of histone deacetylase as antitumor agents: A critical review. *Bioorganic Chemistry*, 2016, 67, 18-42.

[11] M. Alessio, I. Zanellato, I. Bonarrigo, E. Gabano, M. Ravera , D. Osella. Antiproliferative activity of Pt(IV)-bis(carboxylato) conjugates on malignant pleural mesothelioma cells. *J Inor Biochemi* (2013) 129, 52-57.

[12] R. Raveendran, J. P. Braude, E. Wexselblatt, V. Novohradsky, O. Stuchlikova, V. Brabec, V. Gandin and D. Gibson. Pt(IV) derivatives of cisplatin and oxaliplatin with phenylbutyrate axial ligands are potent cytotoxic agents that act by several mechanisms of action. *Chem Sci* (2016) 7, 2381-2391.

[13] V. Novohradsky, L. Zerzankova, J. Stepankova, O. Vrana, R. Raveendran, D. Gibson, J. Kasparkova, V. Brabec. New insights into the molecular and epigenetic effects of antitumor Pt(IV)-valproic acid conjugates in human ovarian cancer cells *Biochemical Pharmacology* (2015) 95, 133-144.

[14] Y. Leng, Z. Marinova, MA. Reis-Fernandes, H. Nau, DM. Chuang. Potent neuroprotective effects of novel structural derivates of valproic acid: potential roles of HDAC inhibition and HSP70 induction. *Neuroscience Lett* (2010) 476, 127-132.

[15] E. Gabano, M. Ravera, I. Zanellato, S. Tinello, A. Gallina, B. Rangone, V. Gandin, C. Marzano, MG. Bottone, D. Osella. An unsymmetric cisplatin-based Pt(IV) derivative containing 2-(2-propynyl)octanoate: a very efficient multi-action antitumor prodrug candidate. *Dalton Trans* (2017) 46(41):14174-14185.

[16] E. Magnani, E. Bettini. Resazurin detection of energy metabolism changes in serum-starved PC12 cells and of neuroprotective agent effect. *Brain Res Protoc* (2000) 5, 266–272.

[17] A. Walzl, C. Unger, N. Kramer, D. Unterleuthner, M. Scherzer, M. Hengstschläger, D. Schwanzer-Pfeiffer, H. Dolznig. The Resazurin Reduction Assay Can Distinguish Cytotoxic from Cytostatic Compounds in Spheroid Screening Assays. *J Biomol Screen* (2014) 19(7), 1047-59.

[18] A. Ghezzi, M. Aceto, C. Cassino, E. Gabano, D. Osella. Uptake of antitumor platinum(II)-complexes by cancer cells, assayed by inductively coupled plasma mass spectrometry (ICP-MS). *J Inorg Biochem* (2004) 98, 73-78.

[19] M. Ravera, E. Gabano, I. Zanellato, I. Bonarrigo, M. Alessio, F. Arnesano, A. Galliani, G. Natile, D. Osella. Cellular trafficking, accumulation and DNA platination of a series of cisplatin-based dicarboxylato Pt(IV) prodrugs *J Inorg Biochem* (2015) 150, 1-8.

[20] KJ. Livak, TD. Schmittgen. Analysis of relative gene expression data using real-time quantitative PCR and the 2^(-ΔΔC) method. *Methods* (2001) 25, 402-408.

[21] J. Malina, C. Hofr, L. Maresca, G. Natile, V. Brabec. DNA interactions of antitumor cisplatin analogs containing enantiomeric amine ligands. *Biophysic J* (2000) 78, 2008-2021.

[22] E. Ratzon, Y. Najajreh, R. Salem, H. Khamaisie, M. Ruthardt, J. Mahajna. Platinum (IV)-fatty acid conjugates overcome inherently and acquired Cisplatin resistant cancer cell lines: an in-vitro study. *BMC Cancer* (2016) 16, 140-150.

[23] S. Goschl, HP. Varbanov, S. Theiner, MA. Jakupec, M. Galanski, BK. Keppler. The role of the equatorial ligands for the redox behavior, mode of cellular accumulation and cytotoxicity of platinum(IV) prodrugs. *J Inorg Biochem* (2016) 160, 264-274.

[24] V. Novohradsky, I. Zanellato, C. Marzano, J. Pracharova, J. Kasparkova, D. Gibson, V. Gandin, D. Osella, V. Brabec. Epigenetic and antitumor effects of platinum (IV)-octanoato conjugates. *Sci Rep* (2017) 7, Article number 3751.

[25] T. Nolan, RE. Hands, SA. Bustin. Quantification of mRNA using real-time RT-PCR. *Nat Protoc* (2006) 1, 1559-1582.

[26] A. Fernandez-Alvarez, C. Llorente-Izquierdo, R. Mayoral, N. Agra, L. Bosca, M. Casado, P. Martin-Sanz. Evaluation of epigenetic modulation of cyclooxygenase-2 as a prognostic marker for hepatocellular carcinoma. *Oncogenesis* (2012) 1, e23.

[27] P. Bose, Y. Dai, S. Grant. Histone deacetylase inhibitor (HDACI) mechanisms of action: emerging insights. *Pharmacology & Therapeutics* (2014) 143, 323-336.

# *Chapter 4*

# *Pt(IV) multifunctional 1R,2R-diamine-based Pt(IV) prodrug containing the novel HDACi, POA: induction of immunogenic cell death on colon cancer*

## *4.1 Introduction*

As previously reported in Chapter 1, the chemistry of Pt(IV) allows to design multifunctional prodrugs. Nowadays, the majority of such Pt(IV) anticancer complexes is based on the cisplatin framework, whereas the oxaliplatin scaffold is less employed. Importantly, in clinic oxaliplatin (Eloxatin™) is used to treat the advanced colorectal cancer (the third most common tumor worldwide) [1], where cisplatin and carboplatin exhibit minor activity [2]. The anticancer effect of oxaliplatin on colon cancer cells is not simply due to the DNA-damaging activity of the Pt-based drug (Chapter 1), but it is also related to the reversion of the immunoescape (one of the hallmarks of cancer, previously reported in Chapter 1). The reversion of the immune evasion mechanism consists in activation of the immune T cells, able to recognize and kill cancer cells. Considering the ability of immune cells to establish a specific immunological memory, T cells activation can ensure a protection against the specific malignant cell transformation and invasion, promoting a long-lasting remission. Therefore, stimulation of the antitumor T cell

immunity is nowadays considered the forefront strategy for the next-generation of anticancer therapies [3] [4].

The dichlorido analogue of oxaliplatin (*i.e.* (*SP*-4-2)-dichlorido(cyclohexane-1*R*,2*R*-diamine)platinum(II), [$PtCl_2$(dach)] (Figure 4.1), might be a good synthon for the design of efficient Pt(IV) combos, specifically directed towards colon cancer. This Pt(II) complex was originally tested along with oxaliplatin, but it was discarded because of its very poor water solubility and quick hydrolysis [5]. However, [$PtCl_2$(dach)] exhibited good anticancer activity when gradually released from block copolymer micelles or lipiodol suspensions in a phase I clinical trial to treat hepatocellular carcinoma [6]. Thus, its transformation in a quite inert and more water soluble Pt(IV) complex, could ameliorate its pharmacokinetics [7] [8].

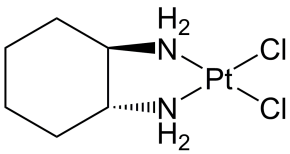


[$PtCl_2$(dach)]

Figure 4.1: The dichlorido analogue of oxaliplatin, (*SP*-4-2)-dichlorido(cyclohexane-1*R*,2*R*-diamine)platinum(II), [$PtCl_2$(dach)].

Epigenetic drugs, as HDACi, are gaining increasing attention for the therapy of colon cancer [9]. Moreover, the cisplatin-based Pt(IV) combo, **1**, bearing the strong HDACi, POA, as axial ligand, exibithed excellent *in vitro* and *in vivo* antitumor activity (Chapter 3).

For all these reasons, the biological activity on colon cancer of a new dach-based Pt(IV) prodrug candidate, containing POA as axial ligand, **3**, was investigated (Figure 4.2). As reported in Chapter 3 for complex **1**, since POA is a chiral molecule, complex **3** containing racemic POA was tested along with its separated isomers, **3R** (containing R-POA) and **3S** (containing S-POA), and the reference compounds cisplatin, oxaliplatin, [$PtCl_2$(dach)], free POA, and **1** (described in Chapter 3).

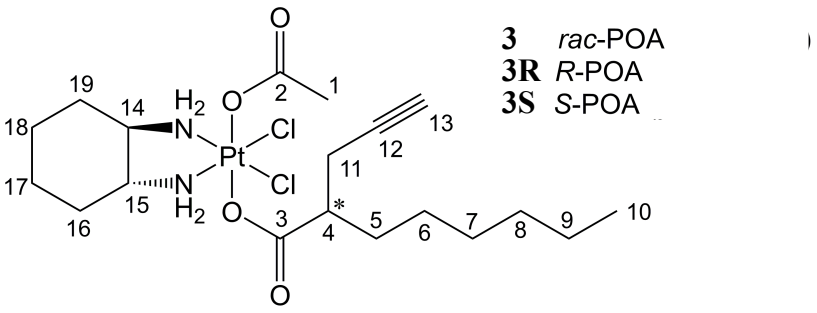


Figure 4.2: Sketch of the Pt(IV) complexes under investigation.

# *4.2 Material and methods*

## *4.2.1 Cell culture*

HCT 116 were purchased from ECACC, as previously reported in Chapter 3, whereas the other human colon carcinoma cell lines, HT29 and SW480, are a kind gift of Prof. Claudia Cantoni (University of Genova, Italy). The mouse colon adenocarcinoma CT26 cell line is a kind gif of Prof. Enzo Terreno (University of Turin, Italy). RPMI 1640 medium was used for SW480 and CT26, whereas HCT 116 and HT29 were grown in McCoy's 5A medium. All media were supplemented, and cell culture and treatment were carried out, as previously described in Chapter 3.

## *4.2.2 Compounds and drug candidates*

The Pt(IV) complexes under investigation were designed, synthetized and characterized in Prof. Osella's bioinorganic laboratory (University of Piemonte Orientale, DiSIT, Italy). In particular, complex **1** were prepared as described in Chapter 3, whereas the synthesis of complex **3** started with the oxidation of [$PtCl_2$(dach)] with hydrogen peroxide in acetic acid to get the mono-hydroxido intermediate. This synthon was turned into the corresponding dicarboxylato complex

**3** by reaction with POA [10]. [$PtCl_2$(dach)] was prepared according to published procedures [11] [12].

In order to prepare the stock solutions of the complexes under investigation for the following biological tests, cisplatin was dissolved in 0.9% w/v NaCl aqueous solution brought to pH = 3 with HCl (final stock concentration 1 mM) (Chapter 3), oxaliplatin (Sigma-Aldrich) was dissolved in Milli-Q water, aliquoted and stored at –80 °C (final stock concentration 2.5 mg $mL^{-1}$, 6.3 mM), whereas [$PtCl_2$(dach)] was freshly dissolved in DMSO (final stock concentration 5 mM). The Pt(IV) complexes were dissolved in absolute ethanol (final stock concentration 5 mM) and stored at -18 °C. The stock concentrations were confirmed with ICP-MS measurements. The mother solutions were diluted in complete medium to the required concentration range and, where present, the total co-solvent concentration never exceeded 0.1% v/v (this concentration was found to be non-toxic to the cells tested as control). A commercial racemic mixture of POA (stock concentration 4.8 M) was purchased by TCI (Chapter 3).

## *4.2.3 Antiproliferative activity*

The growth inhibition of the compounds under investigation was assessed by means of the resazurin reduction assay, as described in detail in Chapter 3.

## *4.2.4 Cellular accumulation*

Around $5\times10^6$ HCT 116 cells were seeded in 25 $cm^2$ flasks and allowed to growth until around 80% of confluence and then treated for 4h with the complexes under investigations (10 μM for cisplatin, oxaliplatin and [$PtCl_2$(dach)], 1 μM for **1** and **3**) in complete medium. Then, the experiment was carried out as previously described in detail in Chapter 3.

## *4.2.5 Chromatin staining*

$2\times10^5$ HCT 116 cells were seeded on Nunc™ Lab-Tek™ 4-chamber slides and allowed to attach for 24 h. The following day the treatment was performed with 1 μM complex **3** or [$PtCl_2$(dach)], or 5 mM POA. Then, the experiment was carried out as described in Chapter 3. Pictures were taken at 40× magnification.

## *4.2.6* In vivo *experiments*

*In vivo* experiments were carried out at Center of Excellence for Preclinical Imaging of University of Turin at the BioIndustry Park of Canavese (Colleretto Giacosa, Italy). A total of 18 BALB/c male mice (Envigo RMS srl, San Pietro al Natisone, Udine, Italy) 5 weeks old at weight of 20-25 g were fed ad libitum with standard diet (Special Diets Services Ltd, Witham, Essex, England). During the entire period of the study the animals were maintained in conditioned and at limited access environments (mean temperature: 22°C; lighting: controlled to give a daily 12 h photoperiod). All the procedures involving the animals were performed according to the national and international laws on experimental animal (L.D. 26/2014; Directive 2010/63/EU) and to the approved experimental protocol procedure (Authorization no. 229/2016-PR). No validated non-animal alternatives are known to meet the objectives of the study. After a period of acclimation (5 days) tumor induction was performed as follows. CT26 cells were grown in RPMI 1640 medium supplemented with 10% fetal bovine serum, 100 IU $mL^{-1}$ penicillin and 100 μg $mL^{-1}$ streptomycin. After two washes with PBS, cells ($1.5\times10^6$) were suspended in 0.2 mL of serum-free medium and injected subcutaneously in the right flank of each mouse. Tumors were let grow approximately 10 days until the tumor become visible in each animal (100-150 $mm^3$). Then, mice were randomly assigned to 6 experimental groups (3 animals per group) and the chemotherapeutic treatments were started. For each administration route (i.e. *per os* and i.v.) each group received **3**, oxaliplatin, or

vehicle. The reference drug oxaliplatin was immediately dissolved before use in double distilled water and the resulting solution was protected from light, whereas **3** was dissolved in vehicle solution (20% v/v Cremophor EL, 20% v/v PEG400 and 60% v/v saline solution). Schedules of two parallel experiments are described in results and discussion. Body weight was recorded every two days during the observation period. Animals obviously in pain or showing signs of severe distress were sacrificed. Criteria for making the decision to sacrifice severely suffering animals, and guidance on the recognition of predictable or impending death, are the subject of an OECD Guidance Document.

Tumor growth was followed by electronic caliper measurement every two days. Tumor volume ($mm^3$) was calculated according to the formula $(W^2 \times L)/2$, where W and L are the maximum width and length of the tumor. Quantitative evaluation of body weight and tumor volume were performed. The antitumor effect was evaluated by comparing the tumor size among groups. Magnetic Resonance Imaging (MRI) acquisitions were performed at the end of observation period on one representative animal for each experimental group. Mice were anesthetized under 0.5-2% isoflurane gas anesthesia ($O_2$ 95.0%). MRI was performed on a 7 Tesla MRI scanner (Pharmascan MRI 7T, Bruker, Germany) using Rare sequences. The $T_2$-weighted images were acquired with the optimized parameters for high-resolution images with a good contrast to detect the tumor mass. Organs from each animal of experimental groups (tumor, kidneys, spleen, liver, heart, and lungs) were collected at sacrifice and divided in two equal parts: one part was formalin-fixed and paraffin-embedded and the other one was stored at -20 °C for quantitative determination of the platinum content. The Pt accumulation was measured by means of ICP-MS analysis on dried samples of 5-20 mg of each organ in triplicate after microwave-assisted digestion (microwave power = 1200 W, temperature = 200 °C, digestion time = 45 min, Milestone Start D, Milestone Srl, Sorisole, Italy) in a mixture containing 80% v/v of $HNO_3$ (70% w/w) and 20% v/v of $H_2O_2$ (30% w/w) and following dilution with 1%

v/v $HNO_3$. Slices (5 µm thick) were obtained from the paraffin embedded organs by rotative microtome and stained by hematoxylin/eosin procedure for microanatomical examination to identify tissue suffering and alteration. CD8 and CD68 immunohistochemistry was performed on spleen and tumor tissue slides of several experimental groups to identify cytotoxic lymphocytes (namely $CD8^+$ T cells) and macrophages (namely $CD68^+$ cells); for both rabbit polyclonal anti-mouse (Abcam: ab203035 and ab125212, Cambridge, UK) was used as primary antibody, revealed using biotinylated secondary antibody and avidin/biotinylated enzyme complex (Vectastain Elite kit, Vector Laboratories, Burlingame, CA, USA) together with 3,3′-diaminobenzidine as chromogen (DAB chromogen kit Vector Laboratories, Burlingame, CA, USA).

The Oxidative Stress Detection Kit (OxyIHC, S7450; Millipore USA) was used to perform immunohistochemical evidences about **3**-induced oxidative stress in liver, according with manufacturer instructions.

### *4.2.7 Statistical analysis*

Statistical analysis was performed as previously described in Chapter 3.

## *4.3 Results and discussion*

### *4.3.1 Antiproliferative activity*

The half-maximal inhibitory concentrations, $IC_{50}$, were measured for the Pt(IV) complexes **3**, **3R** and **3S**, along with the reference compounds cisplatin, oxaliplatin, [$PtCl_2$(dach)], free POA, and the racemic cisplatin-based derivate **1**. The complexes under investigation were tested on three human colon cancer cell lines with different levels of aggressiveness and tumorigenicity [13], namely HCT 116, HT29 and

SW480. In addition, all the compounds were assayed on CT26 mouse colon carcinoma cell line, in the perspective of *in vivo* experiments.

The results (Table 1) showed that the activity of the isomers **3R** and **3S** was almost identical, within the experimental error, to that of **3**, as already observed in Chapter 3 for the cisplatin-based analogue **1**. Moreover, the Pt(IV) complexes **3**, **3R** and **3S** were one or two orders of magnitude more active than the Pt(II) reference models. Importantly, as previously reported in Chapter 3, the free ligand POA is almost inactive within the same range of concentrations ($IC_{50}$ > 100 μM), also on the newly introduced cell lines.

| **Compound** | **$IC_{50}$ [μM]** | | | |
|---|---|---|---|---|
| | **HCT 116** | **HT-29** | **SW480** | **CT26** |
| POA | 439±279 | 970±80 | 470±90 | 200±20 |
| Cisplatin | 2.3±0.3 | 2.7±0.1 | 2.6±0.2 | $(4.1\pm0.6)\times10^{-1}$ |
| Oxaliplatin | 1.2±0.1 | $(9.2\pm0.9)\times10^{-1}$ | $(4.7\pm0.2)\times10^{-1}$ | 1.5±0.5 |
| $[PtCl_2(dach)]$ | $(2.7\pm0.1)\times10^{-1}$ | $(2.4\pm0.2)\times10^{-1}$ | $(1.8\pm0.1)\times10^{-1}$ | $(4.6\pm0.3)\times10^{-1}$ |
| **3** | $(1.0\pm0.1)\times10^{-2}$ | $(1.5\pm0.6)\times10^{-2}$ | $(8.1\pm0.8)\times10^{-3}$ | $(7.1\pm0.6)\times10^{-3}$ |
| **3R** | $(9.1\pm0.6)\times10^{-3}$ | $(1.5\pm0.1)\times10^{-2}$ | $(7.4\pm0.6)\times10^{-3}$ | $(8.8\pm0.6)\times10^{-3}$ |
| **3S** | $(1.1\pm0.7)\times10^{-2}$ | $(1.3\pm0.4)\times10^{-2}$ | $(8.2\pm0.7)\times10^{-3}$ | $(6.3\pm0.8)\times10^{-3}$ |
| **1** | $(2.9\pm0.9)\times10^{-2}$ | $(8.0\pm0.8)\times10^{-2}$ | $(3.7\pm0.6)\times10^{-2}$ | $(4.4\pm0.3)\times10^{-2}$ |

Table 1: Antiproliferative activity ($IC_{50}$) obtained after 72 h of continuous treatment of human colon carcinomas HCT 116, HT-29, and SW480, and mouse colon carcinoma CT26 cell lines. Data are means ± standard deviation of at least three independent replicates.

## *4.3.2 Cellular accumulation*

The Pt cellular uptake, expressed as accumulation ratio (AR), being the ratio between the intra- and extracellular Pt concentration (described in detail in Chapter 3), of all the Pt compounds under investigation, was assessed on HCT 116 cells.

Figure 4.3 shows that the ARs of **3**, **3R** and **3S** are very similar to each other (within the experimental error) and by far higher than those of the reference drugs, cisplatin, oxaliplatin and [$PtCl_2$(dach)]; this is in agreement with what reported in Chapter 3 for the corresponding cisplatin-like Pt(IV) prodrug **1**.

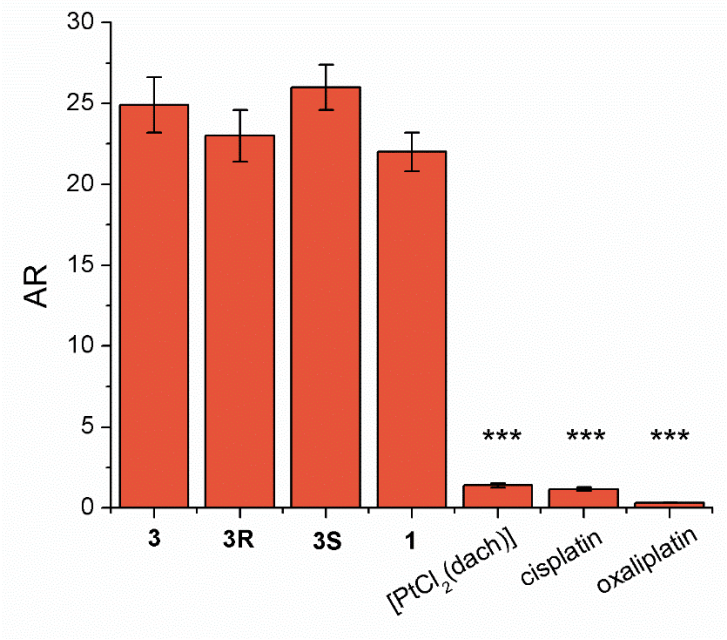


Figure 4.3: Accumulation ratio (AR) of **3**, **1**, [$PtCl_2$(dach)], cisplatin, and oxaliplatin, measured on HCT 116 colon cancer cells treated for 4 h with the compounds. Data are means ± standard deviation of at least three independent replicates and were compared to **3** by means of a one-way ANOVA-Tukey test (no indication = not significant; * $p<0.05$; ** $p<0.01$; *** $p<0.001$).

Based on the above reported results, the following *in vitro* and *in vivo* experiments were planned simply employing complex **3**, since its activity was comparable to that of the isomers **3R** and **3S**.

## *4.3.3 Epigenetic activity*

Two active moieties are released by compound **3** upon intracellular reduction, which are [$PtCl_2$(dach)] and the axil ligand POA. On the one hand [$PtCl_2$(dach)] undergoes rapid hydrolysis in the cytosol, being able to give DNA adducts. On the other hand, the released POA should exert its HDACi activity, as previously observed in Chapter 3 for the cisplatin-based derivate **1**. This hypothesis was verified on HCT 116 cells challenged for 4h with cisplatin, **3** and free POA, by means of Hoechst 33342 staining. Indeed, this dye binds the DNA, highlighting the regions of condensed DNA (heterochromatin) as brighter nuclear foci that decrease in number and size following chromatin relaxation. Thus, punctuated nuclear pattern is visible on control cells and on those exposed to cisplatin (Figure 4.4 a and b), whereas chromatin decondensation and DNA relaxation were clearly observed in cells treated with **3** and POA, underlying that the epigenetic activity of free POA is retained in the Pt(IV) complex **3** (Figure 4.4 c and d).

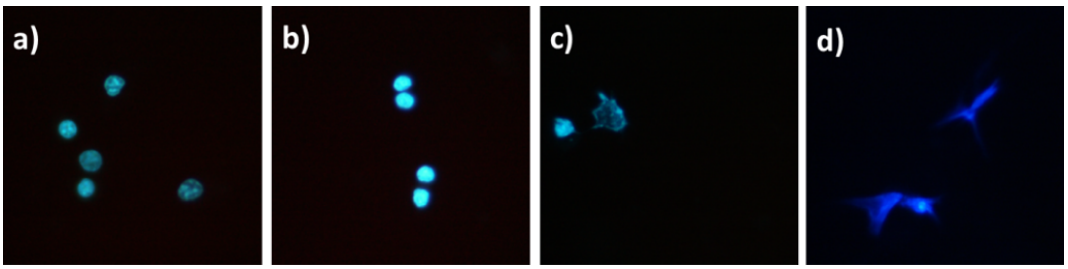


Figure 4.4: HCT 116 cells treated for 4 h with a) fresh medium (control); b) [$PtCl_2$(dach)], 1 µM; c) **3**, 1µM; d) POA, 5 mM. Pictures were taken by using a fluorescence microscope (standard DAPI filters, 400× magnification) on living cells immediately after Hoechst 33342 staining.

## *4.3.4* In vivo *activity*

As previously reported in Chapter 1, Pt(IV) prodrugs were designed for oral administration, being satraplatin the prototype tested in clinical trials. However the predictions of anticancer activity based on *in vitro* experiments, are not always in accordance with the results of those performed *in vivo*, especially for Pt(IV) complexes orally administered [14].

The simultaneous presence of [$PtCl_2$(dach)] and POA made the Pt(IV) complex **3** very lipophilic and this could hamper oral administration. Indeed, all successful oxaliplatin-based Pt(IV) prodrugs containing very lipophilic axial ligands have so far been administered intravenously (i.v.) or intraperitoneally (i.p.) [15] [16].

A pool of BALB/c mice bearing the highly aggressive syngeneic CT26 mouse colon carcinoma, an experimental model extensively used in literature for this kind of study [17], was chosen as test system. Two *in vivo* experiments were planned in parallel (Scheme 1): the former (experiment I) featuring the oral administration of **3** (gavage) and the latter (experiment II) characterized by the administration of **3** i.v. (tail vein). The comparison between the two administration routes (i.e. *per os* and i.v.), allows to verify the better administration of complex **3**, in terms of efficacy/toxicity balancing.

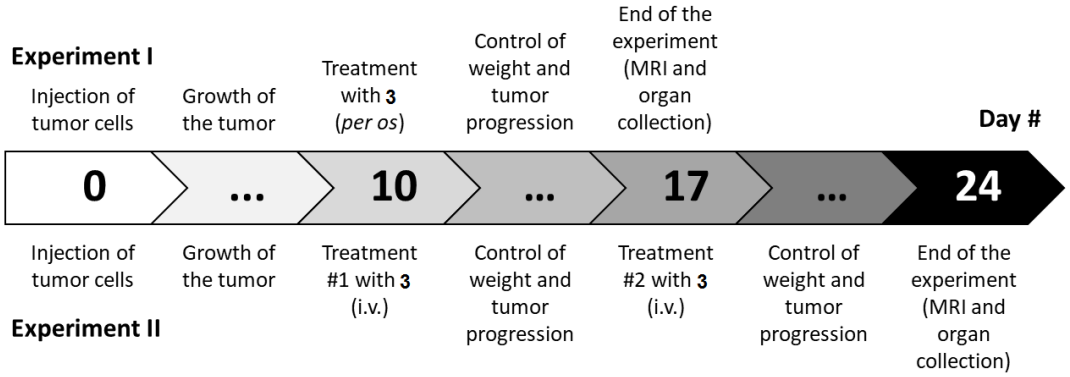


Scheme 1: General scheme of the *in vivo* experiments performed on BALB/c mice bearing syngeneic CT26 mouse colon carcinoma treated with **3**.

In experiment I, three animals received only the vehicle solution (20% v/v Cremophor EL, 20% v/v PEG400, and 60% v/v saline solution) *per os* (control), three animals received the reference drug oxaliplatin dissolved in distilled water i.v. (10 mg $kg^{-1}$, weekly), and three animals received compound **3** dissolved in the vehicle solution *per os* (20 mg $kg^{-1}$, daily). The treatment schedule for oxaliplatin was selected according to standard protocols designed to optimize its efficacy and minimize the occurrence of side effects [18]. The schedule for **3** in experiment I was identical to that successfully employed for the corresponding cisplatin-based Pt(IV) prodrug **1** and for the *bis*-VPA derivative **2**, which is described in detail in Chapter 3.

As shown in Figure 4.5, the vehicle solution administered both *per os* and i.v. did not induce body weight loss in control animals, as well as the i.v. administration of oxaliplatin and **3** at least up to two weeks (mean body weight of each cohort ranging from 99 to 110% of the initial mean weight). On the contrary, administration of **3** *per os* (oral gavage, 20 mg $kg^{-1}$, daily) caused within a week elevated cachexia as demonstrated by a body weight loss >20%. Moreover, the inspected mice showed clear signs of pain. Therefore, for ethical reason, experiment I was stopped after a week (day 17) from the beginning of treatment (day 10). Despite of these heavy side

effects, in experiment I the tumor growth inhibition caused by **3** was higher than that caused by oxaliplatin (53% *vs.* 25% respectively) (Figures 4.6 and 4.7).

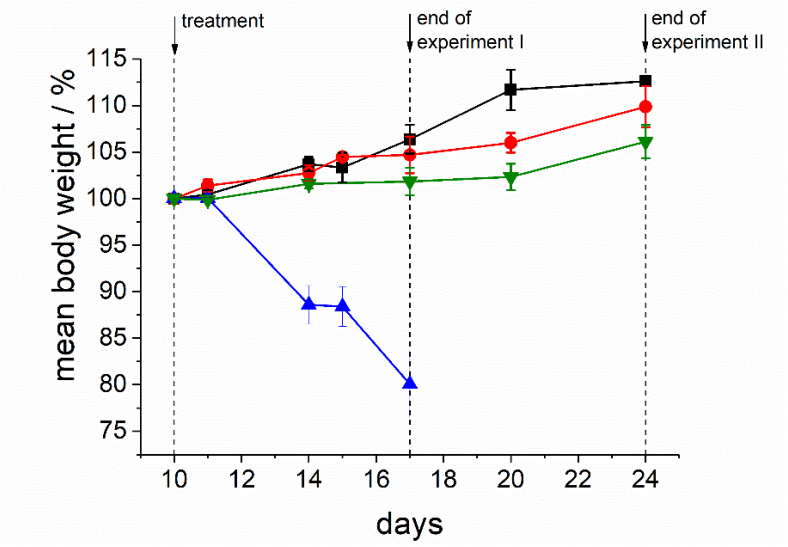


Figure 4.5: Mean body weight % ± standard deviation of BALB/c mice. Black square and line: control; red circle and line: oxaliplatin; upward blue triangles and line: **3** *per os*; downward green triangles and line: **3** i.v..

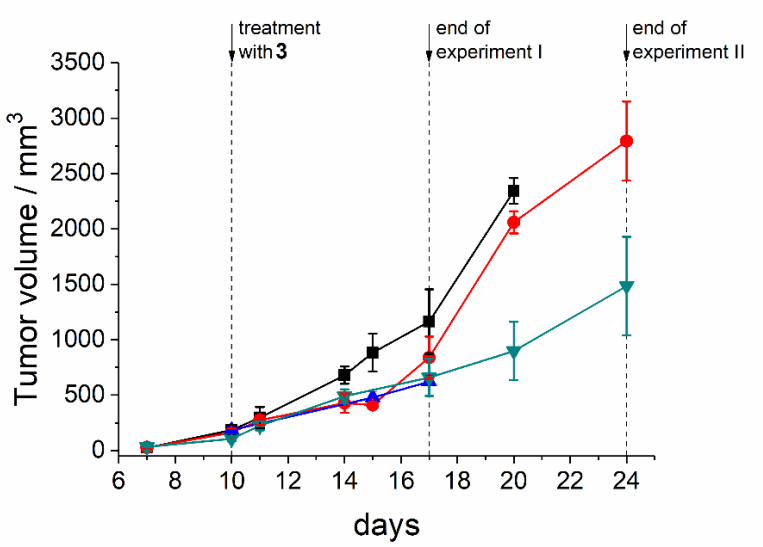


Figure 4.6: Tumor growth inhibition of subcutaneous CT26 cell implant in BALB/c mice. Data are means ± standard deviation. Black squares and line: control; red circles and line: oxaliplatin i.v.; upward blue triangles and line: **3** *per os*; downward green triangles and line: **3** i.v..

In experiment II, the performance of **3** (administered i.v.) was rather promising with respect to reference oxaliplatin. Indeed **3** caused an inhibition of tumor growth of 56% one week after treatment and of 38% after a further week compared to 25% and 5% caused by oxaliplatin, respectively (Figures 4.6 and 4.7). Interestingly, the route of administration did not affect the activity of **3**, since after 1 week (day 17) almost the same tumor growth inhibition was observed: 53% *per os vs.* 56% i.v. (Figure 4.6). Noteworthy was the persistence of the tumor growth inhibition caused by **3**, compared to the Pt(II) reference drug, at least during the time interval of experiment II. Indeed, on the contrary, oxaliplatin showed decreasing activity (Figure 4.7).

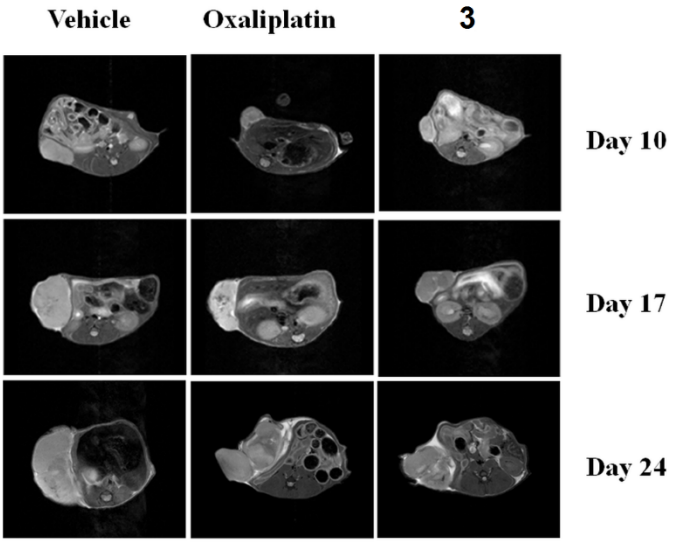


Figure 4.7: Images panel obtained by Magnetic Resonance Imaging (MRI) acquisition of mice with implanted tumor (light grey mass on the left), at the beginning of the treatments (day 10), at the end of experiment I (day 17) and the end of experiment II (day 24).

## *4.3.5 Pt accumulation and organ histology*

Organs were collected at the end of each experiment and split into two samples to perform both the determination of Pt organ content and microanatomical analysis. Complex **3** exhibited higher cellular accumulation than that of oxaliplatin in almost all tissues, including the tumor mass (Figure 4.8), where the values were in line with those observed for the same animal model treated with similar lipophilic Pt(IV) derivatives [16] [19].

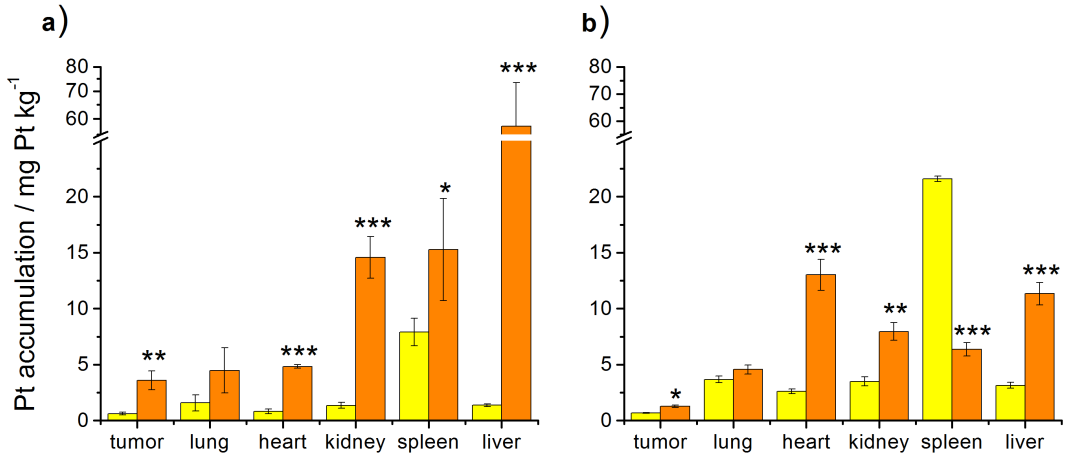


Figure 4.8: Pt organ accumulation (mg Pt $kg^{-1}$ of dry weight mass), a) recovered at the end of experiment I (yellow bars: oxaliplatin i.v.; orange bars: complex **3** *per os*); b) recovered at the end of experiment II (yellow bars: oxaliplatin i.v.; orange bars: complex **3** i.v.). Data are means ± standard deviations of three experiments in triplicate; for each organ the data of oxaliplatin and **3** were compared with a one-way ANOVA-Tukey test (* $p<0.05$; ** $p<0.01$; *** $p<0.001$).

Tissue suffering and alterations induced by the treatments with oxaliplatin and **3** were checked at the microanatomic level, by a hematoxylin/eosin staining, in the tumor mass and in several organs. The effect on tumor mass caused by **3** was more evident than that caused by oxaliplatin and was comparable in both administration protocols (*per os* and i.v.) (Figure 4.9 a, b, c), in line with the observed tumor growth inhibition at day 17 (Figure 4.6). Indeed, the tumor showed a remarkably different pattern of distribution of heterochromatic nuclei (dark cell nuclei) in both experiments (I and II). Whereas heterochromatic nuclei were mainly located in the cortical region of the control group (Figure 4.9 a), both treatments with the Pt-based drugs increased them in the medullary part of tumor, more evidently in the **3**-treated group (Figure 4.9 c) than in the oxaliplatin-treated group (Figure 4.9 b). This change from euchromatic (pale cell nuclei) to heterochromatic nuclei within the medullary

region indicates an adaptive stress response that may lead to apoptotic or necrotic cell death (described in Chapter 1) [20] [21].

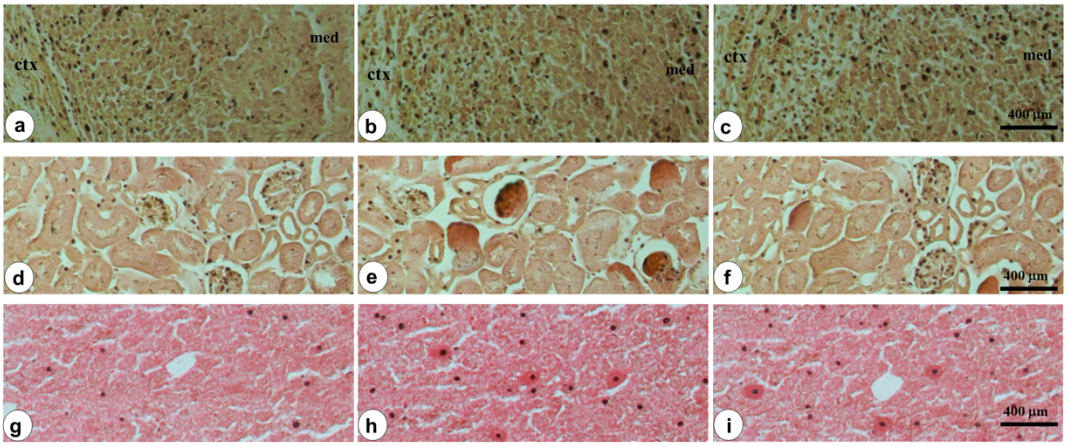


Figure 4.9: Hematoxylin and Eosin staining of organ parenchyma from animals at the end of experiment II. a-c: tumor parenchyma, d-f: kidney parenchyma, g-i: liver parenchyma, a-l: control; b-m: oxaliplatin treated; c-n: complex **3**-treated (med = medullary, ctx = cortical zone of the tumor).

The kidney parenchyma after oxaliplatin administration revealed wide alteration of microanatomical structure, resulting in diffuse eosinophilic cells and signs of glomerular alteration, as glomerular tuft shrinkage and hyperchromic picture (Figure 4.9 e), typical of a clear organ suffering status, not observable in control group (Figure 4.9 d). Similarly, in the liver parenchyma oxaliplatin administration caused several signs of cytotoxicity as eosinophilic hepatocytes and remarkable increase of hyperchromic nuclei occurrence (Figure 4.9 h). These findings were in accordance with the well-known organ toxicity of oxaliplatin, and its low systemic toxicity, observed in terms of body weight loss (Figure 4.5) [22]. Whereas mice treated with **3** showed lesser signs of parenchymal alteration in the kidney with respect to oxaliplatin (Figure 4.9 f) in both experiments. In particular, lower parenchymal alterations were observed after i.v. administration (experiment II) compared to the oral administration (experiment I) (Figure 4.10).

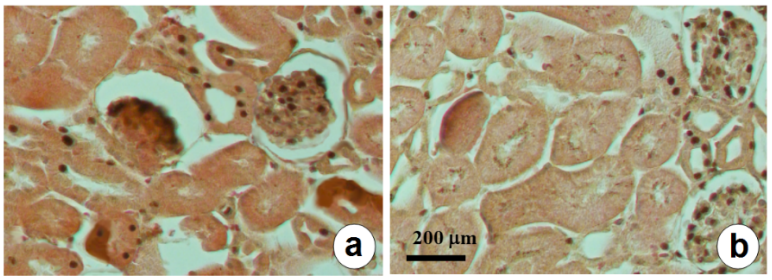


Figure 4.10: Hematoxylin and Eosin staining of kidney parenchyma; a: complex **3**-treated *per os*; b: complex **3**-treated i.v..

Also in the liver, the i.v. protocol caused minor parenchymal alterations compared to oxaliplatin treatment (Figure 4.9 i) in both experiments. The hepatotoxicity of Pt-based drugs can arise from their ability to induce ROS production, leading to an increase of cytokines [22]. Most of the Pt(IV) prodrugs are able to increase intracellular basal ROS levels. This is particularly true for the Pt(IV) prodrugs containing in their scaffold indole carboxylic acids in axial position [23]. Metals catalyse oxidation of proteins introducing carbonyl groups in several amino acid residues in a site-specific manner [24]. Therefore, the increase of carbonyl-modified proteins is considered a key biomarker in detecting the direct action of ROS. For this reason, the immunohistochemical detection of these modified proteins in hepatocytes from mice treated with **3** was performed. A wide increase of carbonyl-modified proteins was observed in hepatocytes from mice treated with **3** *per os* (Figure 4.11). Therefore, the observed systemic toxicity of orally administered **3** might be attributed to the extremely high Pt accumulation into the liver (Figure 4.8).

On the contrary, in both experiments, heart and lung did not reveal any signs of suffering or alteration of the organ parenchymal structure in both control and treated groups (Figure 4.12).

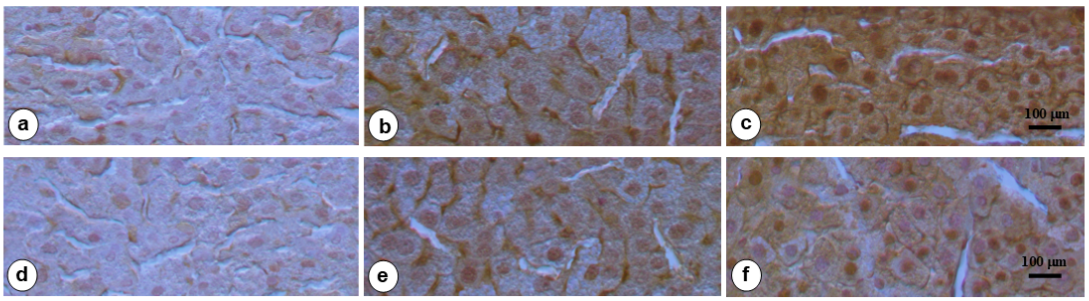


Figure 4.11: Images illustrating the increase of carbonyl modified proteins (brown reaction), as a consequence of direct ROS action. Figures a-c: liver from *per os* **3**-treated mice; figures d-f: liver from i.v. **3**-treated mice.

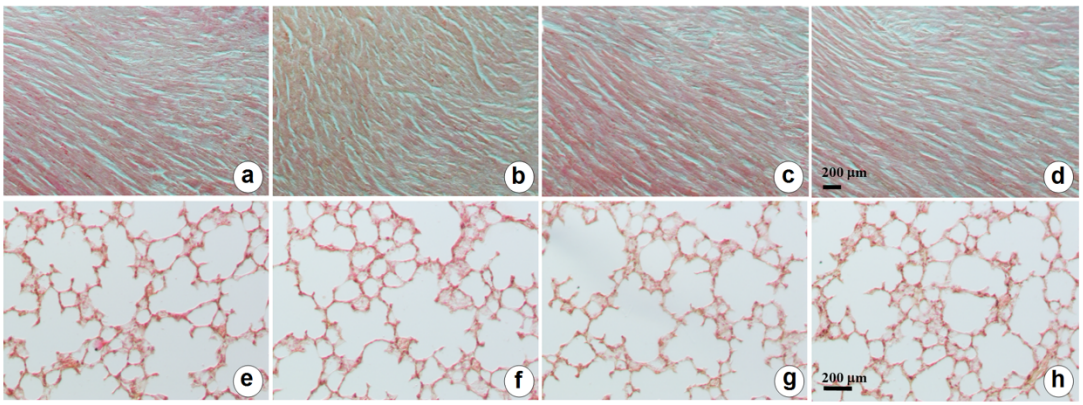


Figure 4.12: Hematoxylin and Eosin staining of heart and lung parenchyma; a, e: control; b, f: oxaliplatin treated; c, g: complex **3** treated *per os*; d, h: complex **3** treated i.v..

High Pt levels were also observed in spleen following oral administration of **3** only, along with volume reduction (Figures 4.8 and 4.13 a, b, c). Spleen volume decrease is a reversible dynamic process observed in patients undergoing platinum-based chemotherapy. The change in spleen volume may correlate with change in the number and function of immune effector cells, indicating splenic activation [25]. On the contrary, splenic volume increase (splenomegaly) indicates oxaliplatin-induced

toxicity [26]. The spleen parenchyma is normally organized in several follicular structures representing the masses of immune effector cells (white pulp) inside a reddish parenchyma (red pulp) in which ageing erythrocytes, cell debris and pathogens are efficiently removed from blood. In both experiments, the spleen revealed an increase of white pulp, more significant in **3**-treated group (Figure 4.13 d, e, f, g). In particular, a remarkable increase of the white pulp was observed in the experiment I (Figure 4.13 f), a hint of splenic hyperactivation.

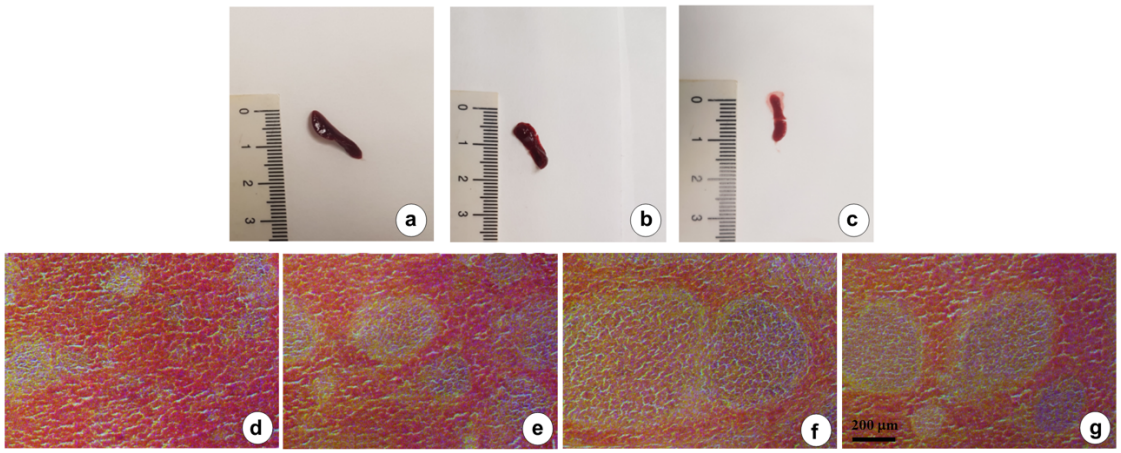


Figure 4.13: Images illustrating alterations in spleen anatomy and structure. Figures a- c: spleen gross anatomy; a: control, b: oxaliplatin treated, c: complex **3**-treated. Figures d-g: spleen parenchyma; d: control; e: oxaliplatin treated; f: complex **3**-treated *per os*; g: complex **3** treated i.v..

Immunohistochemical analysis of cytotoxic lymphocytes and macrophages, namely $CD8^+$ T cells and $CD68^+$ cells, respectively, was performed. This experiment reveals a remarkable increase of these cells in spleen parenchyma of *per os* treated mice, further evidencing the status of splenic hyperactivation (Figure 4.14). Thus, the toxic response of kidney and liver and the splenic hyperactivation of white parenchyma points out that the protocol of oral administration of **3** has to be considered unsatisfactory.

On the contrary, the absence of toxicity, in terms of body weight loss, observed in experiment II correlated with the large decrease of the Pt accumulation in liver, kidney, and spleen (Figure 4.8). Interestingly, the splenic accumulation of oxaliplatin increased with the repetition of the treatment (one week and one administration for experiment I; 2 weeks and 2 administrations for experiment II), whereas that of **3** decreased, probably due to the different pharmacokinetics. In particular, the two different administration routes induce a different occurrence of drugs at systemic levels, being the *per os* administration mediated by intestinal passing that reduce and/or dilute the drug bolus. For these reasons, the i.v. administration of **3** has the advantage of having higher antitumor effect and lower toxicity than oxaliplatin and a more balanced immune response than that observed for oral administration, despite this way was successfully employed for other Pt(IV) derivatives, as satraplatin [27].

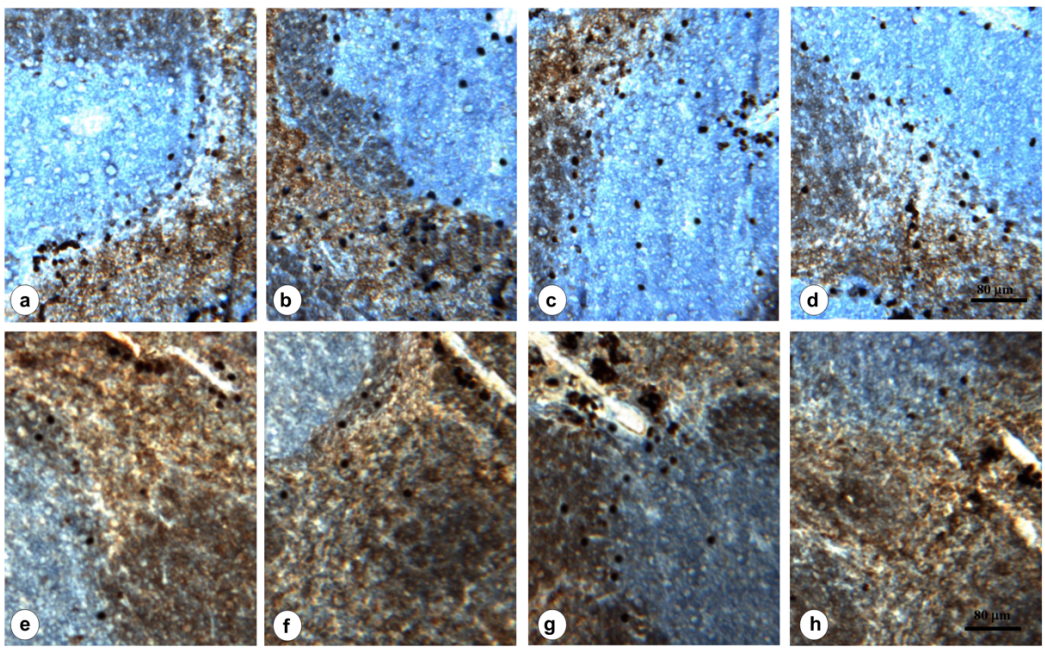


Figure 4.14: Images illustrating the distribution of $CD8^+$ positive lymphocytes and $CD68^+$ macrophages in spleen of several experimental groups. Figures a-d: $CD8^+$ immunohistochemistry in spleen parenchyma; e-h: $CD68^+$ immunohistochemistry in spleen parenchyma.

As previously reported in the Introduction, the immunogenic activity plays an important role in the anticancer propensity of oxaliplatin and its Pt(IV) derivatives. Administration of oxaliplatin (i.p.) inhibited tumor growth and increased tumor-infiltrating activated cytotoxic $CD8^+$ T lymphocytes [28] [29]. Indeed, oxaliplatin-treated dying cancer cells are immunogenic as they express and secrete a specific combination of signals. This molecule restores the recognition of cancer cells by phagocytes of the immune system, essential for antigen presentation to T cell and their differentiation into $CD8^+$ cells [30]. These lymphocytes specifically recognize and kill cancer cells, even in metastatic sites, mediating the last step of the so-called immunogenic cell death (ICD) [4] [31]. Thus, the presence of $CD8^+$ cells within the tumor mass represents an aggression by the immune system by means of ICD. In order to investigate the ability of compound **3** to induce ICD, a CD8 and CD68 immunohistochemistry was performed on tumor tissue slides.

Accordingly, the CD8 immunohistochemistry revealed that, in control group, $CD8^+$ cells were mainly located in the tumor cortical zone (Figure 4.15 a) instead of in the medullary zone (Figure 4.15 d) clustered in very large follicle masses indicating the points of initial tumor invasion. After treatment with **3**, the medullary zone was widely invaded by $CD8^+$ cells (Figure 4.15 f) due to the disadvantage of the cortical zone (Figure 4.15 c). As expected, oxaliplatin treatment also induced the $CD8^+$ cells tumor invasion, albeit less evident than that induced by **3** (Figure 4.15 b, e). Thus, the lipophilic **3** induced a stronger ICD than oxaliplatin itself, in line with previous observations.

Similarly, immunohistochemistry analysis of $CD68^+$ macrophages showed a large display of these cells along tumor parenchyma. A preferential increase in $CD68^+$ cells was observed in the tumor medullary zone of **3**-treated animals (Figure 4.16 g, h). Indeed, it has been reported in literature that some lipophilic oxaliplatin-based Pt(IV) prodrugs exert their antitumor activity on CT26 tumors only in immune-competent BALB/c mice, whereas immune-deficient SCID/BALB/c mice did not

respond to the treatment [19]. As far as **3** generates [$PtCl_2$(dach)] after intracellular reduction, the carrier ligand dach seems to play a role in the ICD [30] [31].

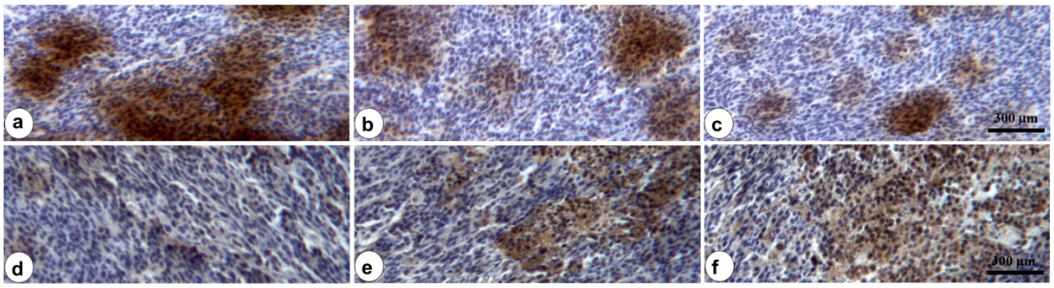


Figure 4.15: Microphotograph panel of immunopositive $CD8^+$ lymphocytes invading the tumor mass. Tumor from animals belonging to experiment II. The dark-brown areas indicate presence and distribution of lymphocytes. a-c: cortical zone of the tumor, d-f: medullary zone of the tumor; a, d: control group, b, e: oxaliplatin treated group, c, f: compound **3**-treated group.

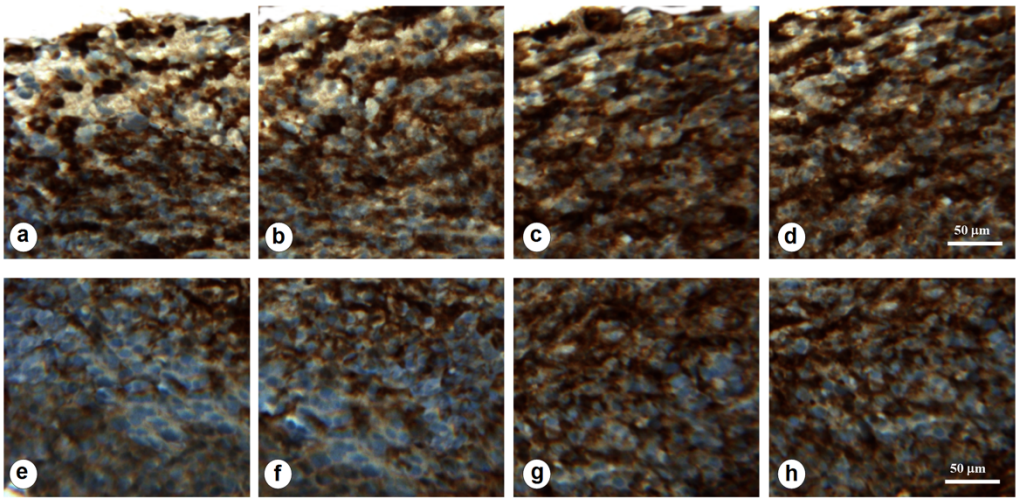


Figure 4.16: Images illustrating the distribution of $CD68^+$ macrophages in tumor tissue of several experimental groups. Figures a-d: $CD68^+$ immunohistochemistry in tumor parenchyma, cortical zone; e-h $CD68^+$ immunohistochemistry in tumor parenchyma, medullary zone. Figures a, e: control; b, f: oxaliplatin treated; c, g: complex **3** treated *per os*; d, h: complex **3**-treated i.v..

## *4.4 Conclusions*

The *in vitro* activity of the Pt(IV) complex **3**, based on the [$PtCl_2$(dach)] scaffold and containing the chiral POA as axial ligand, was investigated on three human and one mouse colon cancer cell lines, and compared to that of the isomers, **3R** and **3S**, and to references cisplatin, oxaliplatin and [$PtCl_2$(dach)]. As expected from their lipophilicity, all the Pt(IV) complexes were one-two orders of magnitude more active than the Pt(II) compounds, due to their higher cellular uptake. Moreover, the $IC_{50}$ data, as well as the cellular accumulation results, showed that the activity of the enriched isomers **3R** and **3S** was almost identical to that of **3**. Therefore, the latter was used for the following *in vivo* tests, employing a pool of BALB/c mice bearing CT26 colon carcinoma. Orally administered **3** inhibited the tumor growth more efficiently than oxaliplatin (administered i.v.). However, the presence of heavy side effects, attributed to an extremely high Pt accumulation into the liver, limited the success of such protocol. Conversely, the performance of **3** administered i.v. was much more promising, because the tumor growth inhibition was strong and persistent during the time interval of the experiment. Furthermore, i.v. administered **3** showed superior antitumor activity than oxaliplatin, with lower nephro- and hepatotoxicity. Moreover, the massive presence of the activated cytotoxic $CD8^+$ lymphocytes in the medullary zone of tumor parenchyma of mice treated with prodrug **3**, demonstrated that this Pt(IV) complex induced ICD. Both metabolites, [$PtCl_2$(dach)] and POA, released after intracellular reduction, likely contribute to this process. Indeed, POA, a potent epigenetic agent can modulate the reversion of the immunoescape, hence contributing to ICD, due to a more efficient antigen presentation to immune T cells.

# *References*

[1] AJ. Yiu, CY. Yiu. Biomarkers in Colorectal Cancer. *Anticancer Res* (2016) 36(3), 1093-102.

[2] HS. Hochster, LL. Hart, RK. Ramanathan, B. Childs, JD. Hainsworth, AL. Cohn, L. Wong, L. Fehrenbacher, Y. Abubakr, MW. Saif, L. Schwartzberg, E. Hedrick. Safety and efficacy of oxaliplatin and fluoropyrimidine regimens with or without bevacizumab as first-line treatment of metastatic colorectal cancer: Results of the TREE study. *J Clin Oncol* (2008**)** 26, 3523-3529.

[3] J. Dunn, S. Rao. Epigenetics and immunotherapy: the current state of play. *Mol Immunol* (2017) 87, 227-239.

[4] B. Cruickshank, M. Giacomantonio, P. Marcato, S. McFarland, J. Pol, S. Gujar. Dying to be noticed: epigenetic regulation of immunogenic cell death for cancer immunotherapy. *Front Immunol* (2018) 9, 654.

[5] MA. Jakupec, M. Galanski, BK. Keppler. Tumour-inhibiting platinum complexes-state of the art and future perspectives. *Rev Physiol Biochem Pharmacol* (2003) 146, 1-53.

[6] S. Fujiyama, J. Shibata, S. Maeda, M. Tanaka, S. Noumaru, K. Sato, K. Tomita. Phase I clinical study of a novel lipophilic platinum complex (SM-11355) in patients with hepatocellular carcinoma refractory to cisplatin/lipiodol. *Br J Cancer* (2003) 89, 1614-1619.

[7] V. Gandin, C. Marzano, G. Pelosi, M. Ravera, E. Gabano, D. Osella. Trans,cis,cis-bis(benzoato)dichlorido(cyclohexane-1R,2R-diamine) platinum(IV): A prodrug candidate for the treatment of oxaliplatin-refractory colorectal cancer. *ChemMedChem* (2014) 9, 1299-1305.

[8] M. Ravera, E. Gabano, S. Bianco, G. Ermondi, G. Caron, M. Vallaro, G. Pelosi, I. Zanellato, I. Bonarrigo, C. Cassino, D. Osella. Host-guest inclusion systems of Pt(IV)-bis(benzoato) anticancer drug candidates and cyclodextrins. *Inorg Chim Acta* (2015) 432, 115-127.

[9] M. Baretti, NS. Azad. The role of epigenetic therapies in colorectal cancer. *Curr Probl Cancer* (2018) 42, 530-547.

[10] M. Sabbatini, I. Zanellato, M. Ravera, E. Gabano, E. Perin, B. Rangone, D. Osella. Pt(IV) bifunctional prodrug containing 2-(2-propynyl)octanoato axial ligand: induction of immunogenic cell death on colon cancer. *J Med Chem* (2019) 62(7), 3395-3406.

[11] SC. Dhara. A rapid method for the synthesis of cis-[$Pt(NH_3)_2Cl_2$]. *Indian J Chem* (1970) 8, 193-194.

[12] RC. Harrison, CA. McAuliffe. An efficient route for the preparation of highly soluble platinum(II) antitumour agents. *Inorg Chim Acta* (1980) 46, L15-L16.

[13] CE. Dukes. The classification of cancer of the rectum. *J Pathol Bacteriol* (1932) 35, 323-322.

[14] S. Theiner, HP. Varbanov, M. Galanski, AE. Egger, W. Berger, P. Heffeter, BK. Keppler. Comparative in vitro and in vivo pharmacological investigation of platinum(IV) complexes as novel anticancer drug candidates for oral application. *J Biol Inorg Chem* (2015) 20, 89-99.

[15] A. Abu Ammar, R. Raveendran, D. Gibson, T. Nassar, S. Benita. A lipophilic Pt(IV) oxaliplatin derivative enhances antitumor activity. *J Med Chem* (2016) 59, 9035-9046.

[16] J. Mayr, P. Heffeter, D. Groza, L. Galvez, G. Koellensperger, A. Roller, B. Alte, M. Haider, W. Berger, CR. Kowol, BK. Keppler. An albumin-based tumor-targeted oxaliplatin prodrug with distinctly improved anticancer activity in vivo. *Chem Sci* (2017) 8, 2241-2250.

[17] N. Sato, MC. Michaelides, MK. Wallack. Characterization of tumorigenicity, mortality, metastasis, and splenomegaly of two cultured murine colon lines. *Cancer Res* (1981) 41, 2267-2272.

[18] R. Pangeni, SW. Choi, OC. Jeon, Y. Byun, JW. Park. Multiple nanoemulsion system for an oral combinational delivery of oxaliplatin and 5-fluorouracil: preparation and in vivo evaluation. *Int J Nanomedicine* (2016) 11, 6379-6399.

[19] S. Goschl, E. Schreiber-Brynzak, V. Pichler, K. Cseh, P. Heffeter, U. Jungwirth, MA. Jakupec, W. Berger, BK. Keppler. Comparative studies of oxaliplatin-based platinum(IV) complexes in different in vitro and in vivo tumor models. *Metallomics* (2017) 9, 309-322.

[20] HM. Schmitt, CL. Schlamp, RW. Nickells. Role of HDACs in optic nerve damage-induced nuclear atrophy of retinal ganglion cells. *Neuroscience Lett* (2016) 625, 11-15.

[21] A. Bayona-Feliu, A. Casas-Lamesa, O. Reina, J. Bernues, F. Azorin. Linker histone H1 prevents R-loop accumulation and genome instability in heterochromatin. *Nat Commun* (2017) 8, 283.

[22] R. Oun, YE. Moussa, NJ. Wheate. The side effects of platinum-based chemotherapy drugs: a review for chemists. *Dalton Trans* (2018) 47, 6645-6653.

[23] D. Tolan, V. Gandin, L. Morrison, A. El-Nahas, C. Marzano, D. Montagner, A. Erxleben. Oxidative stress induced by Pt(IV) pro-drugs based on the cisplatin scaffold and indole carboxylic acids in axial position. *Sci Rep* (2016) 6, 29367.

[24] ER. Stadtman. Oxidation of free amino acids and amino acid residues in proteins by radiolysis and by metal-catalyzed reactions. *Annu Rev Biochem* (1993) 62, 797-821.

[25] SW. Wen, SJ. Everitt, J. Bedo, M. Chabrot, DL. Ball, B. Solomon, M. MacManus, RJ. Hicks, A. Moller, A. Leimgruber. Spleen volume variation in patients with locally advanced non-small cell lung cancer receiving platinum-based chemo-radiotherapy. *Plos One* (2015) 10, e0142608.

[26] EJ. Jung, CG. Ryu, G. Kim, SR. Kim, HS. Park, YJ. Kim, DY. Hwang. Splenomegaly during oxaliplatin-based chemotherapy for colorectal carcinoma. *Anticancer Res* (2012) 32, 3357-3362.

[27] MJ. McKeage, LR. Kelland, FE. Boxall, MR. Valenti, M. Jones, P. Goddard, J. Gwynne, KR. Harrap. Schedule dependency of orally-administered bis-acetato-ammine-dichlorocyclohexylamine-platinum(IV) (JM216) in-vivo. *Cancer Res* (1994) 54, 4118-4122.

[28] HF. Gou, J. Huang, HS. Shi, XC. Chen, YS. Wang. Chemo-immunotherapy with oxaliplatin and interleukin-7 inhibits colon cancer metastasis in mice. *Plos One* (2014) 9, e85789.

[29] HF. Gou, L. Zhou, J. Huang, XC. Chen. Intraperitoneal oxaliplatin administration inhibits the tumor immunosuppressive microenvironment in an abdominal implantation model of colon cancer. *Mol Med Rep* (2018) 18, 2335-2341.

[30] A. Tesniere, F. Schlemmer, V. Boige, O. Kepp, I. Martins, F. Ghiringhelli, L. Aymeric, M. Michaud, L. Apetoh, L. Barault, J. Mendiboure, JP. Pignon, V. Jooste, P. van Endert, M. Ducreux, L. Zitvogel, F. Piard, G. Kroemer. Immunogenic death of colon cancer cells treated with oxaliplatin. *Oncogene* (2010) 29, 482-491.

[31] A. Terenzi, C. Pirker, BK. Keppler, W. Berger. Anticancer metal drugs and immunogenic cell death. *J Inorg Biochem* (2016) 165, 71-79.

# *Chapter 5*

# *Selective activity against human colon cancer cell lines of cyclohexane- 1R,2R-diamine-based Pt(IV) dicarboxylato anticancer prodrugs*

## *5.1 Introduction*

The Pt(IV) compound **3** has shown a good efficacy against colon cancer, both *in vitro* and *in vivo*, as described in Chapter 4. Thus, in order to discover new potential Pt(IV) combo prodrugs active against colon cancer, the biological properties of three couples of asymmetric Pt(IV) species, based on cisplatin (**series 4**) or oxaliplatin-like [$PtCl_2$(dach)] (**series 5**) skeleton, have been investigated (Figure 5.1). One axial ligand consists of a MCFA unit, linked to the Pt(IV) core as an anion, clofibrate (2-(*p*-chlorophenoxy)-2-methyl- propionic acid, CA) (**4a** and **5a**), or heptanoate (HA) (**4b** and **5b**), or octanoate (OA) (**4c** and **5c**), respectively, whereas the remaining axial position is taken up by a biologically inactive acetate (Figure 5.1). As far as the chosen axial ligands are concerned, CA acts as an agonist for peroxisome proliferator-activated receptors (PPARs) and promotes apoptotic cell death [1], OA induces DNA hypermethylation and reduces mitochondrial membrane potential [2], whereas HA could have epigenetic activity as the other MCFA [3].

In this work, cisplatin, [$PtCl_2$(dach)] and oxaliplatin were also tested for comparison purposes.

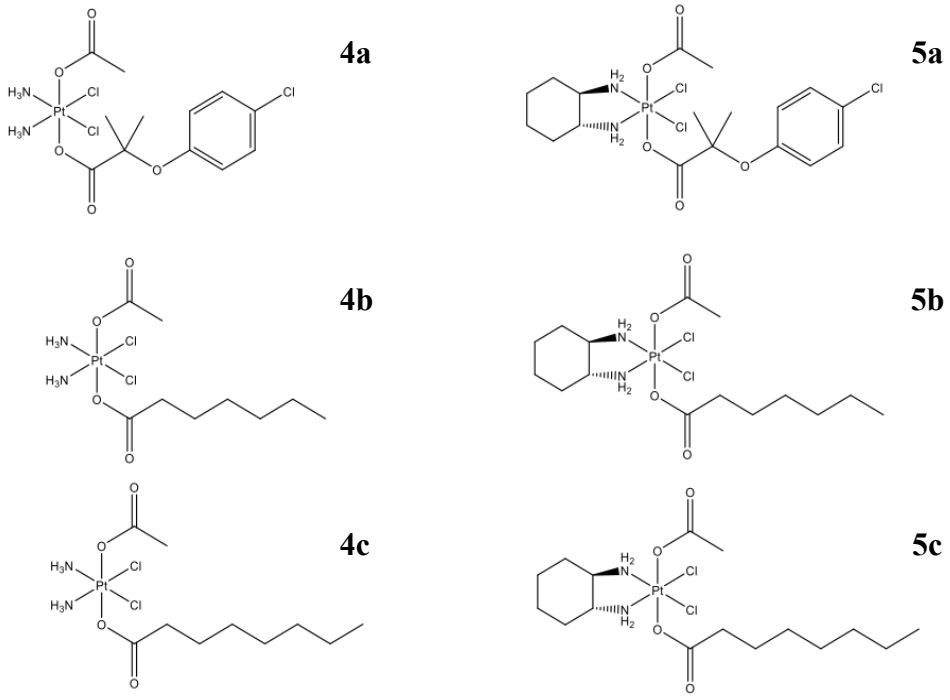


Figure 5.1: Sketch of the two series of Pt(IV) complexes under investigation.

# *5.2 Materials and methods*

## *5.2.1 Cell culture*

A2780 and HCT116 cell lines were purchased from ICLC or ECACC respectively, as described in Chapter 3. HT29 and SW480, are a kind gift of Prof. Claudia Cantoni (University of Genova, Italy) (Chapter 4). A2780 and SW480 were grown in RPMI 1640, whereas McCoy's 5A medium was used for HCT 116 and HT29. All media were supplemented, and cell culture and treatment were carried out, as previously described in Chapter 3.

## *5.2.2 Compounds and drug candidates*

The two series of Pt(IV) complexes under investigation were designed, synthetized and characterized in Prof. Osella's bioinorganic laboratory (University of Piemonte Orientale, DiSIT, Italy). In particular, complexes **4a-c** and **5a-c** were prepared starting from cisplatin or [$PtCl_2$(dach)], respectively, which was oxidized with hydrogen peroxide in acetic acid to get mono-hydroxido intermediates. The final step of the synthesis involves the substitution reaction of the axial hydroxido with CA, HA and OA [4].

In order to prepare the stock solutions of the complexes under investigation for the following biological tests, cisplatin was dissolved in 0.9% w/v NaCl aqueous solution brought to pH = 3 with HCl (final stock concentration 1 mM) (Chapter 3), oxaliplatin was dissolved in Milli-Q water (final stock concentration 2.5 mg $mL^{-1}$, 6.3 mM), whereas [$PtCl_2$(dach)] was freshly dissolved in DMSO (final stock concentration 5 mM) (Chapter 4). The Pt(IV) complexes **4a-4c** were dissolved in absolute ethanol (final stock concentration 3 mM), whereas **5a-5c** were dissolved in DMSO (final stock concentration 4 mM) and stored at -18 °C. The stock concentrations were confirmed with ICP-MS measurements. The mother solutions were diluted in complete medium to the required concentration range and, where present, the total co-solvent concentration never exceeded 0.1% v/v (this concentration was found to be non-toxic to the cells tested as control).

## *5.2.3 Antiproliferative activity*

The growth inhibition of the compounds under investigation was assessed by the use of the resazurin reduction assay, as described in detail in Chapter 3.

## *5.2.4 Cellular uptake*

A2780 cells were seeded in T25 flasks and allowed to grow until around 80% confluence. Then, the treatment was performed for 4 h with the complexes under investigations (10 μM) in complete medium. At time zero, 100 μL of medium was taken out from each sample to check the extracellular Pt concentration. At the end of the exposure, cells were washed three times with PBS, detached from the flasks using 0.05% Trypsin 1× with 2% EDTA (HyClone, Thermo Fisher) and harvested in fresh complete medium. The cell pellet was lysed in 1% w/v sodium dodecyl sulphate and the protein content was determined by means of the bicinchoninic acid method (BCA assay Kit, Pierce ThermoFisher), following manufacturer's instructions. This assay is based on the reduction of $Cu^{2+}$ to $Cu^{+}$ in alkaline conditions. The $Cu^{+}$ is then detected by reaction with BCA, which results in a purple product with absorbance near 562 nm. Since the production of $Cu^{+}$ is a function of protein content, the protein concentration of unknown samples was determined based on a standard curve [5]. The exact volume of the sample was determined by weight. The cell number was computed by a standard curve with known amount of the same cells. Control and cisplatin-treated cells showed the same values as those previously obtained with the method described in Chapter 3. Before the ICP-MS measurement, the $HNO_3$ was diluted to final 1% concentration. The level of Pt found in cells after drug treatment and normalized upon the cell number (cellular Pt uptake) was expressed as ng Pt per $10^6$ cells. In this work, the cellular Pt uptake was used, instead of AR, because the cells were treated with the same concentration of all the compounds under investigation.

## *5.2.5 3D-spheroids model*

3D-spheroids model (which is described later) from HCT 116 cells was obtained by using a microplate-based protocol, similar to those previously reported [6]. 500 cells per well were seeded in U-shaped, 96-well polypropylene plates, put on an orbital mixer (Rotamax 120, Heidolph Instruments) in an incubator (37 °C, 5% $CO_2$). After 4 days cells gave a 300–400 μm diameter spheroid. HCT 116 cells were chosen among the colon cancer cell lines under study since they better grow in these experimental conditions.

The spheroids (after medium removal by gentle aspiration) were challenged with drug-containing medium (200 μL per well) for 72 h, then drug-free medium was replaced twice a week until the experiment was stopped. At the same time points, pictures of at least three spheroids per each experiment were taken at 4× magnification and the dimensions of spheroids were assessed using the native Leica Application Suite software (version 2.0, Leica Microsystems) [7]. The spheroids volume was calculated from the mean diameter, and reported as fold change with respect to the time zero of the treatment ($4^{th}$ day after cell seeding).

## *5.2.6 Statistical analysis*

Statistical analysis was performed as previously described in Chapter 3.

## 5.3 Results and discussion

### 5.3.1 Antiproliferative activity

The half-maximal inhibitory concentrations, $IC_{50}$, were determined for the Pt(IV) prodrugs of **series 4** and **5**, along with the Pt(II) parental species as references. The complexes under investigation were tested on four human cancer cell lines: the Pt(II)-sensitive A2780 ovary adenocarcinoma cells and the cisplatin poorly sensitive (but oxaliplatin sensitive) HCT 116, HT29 and SW480 colon adenocarcinoma cells. Among the compounds tested, the **5a**-**5c** derivatives are the most active, showing $IC_{50}$ values in the nM range (Table 1).

Oxaliplatin was listed in Table 1 because it is the reference metallo-drugs in clinics, but it was excluded from the following comparisons because of its slower activation with respect to all its dichlorido counterparts.

In order to extract a quantitative trend from the bulk of the $IC_{50}$ data, two comparisons on the dichlorido complexes have been done:

i) The ratio R of the activity of cisplatin-based Pt(IV) (**series 4**) vs. cisplatin and of the dach-based Pt(IV) (**series 5**) vs. [$PtCl_2$(dach)], against each cancer cell line, was calculated: R = $IC_{50}$ Pt(II) / $IC_{50}$ Pt(IV), as the antiproliferative activity is the inverse of the corresponding $IC_{50}$ value (Table 2).

ii) The ratio R′ of the activity of cisplatin itself and cisplatin-based Pt(IV) (**series 4**) and the activity of [$PtCl_2$(dach)] itself and dach-based Pt(IV) (**series 5**), against each colon cancer cell line, was calculated, *i.e.* R′ = $IC_{50}$ cisplatin-based / $IC_{50}$ dach-based (Table 3).

| Compound | $IC_{50}$ [μM] | | | |
|---|---|---|---|---|
| | **A2780** | **HCT116** | **HT29** | **SW480** |
| **cisplatin** | $(4.6\pm0.3)\times10^{-1}$ | 2.3±0.1 | 2.7±0.1 | 2.6±0.2 |
| **[$PtCl_2$(dach)]** | $(7.8\pm0.7)\times10^{-2}$ | $(2.7\pm0.3)\times10^{-1}$ | $(2.4\pm0.2)\times10^{-1}$ | $(1.8\pm0.1)\times10^{-1}$ |
| **oxaliplatin** | $(1.71\pm0.08)\times10^{-1}$ | 1.16±0.09 | $(9.2\pm0.8)\times10^{-1}$ | $(4.8\pm0.2)\times10^{-1}$ |
| **4a** | $(8.1\pm0.3)\times10^{-2}$ | $(3.1\pm0.5)\times10^{-1}$ | $(3.7\pm0.8)\times10^{-1}$ | $(3.3\pm0.2)\times10^{-1}$ |
| **5a** | $(1.6\pm0.4)\times10^{-3}$ | $(2.8\pm0.9)\times10^{-3}$ | $(3.4\pm0.7)\times10^{-3}$ | $(2.1\pm0.9)\times10^{-3}$ |
| **4b** | $(1.9\pm0.2)\times10^{-1}$ | $(8.7\pm0.9)\times10^{-1}$ | $(4.5\pm0.8)\times10^{-1}$ | $(4.1\pm0.9)\times10^{-1}$ |
| **5b** | $(3.1\pm0.2)\times10^{-3}$ | $(2.3\pm0.2)\times10^{-3}$ | $(1.6\pm0.6)\times10^{-3}$ | $(2.5\pm0.9)\times10^{-3}$ |
| **4c** | $(4.2\pm0.4)\times10^{-2}$ | $(5.1\pm0.3)\times10^{-1}$ | $(4.4\pm0.9)\times10^{-1}$ | $(4.4\pm0.8)\times10^{-1}$ |
| **5c** | $(3.6\pm0.6)\times10^{-3}$ | $(2.6\pm0.8)\times10^{-3}$ | $(2.2\pm0.7)\times10^{-3}$ | $(1.9\pm0.6)\times10^{-3}$ |

Table 1: Antiproliferative activity ($IC_{50}$) obtained after 72 h of treatment of ovarian A2780 and colon HCT 116, HT29 and SW480 cancer cells lines, with **series 4** and **series 5** complexes compared to cisplatin, [$PtCl_2$(dach)] and oxaliplatin. $IC_{50}$ data are means ± standard deviation of at least three independent replicates.

| Compound | R A2780 | R HCT 116 | R HT29 | R SW480 |
|---|---|---|---|---|
| **4a** | 6 | 7 | 7 | 8 |
| **5a** | 49 | 96 | 71 | 86 |
| **4b** | 2 | 3 | 6 | 6 |
| **5b** | 25 | 117 | 150 | 72 |
| **4c** | 11 | 5 | 6 | 6 |
| **5c** | 22 | 104 | 109 | 95 |

Table 2: The ratio R of the activity of cisplatin-based Pt(IV) (**series 4**) vs. cisplatin and the activity of dach-based Pt(IV) (**series 5**) vs. [$PtCl_2$(dach)] against each cancer cell. R = $IC_{50}$ Pt(II) / $IC_{50}$ Pt(IV). The calculated R values were rounded to the nearest integer.

| Compounds | R′ HCT 116 | R′ HT29 | R′ SW480 |
|---|---|---|---|
| **cisplatin / [$PtCl_2$(dach)]** | 9 | 11 | 14 |
| **4a / 5a** | 111 | 109 | 157 |
| **4b / 5b** | 378 | 281 | 164 |
| **4c / 5c** | 196 | 200 | 232 |

Table 3: The ratio R′ of the activity of cisplatin itself and cisplatin-based Pt(IV) (**series 4**) and the activity of [$PtCl_2$(dach)] itself and dach-based Pt(IV) (**series 5**) against each colon cancer cell line. R′ = $IC_{50}$ cisplatin-based / $IC_{50}$ dach-based. The calculated R′ values were rounded to the nearest integer.

The Pt(IV) complexes, either cisplatin- or dach-based, are more active than the corresponding Pt(II) derivatives, about one or two orders of magnitude, respectively (R ranges from 2 to 11 for **series 4** vs. cisplatin and from 22 to 150 for **series 5** vs. [$PtCl_2$(dach)]). Moreover the presence of the dach carrier ligand confers selectivity towards colon cancer cells with respect to the two ammine carrier ligands, being this selectivity markedly higher for the Pt(IV) complexes (R′ ranges from 9 to 14) than for the Pt(II) derivatives (R′ ranges from 109 to 378).

As a possible contribution to such selectivity, it has been reported that the final [$PtCl_2$(dach)] metabolite generates Pt-DNA adducts structurally different from those caused by cisplatin, hence having different mechanisms for their recognition and processing [8].
Furthermore, the highly tumorigenic HCT 116 cells seemed to be more sensitive to the presence of the dach ligand in the Pt(IV) complexes under investigation, compared to HT29 and SW480 cells.

## *5.3.2 Cellular uptake*

Cellular uptake was measured in A2780 and HCT 116 after 4h CT with the Pt(IV) compounds under investigation and their Pt(II) counterparts. All Pt(IV) complexes were accumulated into the cells to a much greater extent compared to their Pt(II) parental compounds (Figure 5.2), due to the presence of MCFA axial ligands, increasing their lipophilicity. Moreover, the dach-based complexes **5a**, **5b** and **5c** were more internalized than the cisplatin-based ones (**4a**, **4b** and **4c**) in both cell lines (Figure 5.2), as the dach carrier ligand itself contributes significantly to the increase in lipophilicity [4].

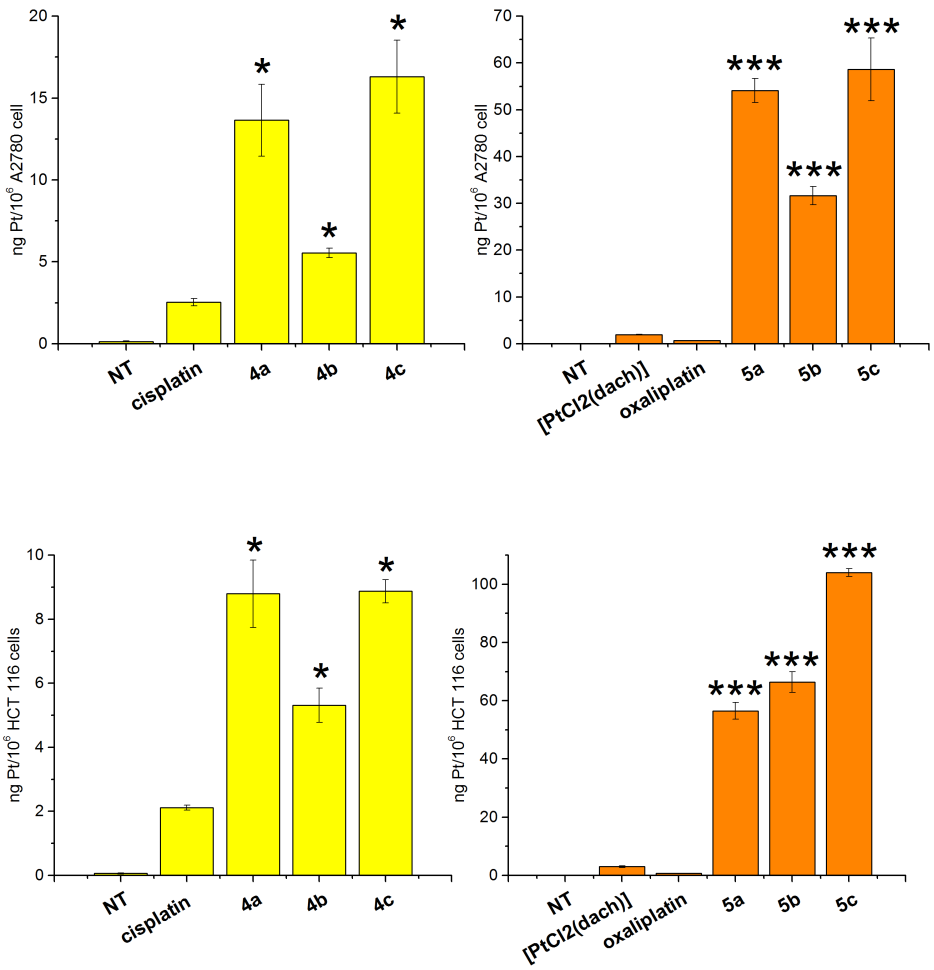


Figure 5.2: Cellular accumulation (ng Pt/ $10^6$ cells) measured on A2780 (upper graphs) and HCT 116 (lower graphs) cells after 4 h treatment with 10 µM cisplatin- (yellow bars) and dach-based (orange bars) complexes compared to their Pt(II) parent compounds. Data are means ± standard deviations of three experiments in triplicate, compared with a one-way ANOVA-Tukey test (* $p<0.05$; ** $p<0.01$; *** $p<0.001$).

### *5.3.3 Prolonged antitumor effect using 3D spheroids model*

The 2D cell monolayer culture model, resulting in a well-controlled and homogeneous environment, facilitates manipulation and microscopic analysis, but is limited by cellular confluence and growth stop. Moreover, such cultures do not perfectly simulate the solid tumor tissue and the associated cancer cellular microenvironment. For these reasons, several kinds of 3D cell models have been proposed in the field of drug discovery and screening, since they simulate features similar to those of *in vivo* tumor tissue. Among these models, multicellular tumor spheroids (MCTS) are one of the most common and versatile scaffold-free methods for 3D cell culture. They are spherical cell aggregates, consisting of an outer ring of proliferating cells (simulating the *in vivo* situation of cancer cells adjacent to blood vessels), of an inner concentric layer of quiescent cells and, finally, of a hypoxic/necrotic core (Figure 5.3). Thus, MCST resemble large solid tumors with respect to their volume growth kinetics, microenvironment and morphological features, gradients of oxygen and nutrient distribution, cell proliferations and drugs access [9]. In addition, they allow the extension of viability experiments for longer times (approximately up to two weeks) than their 2D counterparts, hence distinguishing between antiproliferative activity (growth decrease or arrest for a relatively short period and then re-growth) and cytotoxic activity (no re-growth at all) [10] [11].

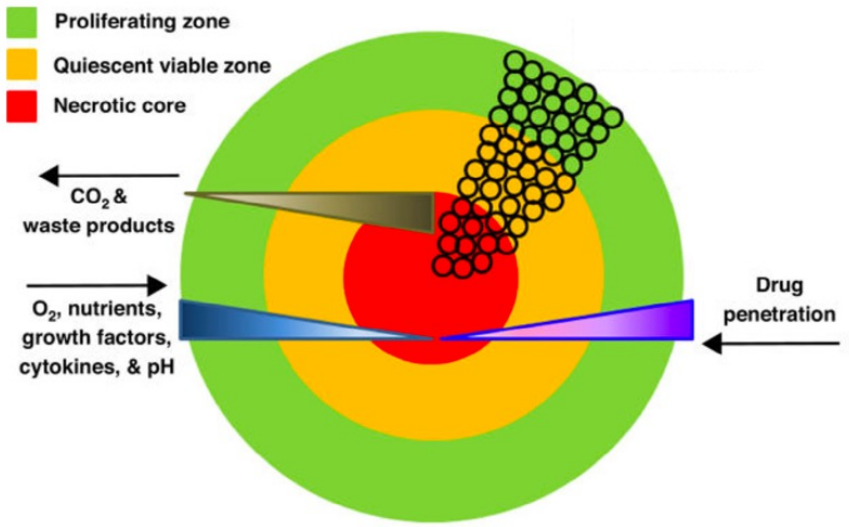


Figure 5.3: Concentric organization of tumor cells in 3D multicellular spheroids. The picture is a modification of that reported in literature [9].

MCST obtained from HCT 116 colon cancer cells (Figure 5.4) were challenged at around $IC_{50}$ and 10 x $IC_{50}$ concentrations of all the Pt complexes under investigation for three days, as usually performed in 2D monolayers models, followed by 11 days of recovery in fresh drug-free medium [12].

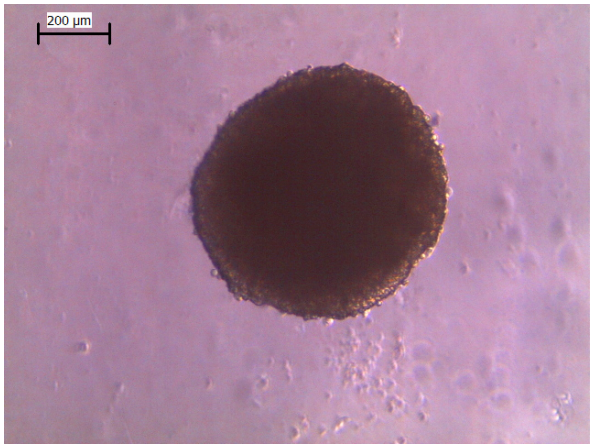


Figure 5.4: Image of MCTS obtained from HCT 116 cancer cells.

As shown in Figure 5.5, when HCT 116 spheroids were treated with Pt(II)-based molecules at concentration ten times higher than the $IC_{50}$ value, the spheroids lost their integrity, giving rise to unshaped aggregates (volume dropped to zero). However, spheroids treated at the $IC_{50}$ value with cisplatin and $[PtCl_2(dach)]$ showed an initial growth arrest, followed by a volume decrease after the 10$^{th}$ day (Figure 5.5 a and b), whereas oxaliplatin caused only a negligible effect (Figure 5.5 c).

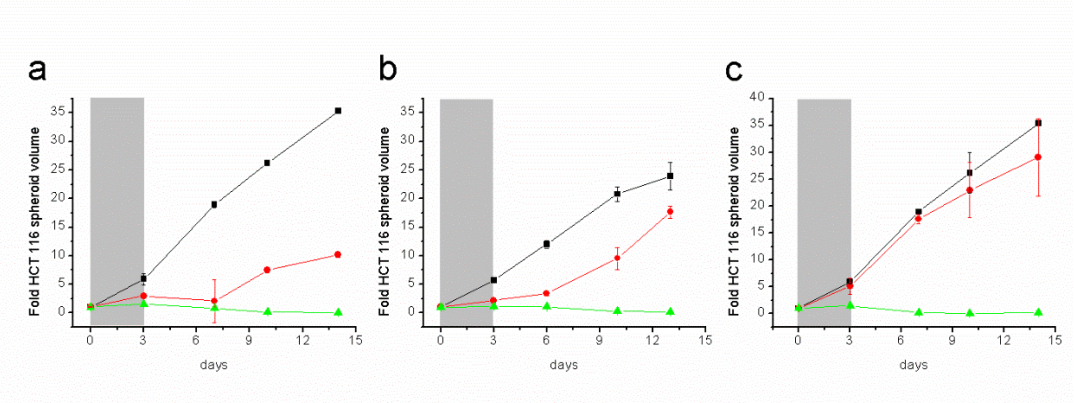


Figure 5.5: Fold volume increase of HCT 116 cancer cell spheroids treated from time zero (corresponding to compact aggregates with 400 μm diameter) to day 3 (grey lane) with around $IC_{50}$ concentration (red circles) or 10 x $IC_{50}$ concentration (upwards green triangles), with respect to control (black squares). The recovery in fresh medium and the size assessment were performed twice a week. Treatment details: a) cisplatin at 2.5 and 10 μM, b) $[PtCl_2(dach)]$ at 0.3 and 3 μM; c) oxaliplatin at 1 and 10 μM.

On the contrary, the Pt(IV) complexes exerted a prolonged antiproliferative action (Figure 5.6 and Figure 5.7). Indeed, spheroids treated with **4b**, **4c**, **5b** and **5c** collapsed, both for $IC_{50}$ value and for ten times higher concentration treatment (Figure 5.6 b, c, e, f), whereas **4a** and **5a** seemed to be slightly less active than the others (Figure 5.6 a, d). Furthermore, the dach-based Pt(IV) derivatives showed a higher potency compared to the corresponding cisplatin-based Pt(IV) complexes on HCT 116 spheroids. In this case the activity is enhanced by three orders of

magnitude, being in the micromolar range for **series 4** and in the nanomolar range for **series 5** complexes.

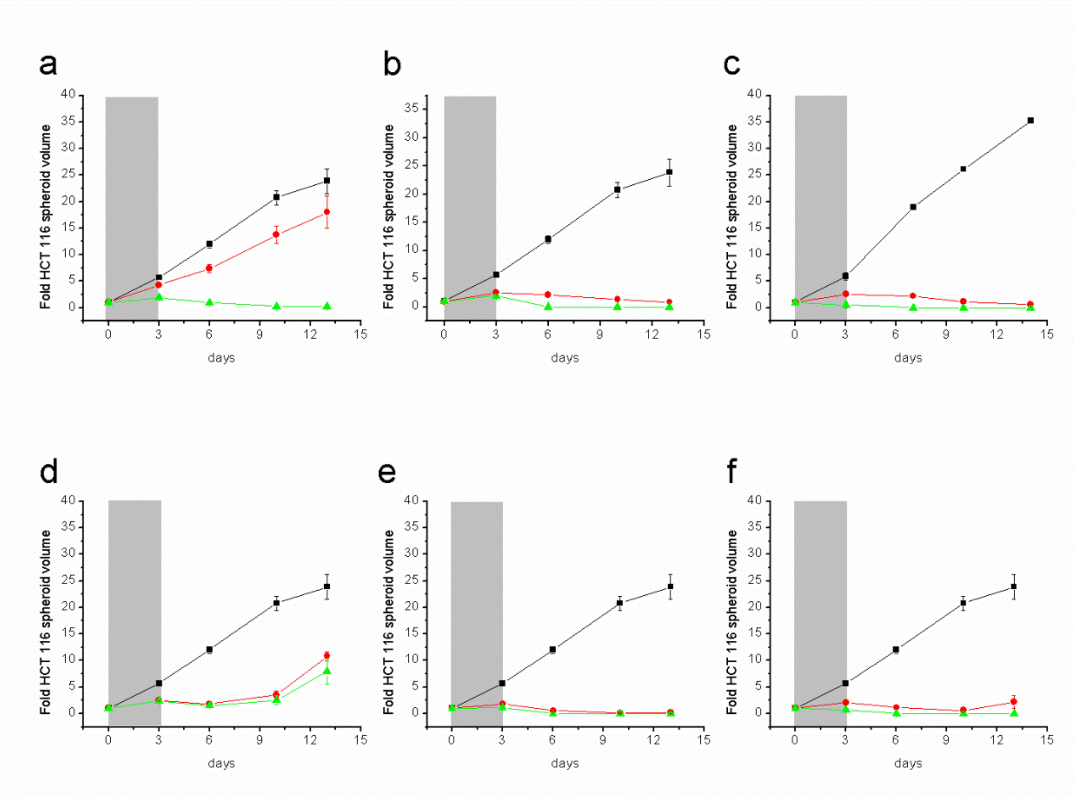


Figure 5.6: Fold volume increase of HCT 116 cancer cell spheroids treated with: a) **4a** at 0.3 and 3 μM, b) **4b** at 1 and 10 μM, c) **4c** at 0.3 and 3 μM, d) **5a** at 0.3 and 3 nM, e) **5b** at 1 and 10 nM, f) **5c** at 0.5 and 5 nM.

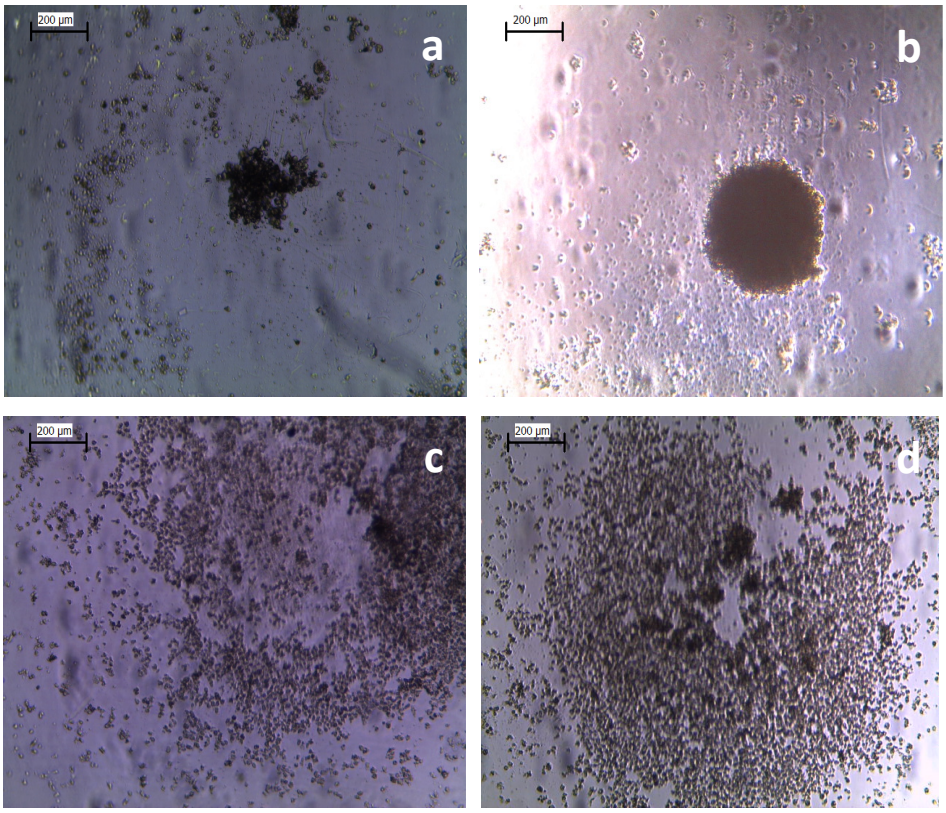


Figure 5.7: Image of MCTS obtained from HCT 116 after 72h of treatment with [$PtCl_2$(dach)] at 10 x $IC_{50}$ concentration (a) or $IC_{50}$ concentration (b) or with **5c** at 10 x $IC_{50}$ concentration (c) or $IC_{50}$ concentration (d).

## *5.4 Conclusions*

The two series of new combo Pt(IV) complexes, based on cisplatin or [$PtCl_2$(dach)] skeleton, exerted a marked antiproliferative activity, both on 2D monolayer cell cultures and on 3D multicellular spheroids, compared to their Pt(II) counterparts. This increase in antiproliferative activity is certainly due to a considerable accumulation in cancer cells of Pt(IV) prodrugs, bearing a lipophilic MCFA axial ligand (*i.e* CA, HA, OA); while the dach carrier ligand itself significantly contributes to such an escalation of lipophilicity. Moreover, the dach-based series showed a higher selectivity towards colon cancer cells, particularly on HCT 116, and the OA seemed to be the most effective synergistic adjuvant for Pt drugs on the tested cell lines.

# *References*

[1] Y. Yokoyama, B. Xin, T. Shigeto, M. Umemoto, A. Kasai-Sakamoto, M. Futagami, S. Tsuchida, F. Al-Mulla and H. Mizunuma. Clofibric acid, a peroxisome proliferator-activated receptor alpha ligand, inhibits growth of human ovarian cancer. *Mol Cancer Ther* (2007) 6, 1379-1386.

[2] V. Novohradsky, I. Zanellato, C. Marzano, J. Pracharova, J. Kasparkova, D. Gibson, V. Gandin, D. Osella, V. Brabec. Epigenetic and antitumor effects of platinum (IV)-octanoato conjugates. *Sci Rep* (2017) 7, Article number 3751.

[3] KN. Tan, TS. McDonald and K. Borges, in *Bioactive Nutraceuticals and Dietary Supplements in Neurological and Brain Disease*, eds. R. R. Watson and V. R. Preedy, Academic Press, San Diego (2015) pp. 461-473.

[4] E. Gabano, M. Ravera, E. Perin, I. Zanellato, B. Rangone, MJ. McGlinchey, D. Osella. Synthesis and characterization of cyclohexane-1R,2R-diamine-based Pt(IV) dicarboxylato anticancer prodrugs: their selective activity against human colon cancer cell lines. *Dalton Trans* (2019) 48(2), 435-445.

[5] JM. Walker. The bicinchoninic acid (BCA) assay for protein quantitation. *Methods Mol Biol* (1994) 32, 5-8.

[6] A. Ivascu, M. Kubbies. Rapid generation of single-tumor spheroids for high-throughput cell function and toxicity analysis. *J Biomol Screen* 11(2006) 922–932.

[7] L. Kamentsky, T. R. Jones, A. Fraser, M. A. Bray, DJ. Logan, KL. Madden, V. Ljosa, C. Rueden, KW. Eliceiri, AE. Carpenter. Improved structure, function and compatibility for CellProfiler: modular high-throughput image analysis software. *Bioinformatics* (2011) 27, 1179–1180.

[8] T. Alcindor, N. Beauger. Oxaliplatin: a review in the era of molecularly targeted therapy. *Curr Oncol* (2011) 18, 18–25.

[9] S. Sant, PA. Johnston. The production of 3D tumor spheroids for cancer drug discovery. *Drug Discov Today Technol* (2017) 23:27-36.

[10] CR. Thoma, M. Zimmermann, I. Agarkova, J. M. Kelm, W. Krek. 3D cell culture systems modeling tumor growth determinants in cancer target discovery. *Adv Drug Delivery Rev* (2014) 69, 29–41.

[11] M. Zanoni, F. Piccinini, C. Arienti, A. Zamagni, S. Santi, R. Polico, A. Bevilacqua, A. Tesei. 3D tumor spheroid models for in vitro therapeutic screening: a systematic approach to enhance the biological relevance of data obtained. *Sci Rep* (2016) 6, 19103.

[12] I. Zanellato, I. Bonarrigo, D. Colangelo, E. Gabano, M. Ravera, M. Alessio, D. Osella. Biological activity of a series of cisplatin-based aliphatic bis(carboxylato) Pt(IV) prodrugs: how long the organic chain should be? *J Inorg Biochem* (2014) 140, 219–227.

# *Chapter 6*

# *Antiproliferative Activity of Pt(IV) Conjugates Containing the Non-Steroidal Anti-Inflammatory Drugs (NSAIDs) Ketoprofen and Naproxen*

## *6.1 Introduction*

As reported in Chapter 1, several agents with different cellular targets have been coordinated to Pt(IV) complexes in order to obtain Pt(IV) bifunctional, or better multifunctional, species. For example, some of them contain the inhibitors of COX enzymes. There are two main isoform of COX, COX-1 and COX-2, responsible for the formation of biological mediators of inflammation (see Chapter 3). COX-1 is constitutively expressed in most tissue, whereas COX-2 level is generally very low, unless induced in response to inflammatory and other physiological stimuli. Moreover, COX-2 expression is also related to pathological processes. Indeed, enhanced COX-2 expression is found in several tumors; thus, it seems to play a role in carcinogenesis [1]. For these reasons, COX inhibitors, as the large family of Non-Steroidal Anti-inflammatory Drugs (NSAIDs), have been suggested for chemoprevention, especially for colon adenocarcinoma [2]. NSAIDs are a chemically different class of drugs, employed for the treatment of fever, pain or inflammation. They exert analgesic and antipyretic effects through the inhibition of COX activity, which catalyze the conversion of arachidonic acid into prostaglandin

$H_2$, which is the precursor for the synthesis of mediators of inflammation as prostaglandins, prostacyclin and thromboxane $A_2$, collectively known as eicosanoids [3] [4]. Unfortunately, NSAIDs exerted a modest tumor growth inhibition when employed as a single agent; however they showed a promising anticancer activity on human colon carcinoma cells, when tested as adjuvant agents [5]. Up to now, the mechanism of action of such anticancer adjuvant effects is not completely understood, but both COX-dependent and -independent pathways seem to play a key role [3] [4].

Classical NSAIDs, including aspirin, naproxen, ibuprofen, indomethacin and several others, inhibit both COX-1 and COX-2. Regrettably, NSAIDs seem to exert the anticancer adjuvant properties by inhibiting the inducible COX-2 only, whereas the inhibition of the constitutive COX-1 is associated to undesirable side effects, such as gastrointestinal toxicity [6] [7] [8].

The first example of a Pt(IV) complex bearing an NSAID as axial ligand, *i.e* acetylsalicylic acid (2-acetoxybenzoic acid, aspirin), is known as asplatin or platin-A (Figure 6.1). This compound showed an antiproliferative activity comparable or slightly higher than that of cisplatin alone and of an equimolar mixture of cisplatin and aspirin [9] [10] [11]. Moreover, asplatin exhibited a better *in vivo* antitumor efficacy, with milder toxicity, compared to cisplatin [10].

Following this research, the study of several Pt(IV) complexes, based on cisplatin, oxaliplatin, or kiteplatin (an isomeric form of $[PtCl_2(dach)]$, introduced in Pt-based drug research many years ago [12]), and containing NSAIDs (*i.e* indomethacin, ibuprofen or wogonin) as axial ligands, has been reported in literature [13] [14] [15].

In this work, two new cisplatin-based Pt(IV) complexes, bearing ketoprofen 2-(3-benzoylphenyl)propanoic acid) (**6**) or naproxen (2-(6-methoxynaphthalen-2-yl)propanoic acid) (**7**) as axial ligand (Figure 6.1), were studied against a panel of human cancer cell lines. Ketoprofen and naproxen are two conventional NSAID propionic acid derivates, acting as inhibitors of both COX-1 and COX-2 [8] [16].

Cisplatin, oxaliplatin, but also asplatin and the free axial ligands (*i.e* ketoprofen and naproxen) were also tested for comparison purposes.

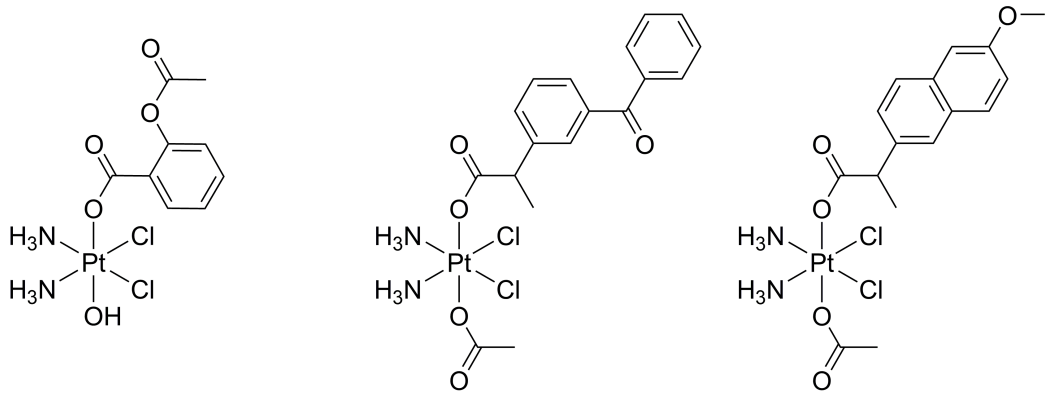

**Asplatin or platin-A** **6** **7**

Figure 6.1: Sketch of the Pt(IV) complexes under investigation.

# *6.2 Materials and methods*

## *6.2.1 Cell culture*

A2780, A549 and HCT116 cell lines were purchased from ICLC or ECACC, as described in Chapter 3, whereas HT29 and SW480 are a kind gift of Prof. Claudia Cantoni (University of Genova, Italy) (Chapter 4). Biphasic malignant pleural mesothelioma cell line, MSTO-211H was purchased from ICLC (ICLC HL01018). RPMI 1640 medium was used for A2780, A549, SW480 and MSTO-211H cell lines, whereas HCT 116 and HT29 cells were grown in McCoy's 5A medium. All media were supplemented, and cell culture and treatment were carried out, as previously described in Chapter 3.

## *6.2.2 Compounds and drug candidates*

The Pt(IV) complexes under investigation were designed, synthetized and characterized in Prof. Osella's bioinorganic laboratory (University of Piemonte Orientale, DiSIT, Italy). In particular, complexes **6** and **7** were prepared starting from cisplatin, which was oxidized with hydrogen peroxide in acetic acid to get the corresponding mono-hydroxido intermediate. The presence of a carboxylic functionality in the structure of ketoprofen and naproxen allows an easy coordination to the Pt(IV) core through an "esterification" reaction of the hydroxido synthon with the acyl chloride of the NSAIDs [17]. Whereas the reference compound asplatin has been prepared according to the procedure reported by Dhar *et al.*, by reacting (*OC*-6-44)-diamminedichloridodihydroxidoplatinum(IV) with the anhydride of acetylsalicylic acid [18].

In order to prepare the stock solutions of the complexes under investigation for the following biological tests, cisplatin was dissolved was dissolved in 0.9% w/v NaCl aqueous solution brought to pH = 3 with HCl (final stock concentration 1 mM) (Chapter 3), whereas oxaliplatin was dissolved in Milli-Q water (Chapter 4). All Pt(IV) complexes were dissolved in absolute ethanol (final stock concentration 5 mM for asplatin and **6**, and 1 mM for **7**) and stored at -18 °C. The mother solutions were diluted in complete medium to the required concentration range and, where present, the total co-solvent concentration never exceeded 0.2% (this concentration was found to be non-toxic to the cells tested as control). The stock concentrations were confirmed with ICP-MS measurements. Aspirin (Sigma-Aldrich), ketoprofen and naproxen (Alfa Aesar-Thermo Fisher Scientific) were freshly dissolved in 0.1 M $NaHCO_3$ (final stock concentration 5 mM for aspirin and ketoprofen and 2.5 mM for naproxen).

## 6.2.3 Antiproliferative activity and combination index

The growth inhibition of the compounds under investigation was assessed by the use of the resazurin reduction assay, as described in detail in Chapter 3.

In order to verify the synergy between NSAIDs and cisplatin, HCT 116 and HT-29 cells were treated with increasing concentrations of cisplatin, ketoprofen or naproxen, and a mixture cisplatin:NSAIDs in a fixed 1:500 molar ratio, according to their respective $IC_{50}$ values. The experiment was repeated three times. According to the method of Chou and Talalay [19] [20] [21], the interaction between cisplatin and NSAIDs was computed in terms of combination index (*CI*) for mutually non-exclusive drugs by using the following equation:

$$CI = \frac{C1_m}{C1_a} + \frac{C2_m}{C2_a} + \frac{C1_m C2_m}{C1_a C2_a}$$

where *C*1 and *C*2 are the concentrations of drugs 1 and 2 used in the mix ($C1_m$ and $C2_m$) or alone ($C1_a$ and $C2_a$) to obtain the same fraction affected ($f_{a,}$), *i.e*. the fraction of cells affected by such a treatment. Based on the actual experimental data, the *CI* values were calculated by solving the equation over an entire range of $f_a$ (from 0.1 to 0.9, obtained from 90 to 10% level of residual viability, upon sigmoidal regression). These data were then used to generate *CI vs.* $f_{a,}$ plots, which is an effect-oriented means of presenting synergism or antagonism. *CI* is defined in such a way that $CI = 1$ indicates simple additive effect, and $CI < 1$ and a $CI > 1$ indicate synergism and antagonism, respectively.

## 6.2.4 Cellular uptake

Around $5x10^6$ A2780 cells were seeded in 25 $cm^2$ flasks and allowed to growth until around 80% of confluence and then treated for 4h with the complexes under investigations (10 μM) in complete medium. Then, the experiment was carried out as previously described in detail in Chapter 3.

## *6.2.5 Quantitative PCR (RT-qPCR)*

HCT 116 and A549 cells ($2\times10^6$) were seeded on 25 $cm^2$ flasks and allowed to attach for 24 h. The treatment was performed with equitoxic concentrations (*i.e.*, HCT 116: 3 μM for both complexes **6** and **7**, 1 mM for both ketoprofen and naproxen, and 30 μM for cisplatin; A549: 5 μM for both complexes **6** and **7**, 1 mM for both ketoprofen and naproxen, and 50 μM for cisplatin). After 24 h, RNA was extracted and purified by DNAse treatment with a commercial kit (RNASPIN MINI, GE Healthcare); then it was quantified, checked for purity and retrotranscribed (RT) to cDNA as previously described in Chapter 3. RT-qPCR was performed in triplicate on each sample (10 ng) to detect the expression levels of BAD, BAX, COX-2, NAG-1, and the reference genes RNA18S, HPRT1, GAPDH. Primer sequences were designed using the NCBI tool and checked for target specificity including splice variants (Table 1). Reactions and all data analyses were performed as previously described in Chapter 3.

| Gene | Accession n. | Forward | Reverse | Product length (bp) |
|---|---|---|---|---|
| COX-2 | M90100.1 | CCCTGAGCATCTACGGTTTG | CATCGCATACTCTGTTGTGTTC | 107 |
| GAPDH | NG_007073.2 | ATCCCTGAGCTGAACGGGAA | GGCAGGTTTTTCTAGACGGC | 99 |
| HPRT1 | NM_000194.2 | TTGCTTTCCTTGGTCAGGCA | ATCCAACACTTCGTGGGGTC | 85 |
| RNA18SN1 | NR_145820.1 | CGTCTGCCCTATCAACTTTCG | TGCCTTCCTTGGATGTGGTAG | 124 |
| BAX | NM_001291428.1 | GACCATCTTTGTGGCGGGAG | GAGGAAAAACACAGTCCAAGGC | 94 |
| BAD | NM_004322.3 | GAGACCTGTGCGCCGTCA | AGGACCTCAGTCTCCCCTCAG | 74 |
| Bcl2a | NM_000633.2 | CTTTGAGTTCGGTGGGGTCA | GGGCCGTACAGTTCCACAAA | 162 |
| NAG-1/GDF15 | NM_004864.3 | TTGCGGAAACGCTACGAGG | GCACTTCTGGCGTGAGTATCC | 115 |



Table 1: Analysis of relative gene expression data using RT-qPCR. The NCBI accession number is reported along with the 5'-3' sequence of the forward and reverse primer and the expected product length.

### 6.2.6 Statistical analysis

Statistical analysis was performed as previously described in Chapter 3.

## 6.3 Results and discussion

### 6.3.1 Antiproliferative activity and combination index

The half-maximal inhibitory concentrations, $IC_{50}$, were determined for **6** and **7**, along with the clinically-employed reference complexes cisplatin and oxaliplatin. Also asplatin, and free ketoprofen, and naproxen were tested for comparison purposes. Six human cancer cell lines were challenged with the compounds under investigation: lung carcinoma A549, colon adenocarcinoma HT29, HCT 116 and SW480, ovarian endometrial adenocarcinoma A2780, and malignant pleural mesothelioma (MPM) with mixed or biphasic phenotype, consisting of both epithelioid and sarcomatoid components, MSTO-211H. The last cell line was added to the panel since promising preclinical results have been reported on the activity of celecoxib on MPM, albeit apparently independent of COX-2 protein level [22].

Before the viability tests the level of COX-2 expression was evaluated in these cell lines by quantitative reverse transcription polymerase chain reaction (RT-qPCR) [23] [24], resulting observably high in A549 and HT29, medium in HCT 116, low in MSTO-211H, and very low in A2780 and SW480 (Figure 6.2).

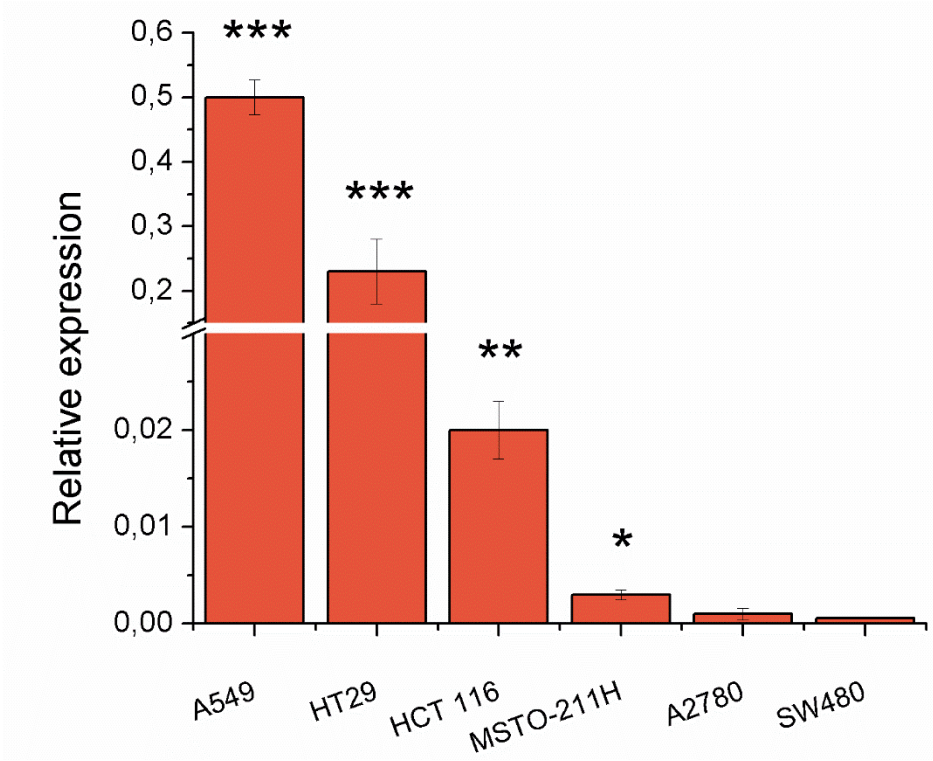


Figure 6.2: COX-2 relative expression in A549, HT29, HCT 116, MSTO-211H, A2780, and SW480 cells. Data are means ± standard deviation of at least three independent replicates and were compared by means of a one-way ANOVA analysis of variance-Tukey test (*$p < 0.05$; **$p < 0.01$; ***$p < 0.001$ *vs.* SW480).

As shown in Table 2, at the first glance, the Pt(IV) complexes **6** and **7** appear to be more active than cisplatin, oxaliplatin, and also asplatin on all cell lines tested ranging from 2 to 24 times. Moreover, the Pt(IV) compound naproxen-bearing **7**, is (almost always) slightly more active than the ketoprofen-bearing one **6**.

| Compound | $IC_{50}$ (μM) | | | | | |
|---|---|---|---|---|---|---|
| | **A549** | **HT29** | **HCT 116** | **MSTO-211H** | **SW480** | **A2780** |
| cisplatin | 3.60±0.90 | 2.72±0.39 | 2.30±0.30 | 1.33±0.35 | 2.27±0.12 | 0.460±0.110 |
| oxaliplatin | 0.74±0.25 | 0.92±0.08 | 1.16±0.09 | 1.01±0.55 | 0.48±0.02 | 0.171±0.008 |
| aspirin | 1672±152 | 2835±885 | 2578±772 | 639±374 | 1607±386 | 1597±455 |
| ketoprofen | 725±69 | 828±229 | 914±185 | 518±296 | 830±173 | 676±36 |
| naproxen | 701±28 | 764±158 | 640±91 | 427±159 | 927±257 | 353±64 |
| asplatin | 6.4±2.7 | 4.42±0.21 | 1.50±0.083 | 1.74±0.21 | 0.217±0.07 | 0.552±0.123 |
| **6** | 0.825±0.388 | 0.486±0.235 | 0.184±0.088 | 0.198±0.035 | 0.0948±0.023 | 0.063±0.033 |
| **7** | 0.486±0.075 | 0.313±0.186 | 0.149±0.076 | 0.161±0.040 | 0.0844±0.0287 | 0.045±0.016 |

Table 2: Antiproliferative activity ($IC_{50}$) obtained after 72 h of treatment of a panel of cancer cell lines (lung A549, colon HT29, HCT 116 and SW480, ovarian A2780 and MPM MSTO-211H cancer cell lines). $IC_{50}$ data are means ± standard deviation of at least three independent replicates.

In order to extract quantitative trends from the bulk of the $IC_{50}$ data, the ratio R of the activity of cisplatin-based Pt(IV) derivatives (*i.e* asplatin, **6**, and **7**) *vs.* the activity of parent cisplatin against each cancer cell has been calculated (Table 3). As previously reported in Chapter 5, since the antiproliferative activity is the inverse of the corresponding $IC_{50}$ value, it follows that: R = $IC_{50}$ (cisplatin) / $IC_{50}$ (Pt(IV) conjugates. Interestingly, the trend of the R values does not follow the level of COX-2 expression. In particular, among the colon cancer cell lines, HCT 116 and SW480 cells, which have lower level of COX-2 with respect to HT29, resulted to be more sensitive to treatments with **6** and **7**. From this reason, the antiproliferative activity seems to be more related to the lipophilicity of the complexes [17] than to the COX-2 expression in these tumor cell lines. Also the antiproliferative activity of the free NSAIDs tested seems to be unrelated to the COX-2 expression, as the $IC_{50}$ values of ketoprofen and naproxen resulted quite similar (in the low mM range) in these cancer cell lines.

| Compound | A549 | HT29 | HCT 116 | MSTO-211H | SW480 | A2780 |
|---|---|---|---|---|---|---|
| asplatin | 0.56 | 0.62 | 2.0 | 0.75 | 1.1 | 0.83 |
| **6** | 4.4 | 5.6 | 17 | 6.7 | 24 | 7.3 |
| **7** | 7.4 | 8.7 | 20 | 8.3 | 27 | 10 |

Table 3: The ratio R of the activity of Pt(IV) conjugates vs. cisplatin against each cancer cell line. R = $IC_{50}$ cisplatin / $IC_{50}$ Pt(IV) complexes.

Moreover, the combination index (CI) values between free cisplatin and the two NSAIDs (*i.e* ketoprofen and naproxen) were calculated for HT29 and HCT 116 , two colon cancer cell lines showing high and medium COX-2 expression, respectively. In all cases, CIs resulted almost additive (around 1) for both cell lines, once again independently from COX-2 expression (Figures 6.3 and 6.4).

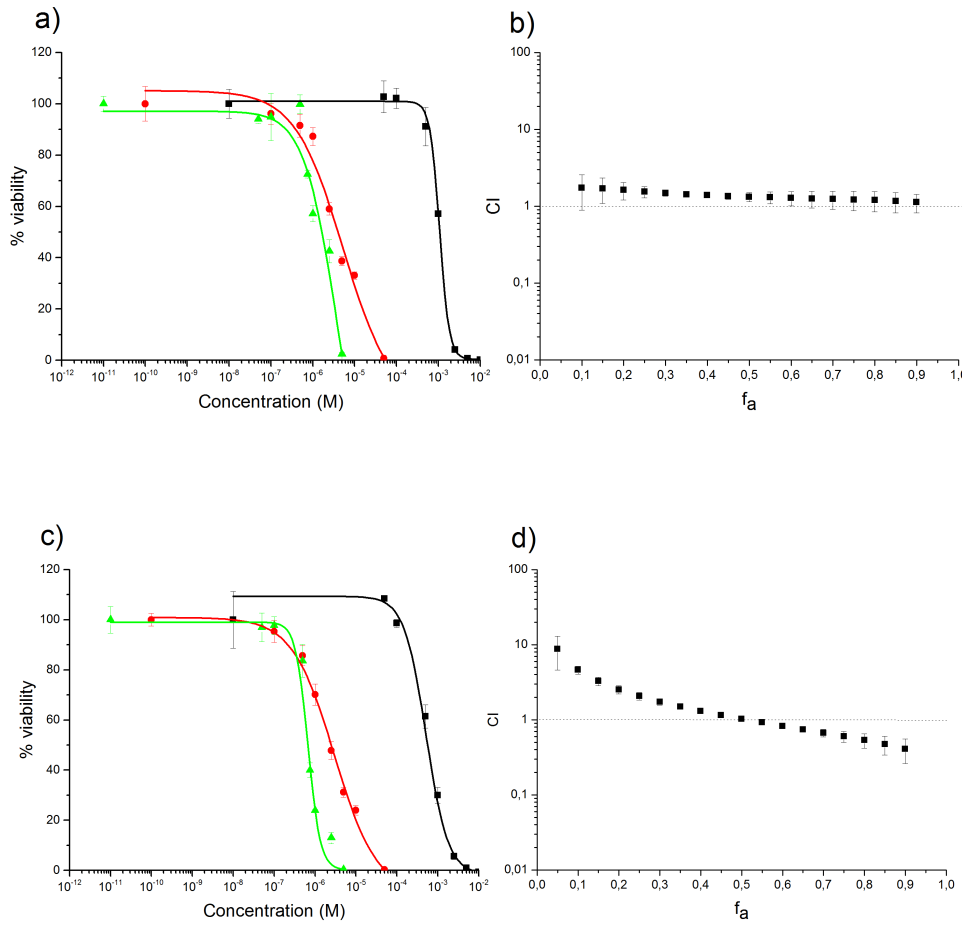


Figure 6.3: a) Residual HCT 116 viability data and concentration response curves (four parameters logistic function) after 72 h of treatment with cisplatin (red circles), ketoprofen (black squares) and a mixture of cisplatin + ketoprofen (final cisplatin:ketoprofen ratio = 1:500, green upward triangles). Data are means ± standard deviation of at least three replicates. b) Fraction affected ($f_a$) data for the 1:500 cisplatin:ketoprofen mix were used to obtain the Combination Index (CI) value by using the equation of Chou and Talalay for mutually non-exclusive drugs. c) Residual HCT 116 viability data and concentration response curves after 72 h of treatment with cisplatin (red circles), naproxen (black squares) and a mixture of cisplatin + naproxen (final cisplatin:naproxen ratio = 1:500, green upward triangles). d) Fraction affected ($f_a$) data for the 1:500 cisplatin:naproxen mix were used to obtain the CI value.

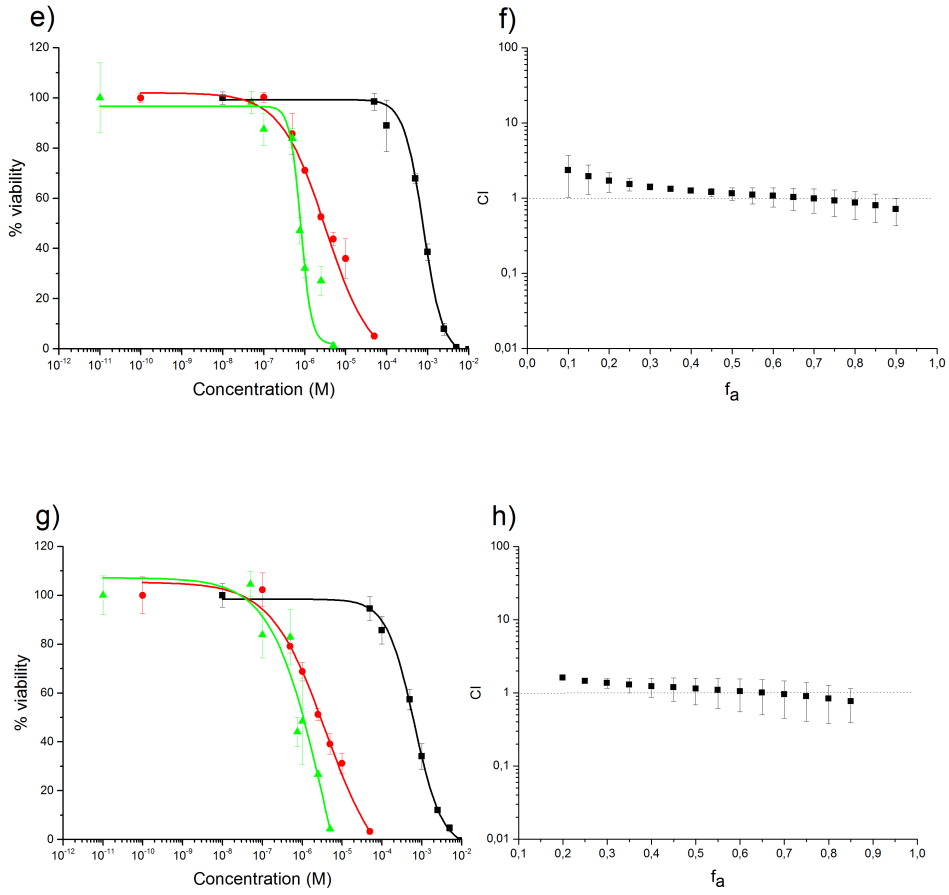


Figure 6.4: e) Residual HT29 viability data and concentration response curves after 72 h of treatment with cisplatin (red circles), ketoprofen (black squares) and a mixture of cisplatin + ketoprofen (final cisplatin:ketoprofen ratio = 1:500, green upward triangles). Data are means ± standard deviation of at least three replicates. f) Fraction affected ($f_a$) data for the 1:500 cisplatin:ketoprofen mix were used to obtain the CI value. g) Residual HT29 viability data and concentration response curves after 72 h of treatment with cisplatin (red circles), naproxen (black squares) and a mixture of cisplatin + naproxen (final cisplatin:naproxen ratio = 1:500, green upward triangles). h) Fraction affected ($f_a$) data for the 1:500 cisplatin:naproxen mix were used to obtain the CI value.

## *6.3.2 Cellular uptake*

The intracellular Pt accumulation of the Pt(IV) compounds **6** and **7**, was assessed on A2780 cells and compared to that of asplatin and cisplatin. This parameter is here expressed as accumulation ratio (AR), *i.e*. the ratio between the intracellular Pt concentration and the extracellular one, as reported in detail in Chapter 3. The AR trend exhibits the differences showed in antiproliferative activity, as the Pt(IV)-NSAID complexes **6** and **7** were more internalized than the others two reference compounds (Figure 6.5). These data confirm that the trend of activity can be explained in terms of lipophilicity of the compounds, which affects their cellular uptake. Thus, these combo Pt(IV) prodrugs enter cells via passive diffusion (one of the main mechanism of cellular uptake of Pt(IV) complexes, as previously mentioned in Chapter 3) more efficiently than their Pt(II) counterparts. Hence this can be defined as *synergistic cellular accumulation* [25].

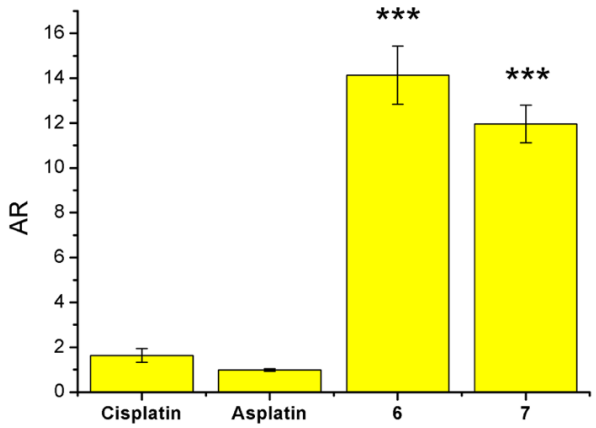


Figure 6.5: Accumulation ratio (AR) of cisplatin, asplatin, **6**, and **7**, measured on A2780 ovarian cancer cells treated for 4 h with 10 μM concentrations of the Pt complexes. Data are means ± standard deviation of at least three independent replicates and were compared by means of a one-way ANOVA analysis of variance-Tukey test (*p < 0.05; **p < 0.01; ***p < 0.001 vs. cisplatin).

## *6.3.3 Modulation of gene expression*

The apparent absence of relationship between COX-2 expression and sensitivity of different cell lines towards the Pt(IV) compounds **6** and **7** or free ketoprofen and naproxen suggests that these drugs might exert their antiproliferative activity through a COX-independent mechanism. Thus, to better understand the biological properties of these drugs a RT-qPCR analysis was performed on two cell lines, A549 and HCT 116, characterized by high and low COX-2 expression, respectively. In this experiment the variation of the expression of five genes (*i.e.*, BAD, BAX, BCL-2, COX-2 and NAG-1) was analyzed.

Since RT-qPCR experiment had to be carried out at shorter time at shorter time intervals (24h) compared to the $IC_{50}$ evaluation (72 h), preliminarily, to perform equitoxic treatments with the Pt(IV) compounds **6**, **7**, or the corresponding free NSAIDs, the $IC_{50}$ values after 24 h of continuous treatment were obtained.

As described in detail in Chapter 1, the main goal of anticancer agents is to increase the levels of pro-apoptotic proteins, as BAX and BAD, or decrease that of anti-apoptotic ones, as BCL-2. Moreover, as previously mentioned, both COX-dependent and -independent pathways seem to play a role in the antitumorigenic mechanism of NSAIDs. Indeed, recent studies have reported the existence of the NSAID activated gene (NAG-1), which is involved in cancer development and progression [26]. It has been demonstrated that the induction of NAG-1 expression by NSAIDs is involved in pro-apoptotic and anticancer activity, both *in vitro* and *in vivo* [27]. Importantly, it is not influenced by COX expression [28], thus, the induced expression of NAG-1 can be related with the antitumorigenic action of NSAIDs, as a COX-independent mechanism [29].

As shown in Figure 6.6, cisplatin, **6** and **7**, had a similar effect on the expression of pro- and anti-apoptotic genes in both cell lines, indicating that cisplatin released by the activation by reduction of the Pt(IV) complexes (described in Chapter 1), plays the major role. Particularly, their main effects was the downregulation of anti-

apoptotic BCL-2, more marked in A549 than in HCT 116 cells, and the upregulation of pro-apoptotic BAX and BAD. On the contrary, contrasting but negligible effects (*i.e.* no changes compared to the regulation threshold) were caused by free ketoprofen and naproxen. In addition, Pt(IV) conjugates and free NSAIDs did not significantly change the COX-2 expression in A549 cells, whereas it slightly increased in HCT 116 cells after treatment with these compounds. This effect may be due to a substantial contribution of cisplatin, as the Pt(II) drug itself increased the expression of COX-2 in HCT 116 cells.

Interestingly, **6** and **7**, and to a lesser extent, free ketoprofen and naproxen, increased the expression of NAG-1 in both cell lines. Also cisplatin caused the upregulation of this gene, thus contributing to the overall stimulation of NAG-1 expression.

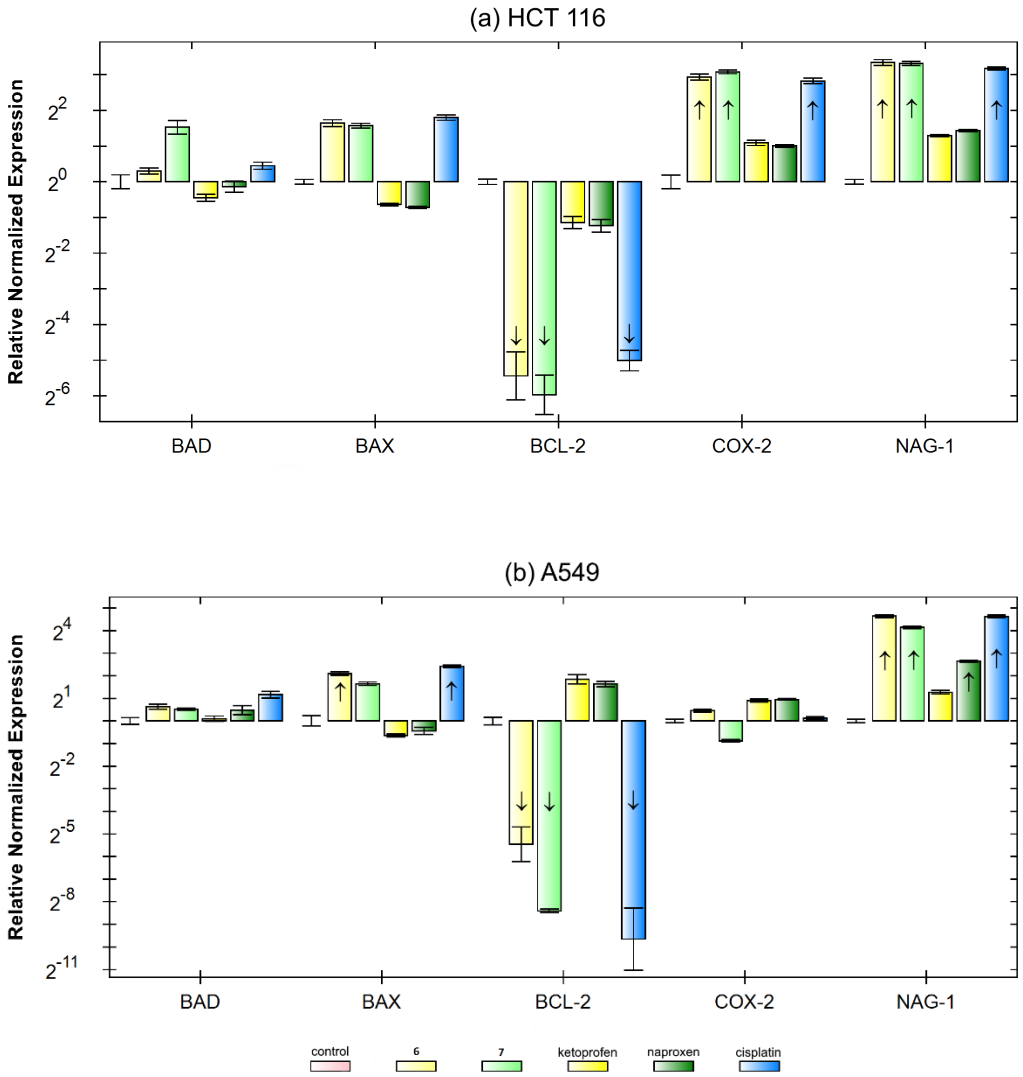


Figure 6.6: Relative gene expression of BAD, BAX , BCL-2, COX-2 and NAG-1 in (a) HCT 116 and (b) A-549 cells following equitoxic 24 h treatments with cisplatin, **6**, **7**, ketoprofen, and naproxen. From left to right of each sequence: control, **6** (light yellow), **7** (light green), ketoprofen (dark yellow), naproxen (dark green), and cisplatin (light blue). The RT-qPCR experiment was performed in triplicate, and results were normalized to references genes in untreated control. The arrows indicate the upregulated (arrow up) or downregulated (arrow down) gene expression with respect to internal threshold value as determined by the CFX Manager software.

## *6.4 Conclusions*

The Pt(IV)-NSAID complexes **6** and **7** showed higher antiproliferative activity on the cancer cell lines under investigation when compared to cisplatin, oxaliplatin, asplatin and the corresponding free NSAIDs, ketoprofen and naproxen. The trend of activity can be explained in terms of lipophilicity of the compounds, that affects their cellular accumulation, hence defined as *synergistic cellular accumulation*. On the contrary, the trend of activity seems to be scarcely dependent on COX-2 gene expression, suggesting that a COX-2-independent mechanism may play a role. This mechanism has been tentatively identified in the activation of the gene NAG-1, having antitumorigenic and pro-apoptotic activity, that may be linked, at least in part, to the chemopreventive activity of NSAIDs. However, analyzing the variation of pro-apoptotic BAD and BAX and anti-apoptotic BCL-2 genes, it appears clearly that cisplatin, released after Pt(IV) $\rightarrow$ Pt(II) reduction, is the component of the combos mainly responsible for the overall antiproliferative activity, also because of its own NAG-1 activation. Thus, most of the biological effects of the Pt(IV) complexes **6** and **7** are related to the releasing of cisplatin. The NSAID axial ligands only increase the overall lipophilicity and hence the cellular accumulation of these combos, offering a minor (additive) contribution in terms of NAG-1 activation.

# *References*

[1] WL. Smith, DL. DeWitt, RM. Garavito. Cyclooxygenases: structural, cellular, and molecular biology. *Annu Rev Biochem* (2000), 69, 145-182.

[2] TT. Yu, XZ. Lao, H. Zheng. Influencing COX-2 activity by COX related pathways in inflammation and cancer. *Mini Rev Med Chem* (2016), 16, 1230-1243.

[3] E. Gurpinar, WE. Grizzle, GA. Piazza. NSAIDs inhibit tumorigenesis, but how? *Clin Cancer Res* (2014), *20*, 1104-1113.

[4] JL. Liggett, XB Zhang, TE. Eling, SJ. Baek. Anti-tumor activity of non-steroidal anti-inflammatory drugs: Cyclooxygenase-independent targets. *Cancer Lett* (2014) 346, 217-224.

[5] J. Lin, PW. Hsiao, TH. Chiu, JI. Chao. Combination of cyclooxygenase-2 inhibitors and oxaliplatin increases the growth inhibition and death in human colon cancer cells. *Biochemical Pharmacology* (2005), *70*, 658-667.

[6] G. Dannhardt, W. Kiefer. Cyclooxygenase inhibitors - current status and future prospects. *Eur J Med Chem* (2001) 36, 109-126.

[7] MJ. Thun, SJ. Henley, C. Patrono. Nonsteroidal anti-inflammatory drugs as anticancer agents: Mechanistic, pharmacologic, and clinical issues. *J Natl Cancer Inst* (2002) 94, 252-266.

[8] P. Patrignani, C. Patrono. Cyclooxygenase inhibitors: from pharmacology to clinical read-outs. *Biochim Biophys Acta* (2015) 1851, 422-432.

[9] RK. Pathak, S. Marrache, JH. Choi, TB. Berding, S. Dhar. The prodrug platin-A: simultaneous release of cisplatin and aspirin. *Angew Chem Int Ed Engl* (2014) 53, 1963-1967.

[10] QQ. Cheng, HD. Shi, HX. Wang, YZ. Min, J. Wang, YZ. Liu. The ligation of aspirin to cisplatin demonstrates significant synergistic effects on tumor cells. *Chem Commun (Camb)* (2014) 50, 7427-7430.

[11] QQ. Cheng, HD. Shi, HX. Wang, J. Wang, YZ. Liu. Asplatin enhances drug efficacy by altering the cellular response. *Metallomics* (2016) 8, 672-678.

[12] JD. Hoeschele, HDH. Showalter, AJ. Kraker, WL. Elliott, BJ. Roberts., JW. Kampf. synthesis, structural characterization, and antitumor properties of a novel class of large-ring platinum(II) chelate complexes incorporating the *cis*-1,4-diaminocyclohexane ligand in a unique locked boat conformation. *J Med Chem* (1994) 37, 2630–2636.

[13] W. Neumann, BC. Crews, MB. Sarosi, CM. Daniel, K. Ghebreselasie, MS. Scholz, LJ. Marnett,; E. Hey-Hawkins. Conjugation of cisplatin analogues and cyclooxygenase inhibitors to overcome cisplatin resistance. *ChemMedChem* (2015) 10, 183-192.

[14] A. Curci, N. Denora, RM. Iacobazzi, N. Ditaranto, JD. Hoeschele, N. Margiotta, G. Natile. Synthesis, characterization, and in vitro cytotoxicity of a Kiteplatin-Ibuprofen Pt(IV) prodrug. *Inorg Chim Acta* (2018) 472, 221-228.

[15] XD. Qin, G. Xu, FH. Chen, L. Fang, SH. Gou. Novel platinum(IV) complexes conjugated with a wogonin derivative as multi-targeted anticancer agents. *Bioorg Med Chem* (2017) 25, 2507-2517.

[16] B. Cryer, M. Feldman. Cyclooxygenase-1 and cyclooxygenase-2 selectivity of widely used nonsteroidal anti-inflammatory drugs. *Am J Med* (1998) 104, 413-421.

[17] M. Ravera, I. Zanellato, E. Gabano, E. Perin, B. Rangone, M. Coppola, D. Osella. Antiproliferative Activity of Pt(IV) Conjugates Containing the Non-Steroidal Anti-Inflammatory Drugs (NSAIDs) Ketoprofen and Naproxen. *Int J Mol Sci* (2019) 24, 20(12).

[18] RK. Pathak, S. Marrache, JH. Choi, TB. Berding, S. Dhar. The prodrug platin-a: simultaneous release of cisplatin and aspirin. *Angew Chem Int Ed Engl* (2014) 53, 1963-1967.

[19] TC. Chou, P. Talalay. Quantitative analysis of dose-effect relationships: the combined effects of multiple drugs or enzyme inhibitors. *Adv Enzyme Regul* (1984) 22, 27-55.

[20] TC. Chou. Theoretical basis, experimental design, and computerized simulation of synergism and antagonism in drug combination studies. *Pharmacol Rev* (2006) 58, 621-681.

[21] TC. Chou. Drug combination studies and their synergy quantification using the Chou-Talalay method. *Cancer Res* (2010) 70, 440-446.

[22] A. Catalano, L. Graciotti, L. Rinaldi, G. Raffaelli, S. Rodilosso, P. Betta, W. Gianni, S. Amoroso, A. Procopio. Preclinical evaluation of the nonsteroidal anti-inflammatory agent celecoxib on malignant mesothelioma chemoprevention. *International J Cancer* (2004) 109, 322-328.

[23] KJ. Livak, TD. Schmittgen. Analysis of relative gene expression data using real-time quantitative PCR and the 2^(-ΔΔC) method. *Methods* (2001) 25, 402-408.

[24] T. Nolan, RE. Hands, SA. Bustin. Quantification of mRNA using real-time RT-PCR. *Nat Protoc* (2006) 1, 1559-1582.

[25] R. Raveendran, JP. Braude, E. Wexselblatt, V. Novohradsky, O. Stuchlikova, V. Brabec, V. Gandin, D. Gibson. Pt(IV) derivatives of cisplatin and oxaliplatin with phenylbutyrate axial ligands are potent cytotoxic agents that act by several mechanisms of action. *Chem Sci* (2016) 7, 2381-2391.

[26] SJ. Baek, JS. Kim, SM. Moore, SH. Lee, J. Martinez, TE. Eling. Cyclooxygenase inhibitors induce the expression of the tumor suppressor gene EGR-1, which results in the up-regulation of NAG-1, an antitumorigenic protein. *Mol Pharmacol* (2005) 67, 356-364.

[27] SJ. Baek, KS. Kim, JB. Nixon, LC. Wilson, TE. Eling. Cyclooxygenase inhibitors regulate the expression of a TGF-beta superfamily member that has proapoptotic and antitumorigenic activities. *Mol Pharmacol* (2001) 59, 901-908.

[28] SJ. Baek, LC. Wilson, CH. Lee, TE. Eling. Dual function of nonsteroidal anti-inflammatory drugs (NSAIDs): Inhibition of cyclooxygenase and induction of NSAID-activated gene. *J Pharmacol Exp Ther* (2002) 301, 1126-1131.

[29] TE. Eling, SJ. Baek, M. Shim, CH. Lee. NSAID activated gene (NAG-1), a modulator of tumorigenesis. *J Biochem Mol Biol* (2006) 39, 649-655.

# *Chapter 7*

## *Concluding Remarks and Perspectives*

Despite the progress made by the research, cancer remains one of the major causes of death worldwide. Nowadays, immunostimulating- and targeted-therapies are considered among the most promising antitumor strategies to get high therapeutic antitumor effects with mild systemic toxicity. However, traditional cytotoxic (DNA-damaging) chemotherapy is still one of the treatments of choice for several highly aggressive cancers. Most of such chemotherapeutic schedules consist of the so-called combination therapy (*i.e.* the administration of two or more additive, or better synergistic, drugs together). Within this context, the three FDA-approved Pt(II) drugs, cisplatin, carboplatin and oxaliplatin play a key role, being administered in about 50% of anticancer regimens. Unfortunately, their use is hampered by severe side effects, production of drug resistance and poor pharmacokinetic activities. On the contrary, the Pt(IV) complexes are ideally suitable for such approach. They have octahedral geometry, so they are quite inert to substitution and reach intact cancer cells, minimizing the side effects and the off-target reactions. Moreover, the Pt(IV) complexes act as prodrugs, being activated by reduction within hypoxic cancer cells, releasing the corresponding Pt(II) complex and two axial ligands. These ligands can be biologically active molecules, providing an adjuvant or synergistic action with cytotoxic Pt(II) species, and ensuring the synchronous internalization of such Pt(IV) multifunctional drugs (“combo”).

The biological properties of several newly designed, synthetized and characterized multi-action Pt(IV) prodrug candidates have been reported in this Ph.D. thesis.

Epigenetic agents, such as Histone DeAcetylase inhibitors (HDACi), seem to be suitable axial ligands. Indeed, a cisplatin-based Pt(IV) complexes containing the novel histone deacetylase inhibitor 2-(2-propynyl)octanoate (POA) as axial ligand was studied. Since POA has a chiral centre, also its isomers were tested, showed almost identical *in vitro* activity compared to the racemate. The POA-bearing Pt(IV) complex showed a marked *in vitro* antiproliferative activity on a panel of different human cancer lines and also a strong *in vivo* anticancer activity on Lewis lung carcinoma bearing mice, compared with the Pt(II) counterpart (*i.e.* cisplatin). Moreover, albeit having a single HDACi molecule, it exhibited *in vitro* and *in vivo* performances similar or even better to those offered by another Pt(IV) compound, featuring two HDACi (*i.e* VPA) molecules, with a more efficient biodistribution. These promising results have led to the investigation of the biological properties of a Pt(IV) derivate bearing the same POA molecule, but based on the oxaliplatin-analogue *cis*-dichlorido(cyclohexane-1R,2R-diamine)platinum(II) (or [$PtCl_2$(dach)]). The *in vitro* activity of the compound with racemic POA was evaluated on three human and one mouse colon cancer cell lines along with that of its isomers, and also in this case the $IC_{50}$ and the cellular accumulation data showed that the activity of the three POA derivatives is almost identical. Moreover, the Pt(IV) complexes were one or two orders of magnitude more active than the references Pt(II) compounds cisplatin, oxaliplatin and [$PtCl_2$(dach)], due to their high cellular accumulation. Finally, the dach-based Pt(IV) prodrug exerted also a marked *in vivo* anticancer activity on a pool of immunocompetent BALB/c mice bearing CT26 colon carcinoma. When orally administered the Pt(IV) prodrug inhibited the tumor growth more efficient than intravenously administered (i.v.) oxaliplatin. However, such a protocol is limited by the presence of heavy side effects, probably due to an extremely high Pt accumulation into the liver and spleen. Conversely, the performances of the Pt(IV) complex i.v. administered were much more promising in terms of tumor growth inhibition and persistence of the anticancer effects, along with lower nephro- and hepatotoxicity. Noteworthy, the dach-based Pt(IV) complex

containing one POA molecule, was able to induce immunogenic cell death, as demonstrated by the massive presence of the activated cytotoxic $CD8^+$ T lymphocytes. Both metabolites [$PtCl_2$(dach)] and POA, released upon intracellular reduction, seem to contribute to this process, leading to a reversion of the immunoescape mechanisms on colon cancer.

Since this compound has shown a good efficacy against colon cancer, the *in vitro* antitumor activity of three couples of asymmetric Pt(IV) species, cisplatin- or dach-based, containing the bioactive axial ligands clofibrate (2-(*p*-chlorophenoxy)-2-methyl- propionic acid (CA) or heptanoate (HA) or octanoate (OA), was investigated on three different human colon cancer cell lines and on one ovarian cancer cell line. The two series of Pt(IV) prodrugs showed a marked anticancer activity, both on monolayer cell cultures and on 3D multicellular tumor spheroids (MCTS), compared to the Pt(II) counterparts. This potency is certainly due to a considerable accumulation in cancer cells of Pt(IV) prodrugs, bearing a lipophilic axial ligand (*i.e* CA, HA, OA); the dach carrier ligand itself significantly contributes to such an escalation of lipophilicity. Moreover, the dach-based series showed a higher selectivity towards colon cancer cells.

Finally, inhibitors of cyclooxygenase (COX) enzymes, as Non-Steroidal Anti-Inflammatory Drugs (NSAIDs), have been suggested for chemoprevention on colon carcinoma, and cisplatin and several NSAIDs have proved to act additively or synergistically on several cancer cell lines. For these reasons the *in vitro* activity of two cisplatin-based Pt(IV) complexes containing an NSAIDs as axial ligand, (*i.e.* ketoprofen or naproxen) was evaluated. Both Pt(IV) complexes offered good antiproliferative performances on a panel of human cancer cell lines with different levels of COX-2 expression, including a malignant pleural mesothelioma one (a very chemoresistant tumor). The main reason of this increased activity, compared to the reference drug cisplatin, seems to be related to the enhanced lipophilicity of the Pt(IV) species (synergistic cellular accumulation). Indeed, their biological effects resulted almost independent from COX-2 expression, while these NSAID axial

ligands offered an additive contribution in the activation of the NSAIDs activated gene (NAG-1), involving in growth inhibition of cancer cells.

In summary, as demonstrated in this Ph.D. work, an increase in antiproliferative activity of Pt(IV) prodrugs compared to their Pt(II) parent compounds is almost generally expected, as a consequence of the increased lipophilicity and consequently to the higher cellular accumulation, causing, in turn, proportionally higher DNA platination. An increase in lipophilicity can be achieved by using highly lipophilic amines as carrier ligands, as in the case of satraplatin, which entered in several clinical trials. This complex produces Pt(II) metabolites different from those usually employed in the clinic (*i.e.* cisplatin and oxaliplatin), also influencing the sensitivity towards different tumors. Alternatively, the addition of long-chain aliphatic carboxylic acids as axial ligands leads to an increase of lipophilicity in cisplatin- or oxaliplatin-based Pt(IV) compounds. The use of axial ligands with further biological properties,synergistic or additive with respect to those of the Pt(II) drugs, leads to these Pt(IV) multi-action complexes with promising pharmacological profile. These axial ligands are generally bioactive *per se* at concentrations higher than those of the Pt(II) metabolites. However, the *synergistic cellular accumulation* of the Pt(IV) prodrug allows a more efficient cellular accumulation causing an increase of the local concentration of the second drug (the axial ligand).

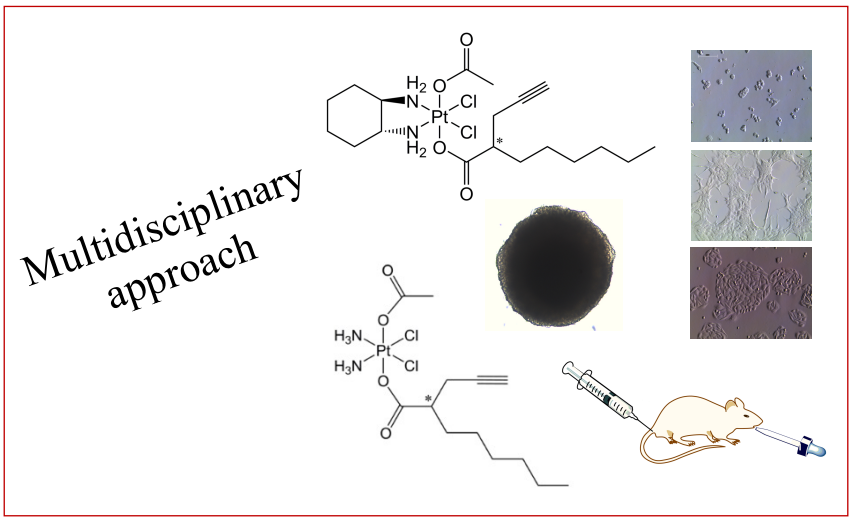

Thus, a multidisciplinary approach, involving inorganic chemists, biochemists and molecular biologists, is needed to understand the real advantages caused by the incorporation of such bioactive molecules in these combo prodrug candidates.

For these reasons, future perspectives of this work could include a further, deeper investigation of the molecular mechanisms triggered in cells by the treatment with both cisplatin- and dach-based Pt(IV) prodrugs, containing the epigenetic agent POA as axial ligand. Indeed, among all the potential combos studied in this work, they showed the better *in vitro* and *in vivo* anticancer performances. Moreover, in this context, also other new Pt(IV) complexes, bearing different epigenetic drugs as axial ligand, could be designed, synthetized, characterized and investigated from a biological point of view. Particularly, in order to better understand the multi-action of these drugs, *in vitro* tests both on 2D monolayer cell cultures and on 3D MCTS, which resemble the features of *in vivo* tumor tissue and allow to study long-term effects of the drugs, will be performed. Importantly, also *in vivo* studies will be carried out, to understand how the route of administration can affect the antitumor efficacy and the side effects of these drugs.

Finally, in order to better target the tumor tissue, a passive drug delivery strategy could be exploited. Thus, the biological properties of Pt(IV) complexes bound to several macromolecules or nanoparticles, including micelles and liposome, polymers, carbon nanotubes or other delivery systems could be investigated in detail.

# *List of Publications*

1. E. Gabano, E. Perin, C. Fielden, JA. Platts, A. Gallina, B. Rangone, M. Ravera M. How to obtain Pt(IV) complexes suitable for conjugation to nanovectors from the oxidation of [PtCl(terpyridine)]. *Dalton Trans* (2017) 46(31):10246-10254.

2. E. Gabano, M. Ravera, I. Zanellato, S. Tinello, A. Gallina, B. Rangone, V. Gandin, C. Marzano, MG. Bottone, D. Osella. An unsymmetric cisplatin-based Pt(IV) derivative containing 2-(2-propynyl)octanoate: a very efficient multi-action antitumor prodrug candidate. *Dalton Trans* (2017) 46(41):14174-14185.

3. B. Rangone, B. Ferrari, V. Astesana, I. Masiello, P. Veneroni, I. Zanellato, D. Osella, MG. Bottone. A new platinum-based prodrug candidate: Its anticancer effects in B50 neuroblastoma rat cells. *Life Sci* (2018) 210:166-176.

4. E. Gabano, M. Ravera, E. Perin, I. Zanellato, B. Rangone, MJ. McGlinchey, D. Osella. Synthesis and characterization of cyclohexane-1R,2R-diamine-based Pt(IV) dicarboxylato anticancer prodrugs: their selective activity against human colon cancer cell lines. *Dalton Trans* (2019) 48(2), 435-445.

5. M. Sabbatini, I. Zanellato, M. Ravera, E. Gabano, E. Perin, B. Rangone, D. Osella. Pt(IV) bifunctional prodrug containing 2-(2-propynyl)octanoato axial ligand: induction of immunogenic cell death on colon cancer. *J Med Chem* (2019) 62(7), 3395-3406.

6. M. Ravera, I. Zanellato, E. Gabano, E. Perin, B. Rangone, M. Coppola, D. Osella. Antiproliferative activity of Pt(IV) conjugates containing the Non-Steroidal Anti-Inflammatory Drugs (NSAIDs) ketoprofen and naproxen. *Int J Mol Sci* (2019) 24, 20(12).

7. B. Ferrari, F. Urselli, M. Gilodi, S. Camuso, EC. Priori, B. Rangone, M. Ravera, P. Veneroni, I. Zanellato, E. Roda, D. Osella, MG. Bottone. New platinum-based prodrug Pt(IV)Ac-POA: antitumour effects in rat C6 glioblastoma cells. *Neurotox Res* (2019) doi: 10.1007/s12640-019-00076-0.

# *Acknowledgments*

Desidero innanzitutto ringraziare il Prof. Domenico Osella, mio supervisore, per avermi offerto l'opportunità di intraprendere questo percorso di ricerca, e per l'infinita cortesia e disponibilità dimostratemi nel corso di questi anni, e il Prof. Mauro Ravera per la proficua collaborazione.

Un sentito ringraziamento va alla Dott.ssa Elisabetta Gabano per la sua assidua disponibilità ed infinita pazienza, e per i suoi preziosi consigli, in particolare durante la stesura della tesi.

Un ringraziamento speciale va poi alla Dott.ssa Ilaria Zanellato per il suo prezioso aiuto nella progettazione degli esperimenti e nella successiva analisi dei dati, oltre che per la sua gentilezza e disponibilità. Ringrazio inoltre il Dott. Andrea Gallina, guida paziente durante gli esperimenti svolti all'inizio del mio percorso di Dottorato.

Desidero inoltre ringraziare il Dott. Stefano Tinello e la Dott.ssa Elena Perin per la sintesi e la caratterizzazione dei complessi a base di platino da me testati, ed in particolare ringrazio quest'ultima anche per le analisi effettuate mediante ICP-MS e ICP-OES, ma soprattutto per la sua disponibilità a qualsiasi chiarimento e per il rapporto di amicizia instauratosi durante questi anni.

Ringrazio inoltre per le proficue collaborazioni scientifiche instauratesi durante questo mio percorso di ricerca il Prof. Maurizio Sabbatini e la Dott.ssa Flavia Caprì (Università del Piemonte Orientale), la Prof.ssa Valentina Gandin e la Prof.ssa Cristina Marzano (Università di Padova), il Prof. Enzo Terreno (Università di Torino), la Prof.ssa Maria Grazia Bottone e la Dott.ssa Beatrice Ferrari (Università di Pavia), il Prof. Michael J. McGlinchey (University College Dublin), il Prof. James A. Platts (Cardiff University), e il Consorzio Interuniversitario di Ricerca in Chimica dei Metalli nei Sistemi Biologici (CIRCMSB).

Un ringraziamento va inoltre alla Compagnia di San Paolo (progetto BIPLANES) e all'Università del Piemonte Orientale per il supporto finanziario alla ricerca svolta.

Ringrazio poi Jonathan, Simone, Chiara e Giulia con i quali ho intrecciato questo mio percorso di crescita, sia scientifico che umano, e la Prof.ssa Maria Angela Masini, sempre disponibile ad elargire consigli in ambito biologico…e non solo.
Un ringraziamento speciale va poi alla mia famiglia e alle mie più care amiche, Ilaria e Valentina, per l'impareggiabile supporto e incoraggiamento.
Infine, ringrazio di cuore Alberto, che non smette mai di credere in me.

UNIVERSITÀ DEL PIEMONTE ORIENTALE

DIPARTIMENTO DI
SCIENZE E INNOVAZIONE
TECNOLOGICA

Viale Teresa Michel 11 – 15121
Alessandria AL

# DECLARATION AND AUTHORISATION TO ANTIPLAGIARISM DETECTION

The undersigned Rangone Beatrice student of Chemistry&Biology Ph.D course (XXXII Cycle)

**declares:**

- to be aware that the University has adopted a web-based service to detect plagiarism through a software system called "Turnitin",
- his/her Ph.D. thesis was submitted to Turnitin scan and reasonably it resulted an original document, which correctly cites the literature

**acknowledges:**

- his/her Ph.D. thesis can be verified by his/her Ph.D. tutor and/or Ph.D Coordinator in order to confirm its originality.

Date: 14/11/2019 Signature: